Physics at HERA

Ulrich F. Katz, ZEUS
University of Erlangen

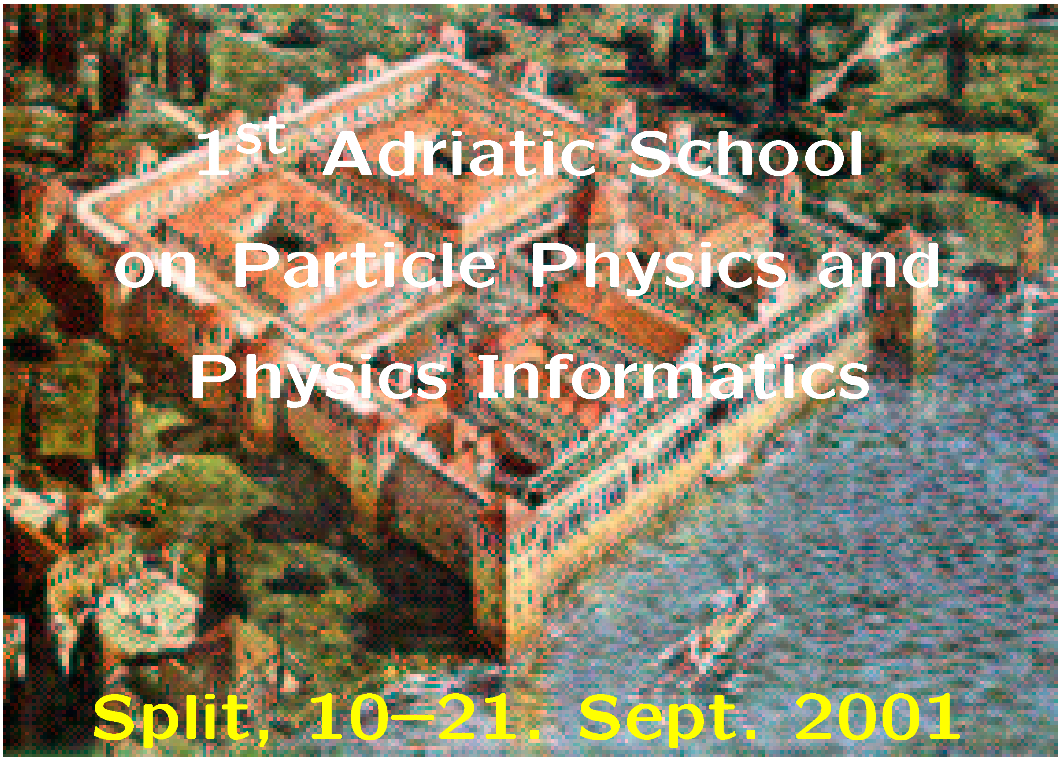

- Introduction:
  deep inelastic scattering at HERA
- DIS cross sections,
  structure functions
  and parton distributions
- DIS analyses and results at high Q^2
- Searches for “new physics”

Introduction: Electron-Proton Collisions at HERA

Overview:

- HERA
  - Experiments
  - Parameters
- Deep inelastic scattering
  - Kinematics
  - Signatures
  - Event topologies
- Example events
- NC and CC cross sections
- Beyond the Standard Model

HERA and its Experiments

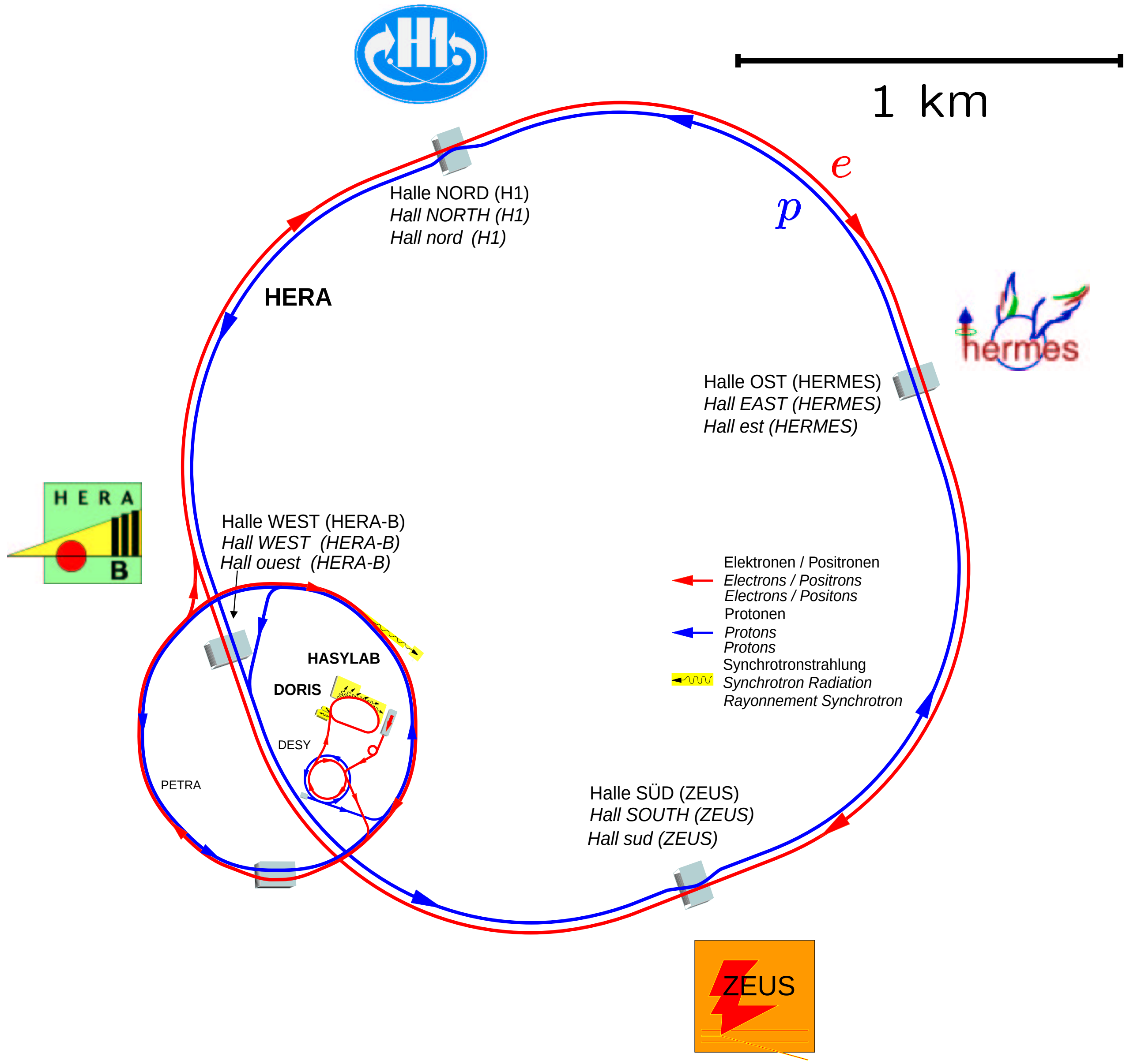

ep collisions at $\sqrt{s} \approx 300$ GeV

e beam (longitudinally polarized) on polarized gas target, $\sqrt{s} \approx 7.5$ GeV;
goal: polarized structure functions

p beam on internal wire target, $\sqrt{s} \approx 40$ GeV;
goal: study hadrons with c and b quarks

HERA: Parameters and Data Sets

Circumference:	6.3 km
Beam energies:	27.5 GeV (e), 820/920 GeV (p, before/after 1997)
Beam currents:	$\lesssim$ 50 mA (e), $\lesssim$ 100 mA (p)
Bunches:	ca. 180 in 210 buckets (some unpaired)
Bunch collision rate:	1/96 ns = 10.4 MHz
Beam life times:	$\sim$ 8 hours (e)
Luminosity:	$\sim 10^{31}\,\mathrm{cm^{-2}\,s^{-1}}$

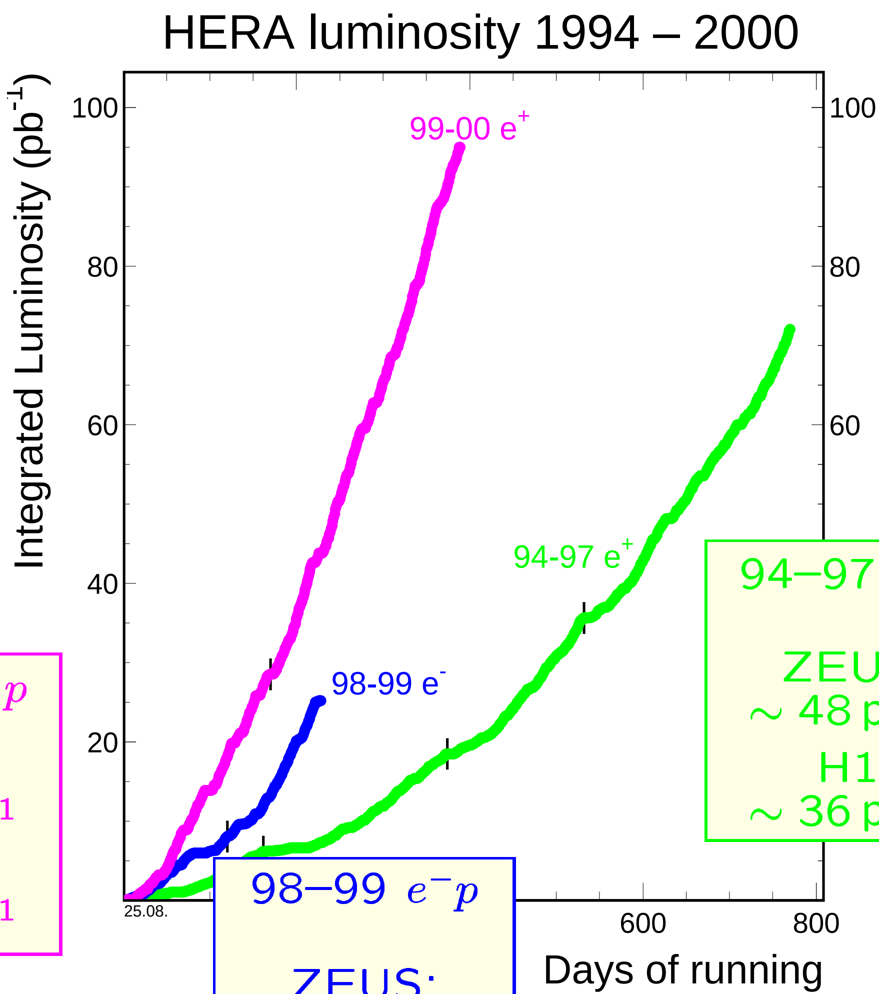

99–00 e^+p

ZEUS: $\sim 70\,\mathrm{pb}^{-1}$

H1: $\sim 70\,\mathrm{pb}^{-1}$

98–99 e^-p

ZEUS: $\sim 16\,\mathrm{pb}^{-1}$

H1: $\sim 15\,\mathrm{pb}^{-1}$

94–97 e^+p

ZEUS: $\sim 48\,\mathrm{pb}^{-1}$

H1: $\sim 36\,\mathrm{pb}^{-1}$

Physics Topics in ep Scattering

ep collisions at HERA offer broad spectrum of reaction channels and physics topics

The following list is neither complete nor are the different items mutually exclusive

- Deep inelastic scattering (DIS)
  - investigation of the parton structure of the proton
  - tests of perturbative QCD (pQCD)
  - electroweak effects (W, Z exchange)
  - study of the transition to the non-perturbative QCD regime
- Photoproduction
  - collision of quasireal photons with protons
  - testing the "photon structure"
  - jet physics ($\rightarrow$ QCD)
  - heavy flavor physics
- Searches for "new physics"
  - new particles (leptoquarks, excited fermions, SUSY particles)
  - anomalous couplings
  - the unexpected
- Diffraction
- Exclusive reactions
- W production
- ...

Cross Sections: Where Experiment Meets Theory

The cross section σ is a measure for the reaction probability

$$\sigma = \frac{N_{\text{reaction}}}{\underbrace{\int_{\text{time}} \mathrm{d}t \, \left[N_{\text{target}} \times (\text{beam flux})\right]}_{\text{integrated luminosity } \mathcal{L}}}$$

Measurement of σ requires knowledge

- of the number of reactions (N_{reaction})
- of the integrated luminosity ($\mathcal{L}$)

$$\sigma = (\text{kin. factor}) \times \underbrace{\left|\mathcal{M}_{fi}\right|^2}_{\substack{\text{square of transition}\\ \text{matrix element}}}$$

- matrix element contains characteristic parameters of interaction (couplings etc.)
- measurement of σ needed to test theory and to determine parameters
- $|\mathcal{M}|$ usually calculated perturbatively ($\rightarrow$ Feynman graphs)

Deep Inelastic ep Reactions in the Quark Parton Model

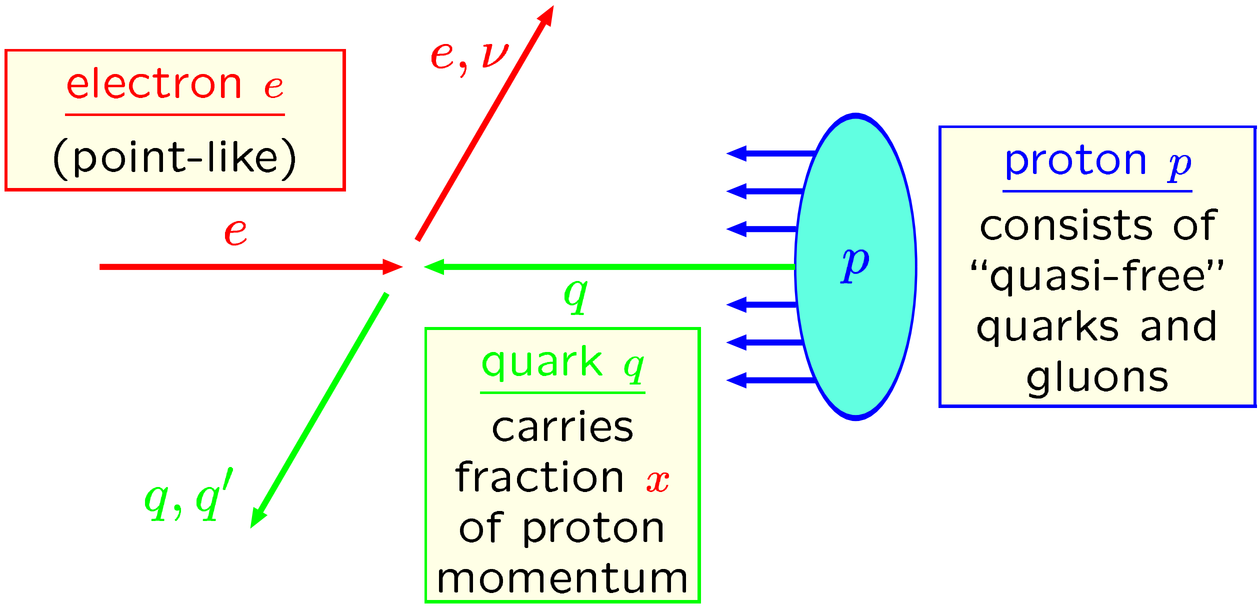

deep inelastic ep scattering (DIS) = incoherent sum of elastic eq scattering:

$$\sigma(ep) = \sum_{q,\bar{q}\ \text{in}\ p} f_{q|p} \cdot \sigma(eq)$$

parton distribution $f_{q|p}(x)$:

probability distribution to find a parton of flavor q with momentum fraction x in the proton

$\sigma(eq)$:

differential eq cross section (depends on scattering angle and eq center-of-mass energy)

Kinematic Variables

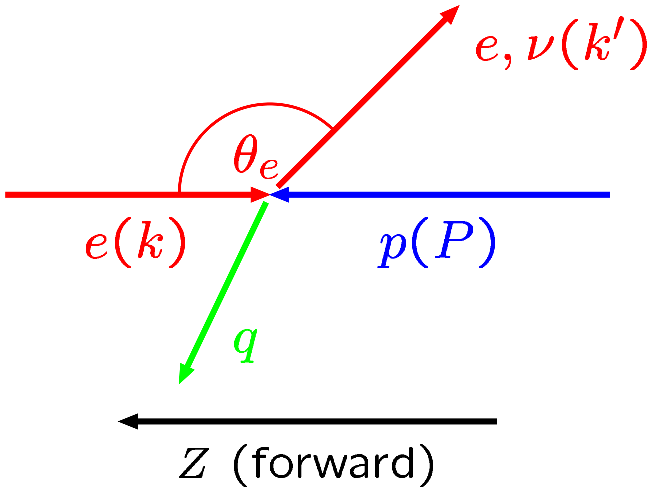

Four-momenta in lab system:

- e (beam): $k = (E_e, 0, 0, -E_e)$
- p (beam): $P = (E_p, 0, 0, E_p)$
- e (scattered): $k' = (E', \ldots)$

Kinematic variables:

square of the ep center-of-mass energy:

$$s = (k + P)^2 = 4E_eE_p$$

four-momentum transfer:

$$q = k - k'; \qquad Q^2 = -q^2 = 2E_eE'(1 + \cos\theta_e)$$

Bjorken scaling variable x:

$$x = Q^2/(2\,q \cdot P) = \text{momentum fraction of quark in proton}$$

inelasticity:

$$y = (q \cdot P)/(k \cdot P) = (1 - \cos\theta_e^*)/2;$$

$\theta_e^* =$ scattering angle in eq center-of-mass system

Q^2, x and y:

$$Q^2 = x \cdot y \cdot s$$

invariant eq mass:

$$M = \sqrt{(k + xP)^2} = \sqrt{xs}$$

The Kinematic Plane of DIS

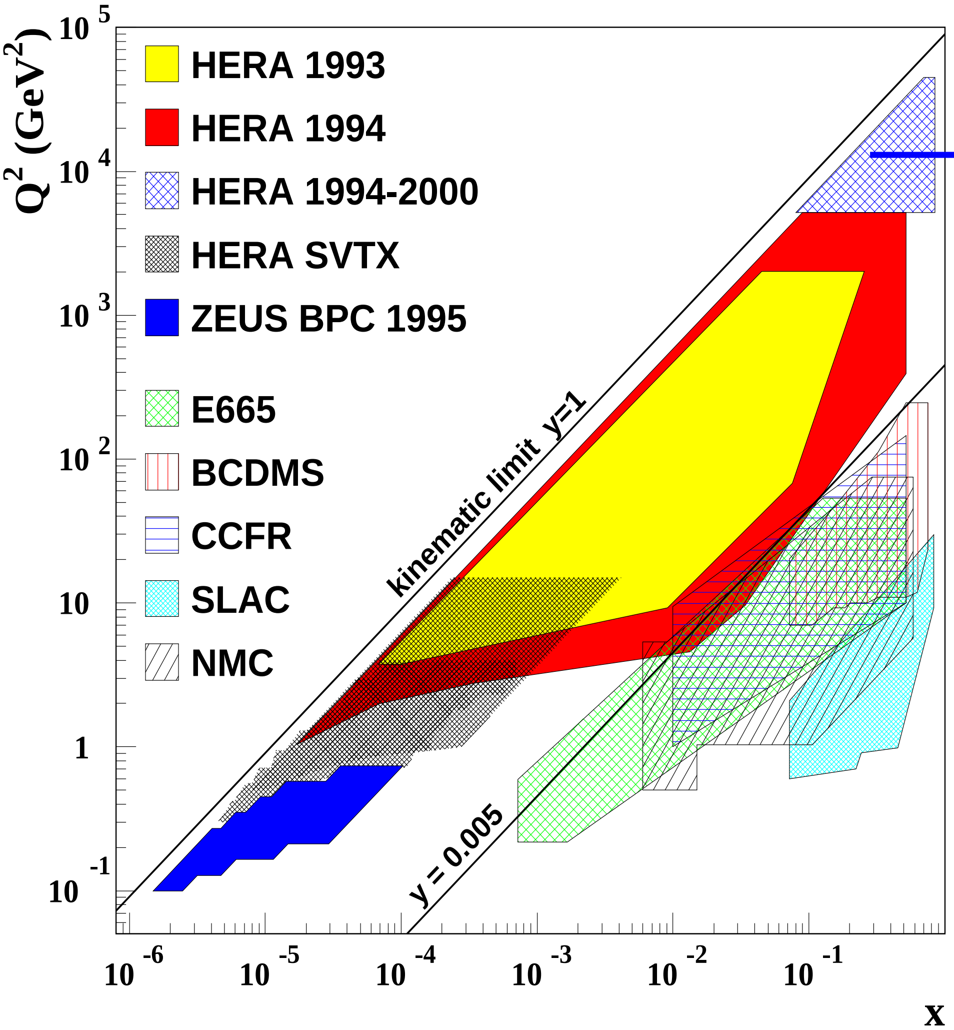

Large
x, Q^2, M
$\Rightarrow$
DIS at electroweak energy scales
($Q^2 \sim M^2_{W,Z}$)
Search for new physics

- HERA extends accessible x and Q^2 region by two orders of magnitude $\Rightarrow Q^2 \gtrsim M^2_{W,Z}$; DIS in this kinematic region was unexplored before HERA.
- Large $Q^2 \Rightarrow$ good spatial resolution ($\Delta x \sim \hbar/\sqrt{Q^2} = \mathcal{O}(10^{-17}\,\text{cm})$)
- Large $x \Rightarrow$ high invariant eq mass ($M = xs \lesssim 200\,\text{GeV}$)

DIS Signatures

Hadronic final state:

- Proton remnant
  jet in forward direction ("remnant jet")
- Scattered quark
  jet in central detector ("current jet")
- Gluon radiation etc.
  further jets in central detector
  [$(n+1)$-jet topology]

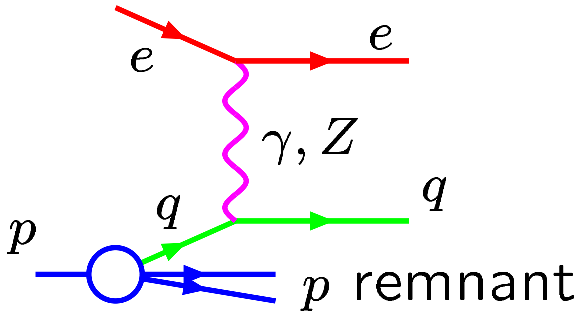

Neutral Current (NC)

- Scattered electron
  $\Rightarrow$ isolated
  $\Rightarrow$ energy $\gtrsim 10\,\text{GeV}$
- One or more
  "central" jets
- Proton remnant
  energy deposition
  around beam pipe
  in p direction

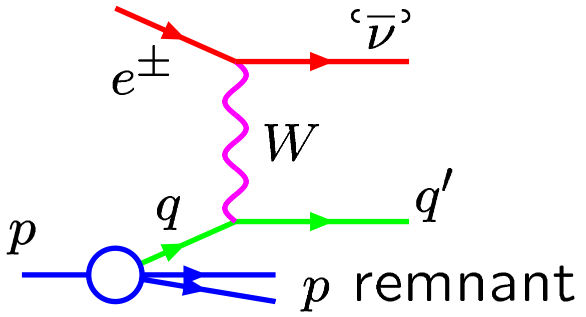

Charged Current (CC)

- Scattered neutrino
  $\Rightarrow$ invisible
  $\Rightarrow$ causes missing
  transverse
  momentum
- Hadronic final state
  $\Rightarrow$ as in NC reactions

Event Topologies at High Q^2

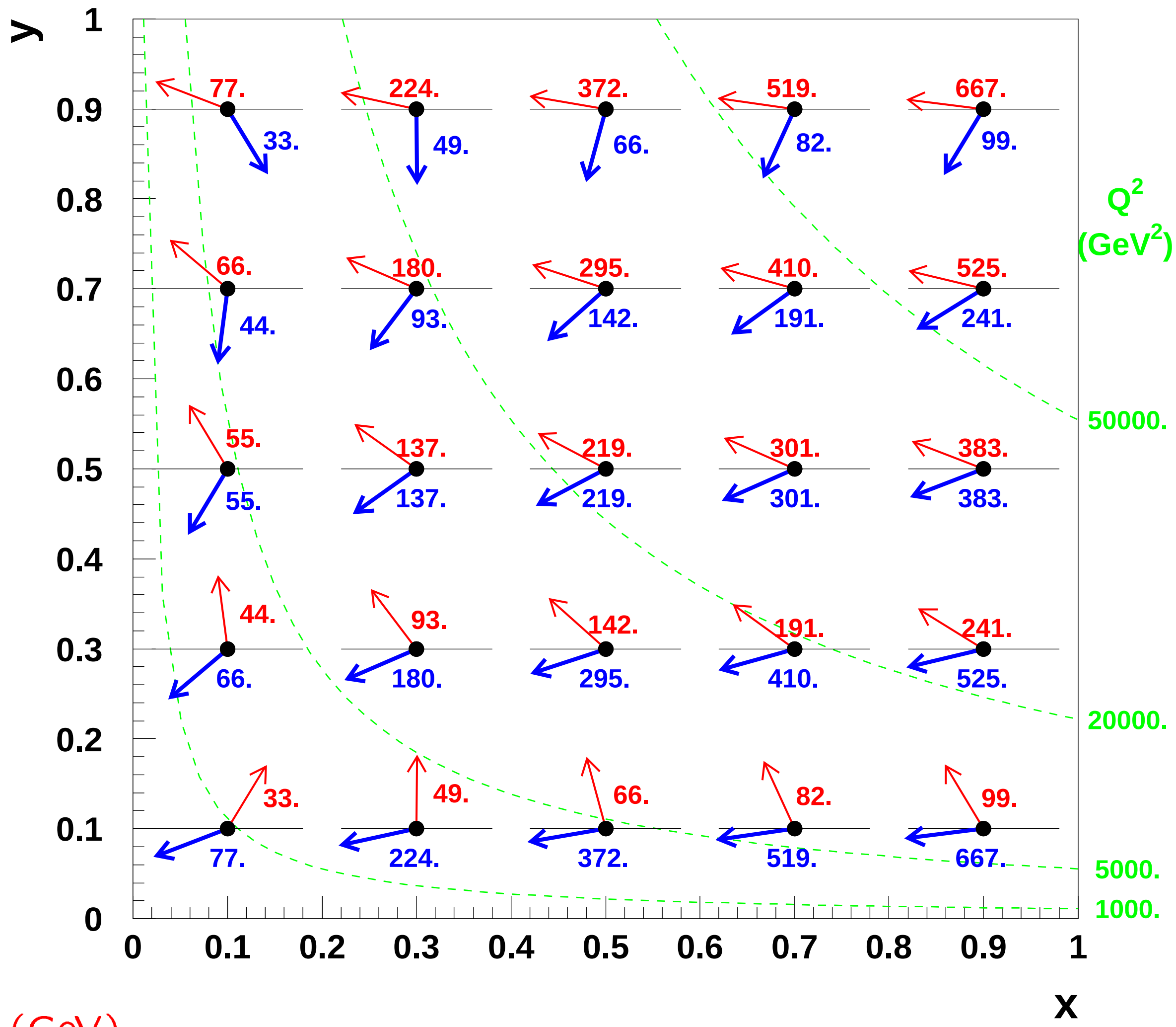

E' (GeV) energy and direction of scattered electron

E_q (GeV) energy and direction of scattered quark

For $Q^2 \gtrsim 1000\,\mathrm{GeV}^2$:

- Scattered electron and current jet have energies of 100 GeV and more
- Electron and jet mostly hit central and forward detector components
- Acceptance problems at $y, 1-y \ll 0.1$

A NC Event in the ZEUS Detector

Scattered electron

- energy in elm. calorimeter
- isolated, single track

$Q^2 \approx 25\,000\ \mathrm{GeV}^2$
$x \approx 0.55$
$y \approx 0.50$
$E' \approx 236\ \mathrm{GeV}$

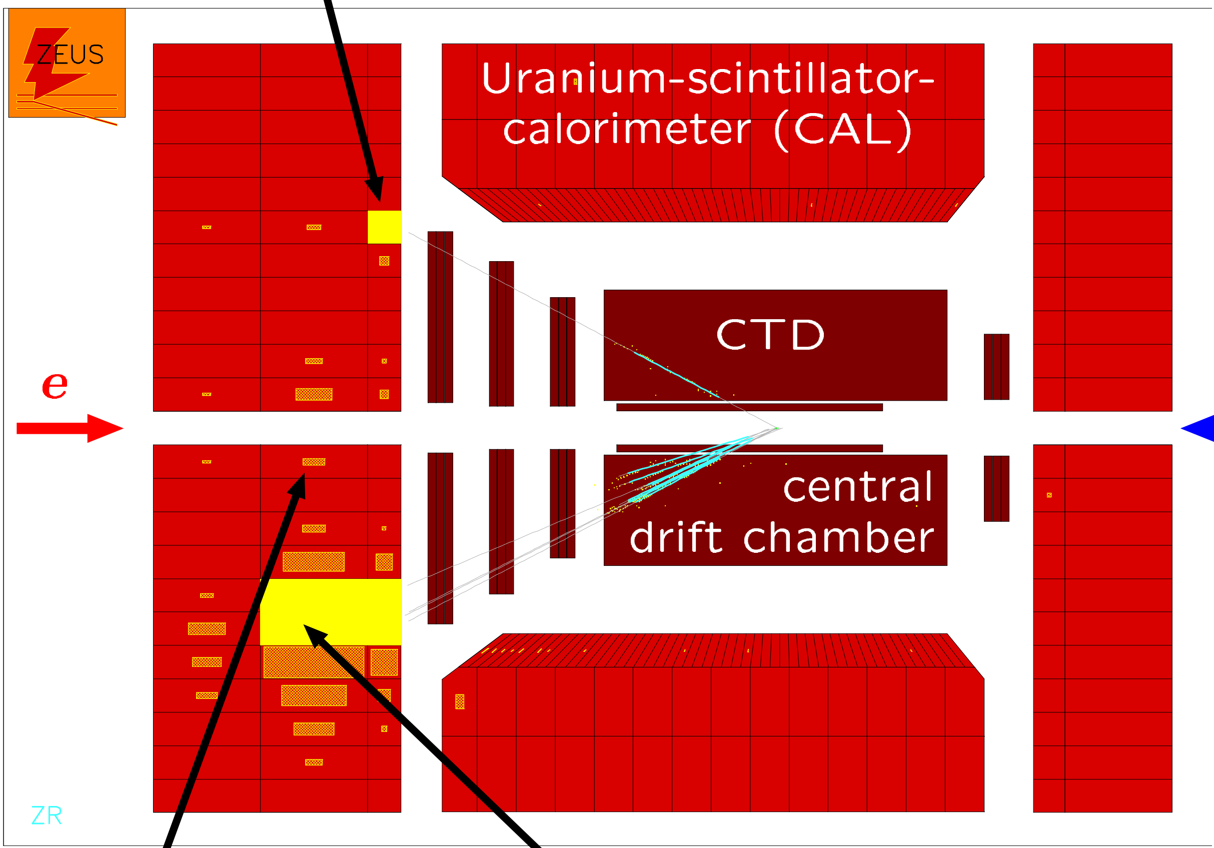

Remnant jet

Current jet

- energy in elm. and had. calorimeter
- many tracks, collimated energy flow

A CC Event in the H1 Detector

Current jet

– energy in elm. and had. calorimeter

– many tracks, collimated energy flow

$Q^2 \approx 20\,000\ \mathrm{GeV}^2$

$x \approx 0.4$

$y \approx 0.49$

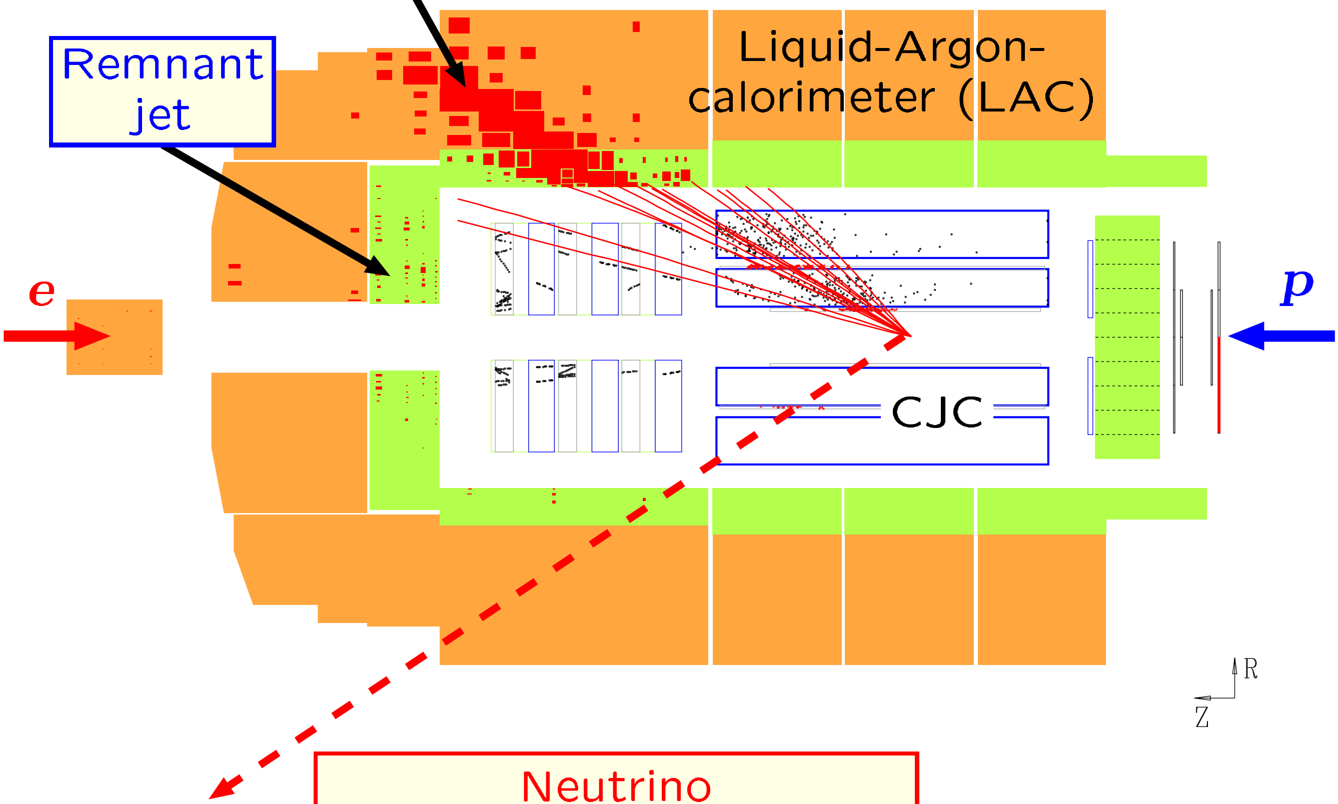

Neutrino

– leaves no signal in the detector

– causes "missing transverse momentum" (missing P_t)

NC and CC Cross Sections

Measurements of dσ/dQ^2 at HERA:

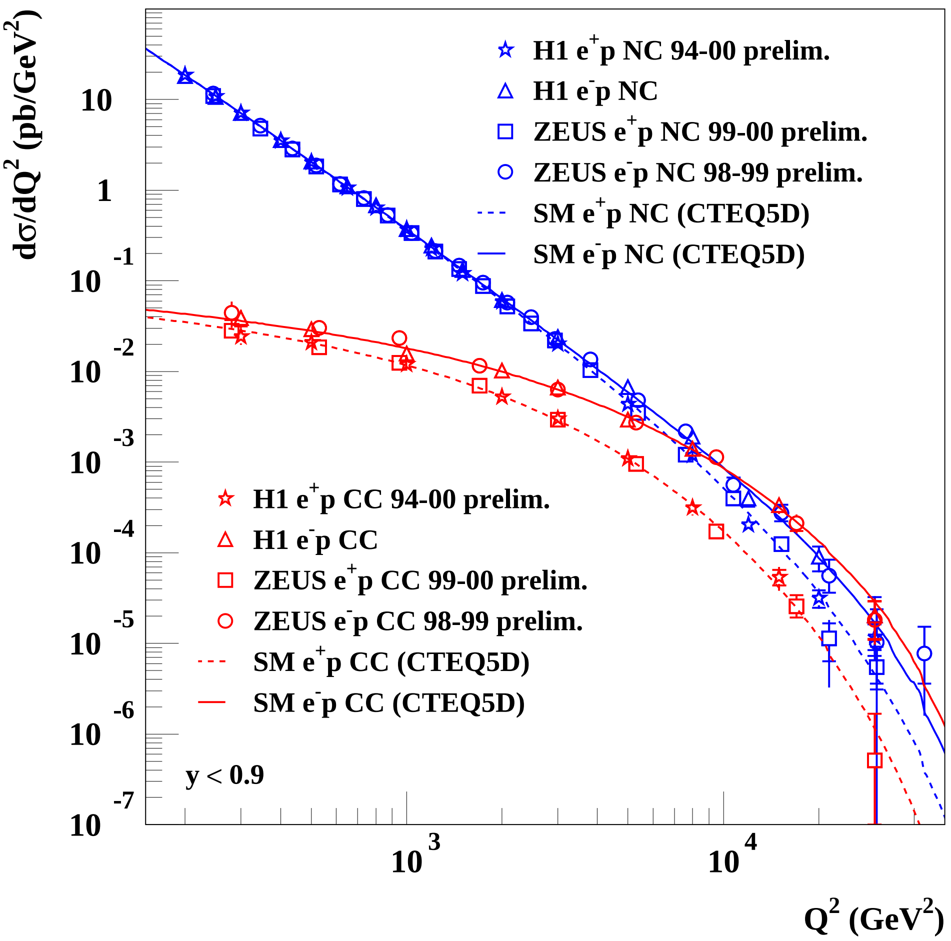

- HERA: first simulteneous measurements of NC and CC reactions, e^+p und e^-p in the same experiment.
- For $Q^2 \gtrsim M^2_{W,Z}$ we have dσ/dQ^2(NC) $\sim$ dσdQ^2(CC) (electroweak unification).
- Cross sections vary by many orders of magnitude, measurements still statistics-dominated at high Q^2.

Beyond the Standard Model

. . . some examples

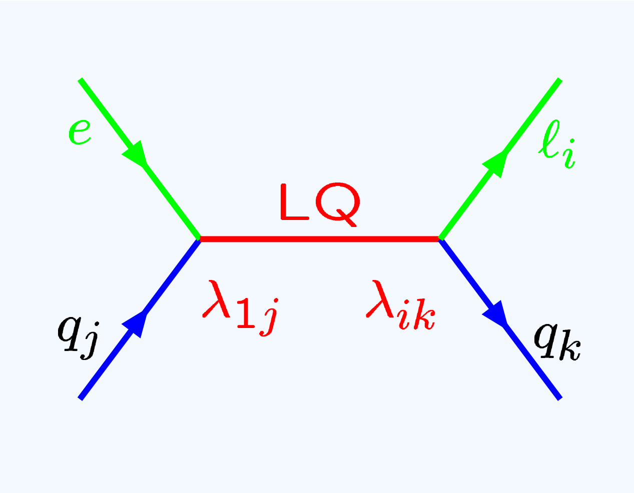

Leptoquark (LQ)

- Narrow resonance in $M = \sqrt{xs}$
- If $\ell = e$: single event indistinguishable from DIS
- But: different angular distribution (y)

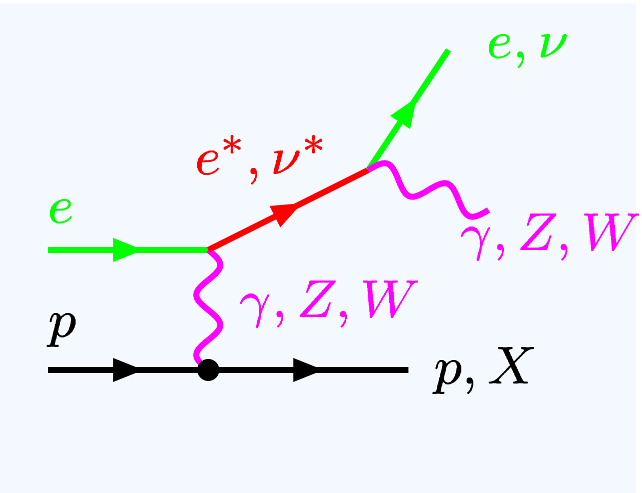

Excited fermions (e^* or ν^*)

- May exist if fermions are composite
- Various decays to fermion+gauge boson
- Event topology different from DIS

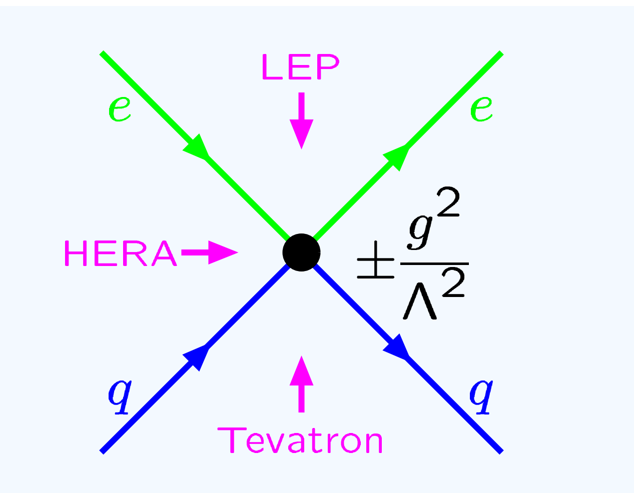

Contact interactions (CI)

- Effective model for processes with energy scale $\gg s$
- E.g. exchange of new gauge boson or of LQ
- DIS cross section modified

DIS Cross Sections, Structure Functions and Parton Distributions

Overview:

- The QPM cross section
  - eq cross sections
  - ep cross sections and structure functions
  - Parton distributions
  - Radiative corrections
- QCD corrections
  - Leading contributions
  - QCD evolution equations
- QCD fits
  - Fit method
  - Experimental data
  - PDFs at high x
- Precision of cross section predictions

The QPM Cross Section

$$\frac{\mathrm{d}^2\sigma}{\mathrm{d}x\,\mathrm{d}Q^2}(x,Q^2) = \sum_q q(x,Q^2)\,\frac{\mathrm{d}\,\hat{\sigma}}{\mathrm{d}Q^2}(x,Q^2) \qquad (*)$$

1

The eq cross section (LO)

$x = \hat{s}/s$ und $Q^2 = y\hat{s} = \hat{s}\cos^2\theta^*/2$ determine eq center-of-mass energy and scattering angle.

$$\frac{\mathrm{d}\,\hat{\sigma}_{\mathrm{NC}}}{\mathrm{d}Q^2} \propto \left| \quad + \quad \right|^2$$

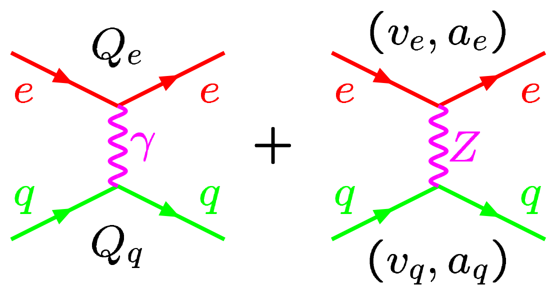

$$v_f = \frac{-I_f^3 + 2\sin^2\theta_W\,Q_f}{2\sin\theta_W\cos\theta_W} \qquad a_f = \frac{-I_f^3}{2\sin\theta_W\cos\theta_W}$$

Q_f = charge of f in units of e

I_f^3 = 3-component of weak isospin

θ_W = Weinberg angle

$$\frac{\mathrm{d}\,\hat{\sigma}_{\mathrm{CC}}}{\mathrm{d}Q^2} \propto \sum_{q'} |V_{qq'}|^2 \left| \quad \right|^2$$

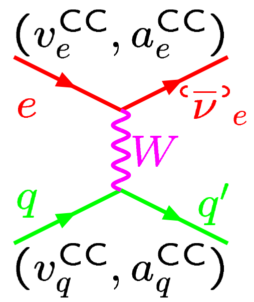

$$v_f^{\mathrm{CC}} = -v_a^{\mathrm{CC}} = \frac{1}{2\sqrt{2}\sin\theta_W}$$

$V_{qq'}$ = Cabbibo–Kobayashi–Maskawa matrix

$\boxed{\text{Note: QCD is not involved at LO !}}$

The QPM Cross Section [2]

2

The parton distributions (PDFs)

- $p(x,Q^2)\mathrm{d}x$ is the probability at given Q^2 to find in the proton a parton of flavor p with momentum fraction between x und $x+\mathrm{d}x$
- "Naïve" QPM: $p(x,Q^2)$ does not depend on Q^2 (scaling)
- Q^2 dependence induced by QCD corrections (see below)

3

The ep cross section

$$\frac{\mathrm{d}^2\sigma_{\mathrm{NC}}(e^\pm p)}{\mathrm{d}x\,\mathrm{d}Q^2} = \frac{2\pi\alpha^2}{Q^4}\left(Y_+F_2^{\mathrm{NC}} \mp Y_- xF_3^{\mathrm{NC}}\right)$$

$$\frac{\mathrm{d}^2\sigma_{\mathrm{CC}}(e^\pm p)}{\mathrm{d}x\,\mathrm{d}Q^2} = \frac{\pi\alpha^2}{8\sin^4\theta_W}\,\frac{1}{\left(Q^2+M_W^2\right)^2}\times \left(Y_+F_2^{\mathrm{CC}\pm} \mp Y_- xF_3^{\mathrm{CC}\pm}\right)$$

$$Y_\pm = 1 \mp [1-y]^2$$

- $F_{2,3} = F_{2,3}(x,Q^2)$ = structure functions
- xF_3 terms violate parity.
- Representation of the DIS cross section in terms of structure functions does not require knowledge of partons.
- Approximation: longitudinal structure function $F_L \approx 0 \Rightarrow F_2 = 2xF_1$ (Callan–Cross relation, ony valid if partons carry spin 1/2).

The QPM Cross Section [3]

4

Structure functions and PDFs

Calculate $d\hat{\sigma}/dQ^2$ and insert in $(*)$
$\Rightarrow$ relation between structure fnct's and PDFs:

NC:

$$F_2^{\mathrm{NC}} = x \sum_{q=d,u,s,c,b} A_q(Q^2)\ [q+\bar{q}]$$

$$xF_3^{\mathrm{NC}} = x \sum_{q=d,u,s,c,b} B_q(Q^2)\ [q-\bar{q}]$$

$$A_q(Q^2) = Q_q^2 - 2Q_q v_e v_q\, P_Z + (v_e^2+a_e^2)(v_q^2+a_q^2)\, P_Z^2$$

$$B_q(Q^2) = -2Q_q a_e a_q\, P_Z + 4 v_e a_e v_q a_q\, P_Z^2$$

$$P_Z = \frac{Q^2}{Q^2+M_Z^2}$$

- t quarks do not contribute to NC reactions at HERA ($2m_t \approx 350\,\mathrm{GeV} > \sqrt{s}$)
- Phase space suppression of c and b quarks in final state is negligible
- Mass effects of c and b quarks in initial state are absorbed in PDFs

CC:

$$F_2^{\mathrm{CC}+}, xF_3^{\mathrm{CC}+} = \sum_{q=d,s} xq \pm \sum_{q=u,c} x\bar{q}$$

$$F_2^{\mathrm{CC}-}, xF_3^{\mathrm{CC}-} = \sum_{q=u,c} xq \pm \sum_{q=d,s} x\bar{q}$$

- b and t contributions are neglected (large m_t and small CKMM elements V_{i3})

Electroweak Radiative Corrections

Virtual corrections

example graphs:

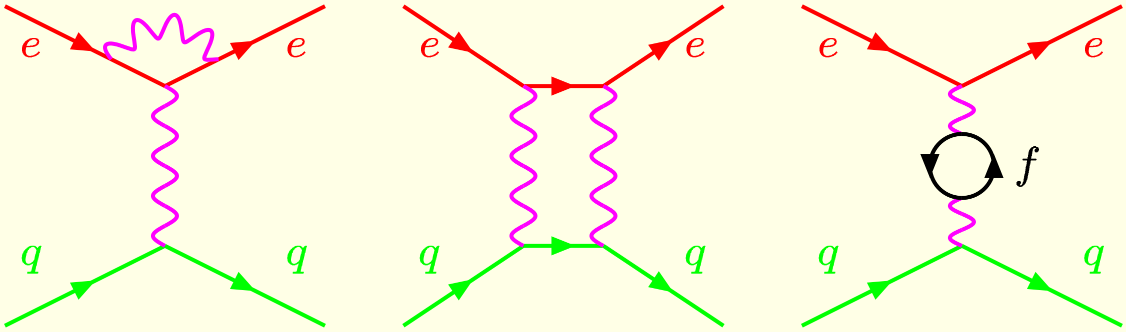

- All corrections at 1-loop level are known and included in MC simulation
- They induce Q^2 dependence of SM parameters (e.g. $\alpha = \alpha(Q^2)$)

Photon radiation

example graphs:

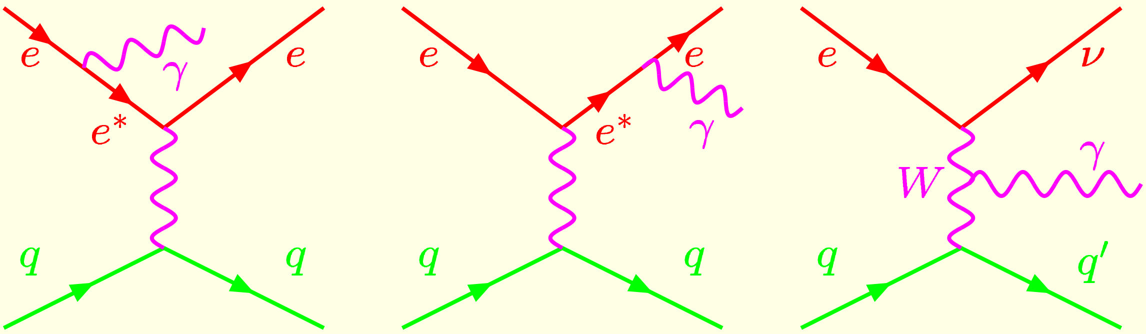

- Dominant: γ radiation from electron lines. Cross section has 3 poles:

$k \cdot k_\gamma \approx 0$	$\vec{k}_\gamma \parallel \vec{k}$, "initial state radiation" (ISR)
$k' \cdot k_\gamma \approx 0$	$\vec{k}_\gamma \parallel \vec{k}'$, "final state radiation" (FSR)
$(k - k' - k_\gamma)^2 \approx 0$	"QED Compton scattering"

- Large corrections: $\sim +50\%$ at $y_e > 0.8$, $x_e < 0.01$; $\sim -30\%$ at $y_e < 0.2$, $x_e > 0.5$
- Uncertainty is largest at high y (a few %)

QCD Corrections

Virtual corrections:

- Leading order:
  gluon loops at quark lines
- Taken into account by correction of α_s
- $\alpha_s \to \alpha_s(Q^2)$ (“running α_s”)

$$\alpha_s(M_Z^2) = 0.1184 \pm 0.0031$$

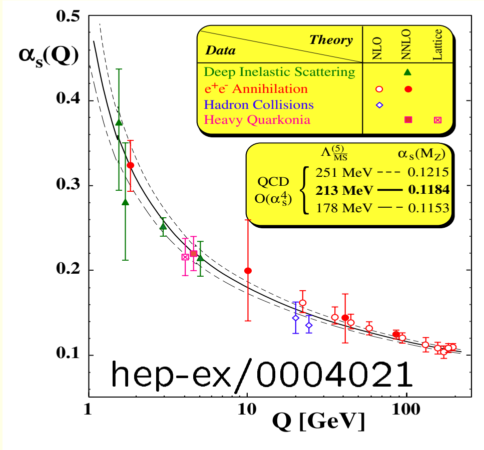

Processes of first order in α_s:

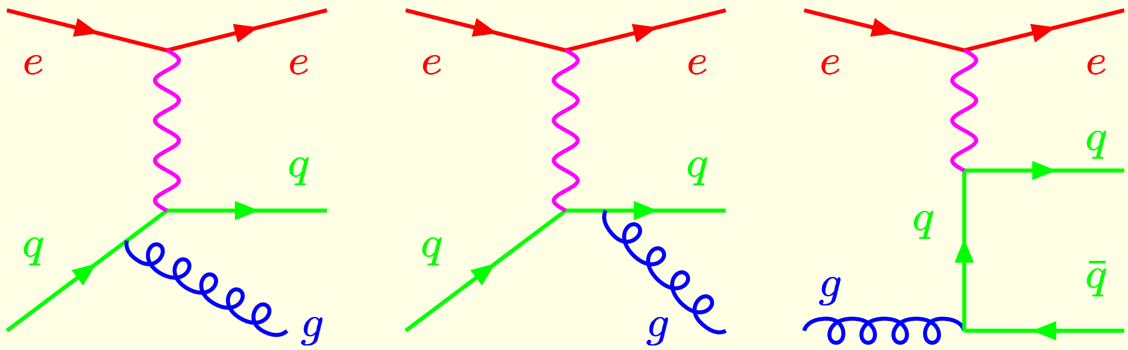

QPM:

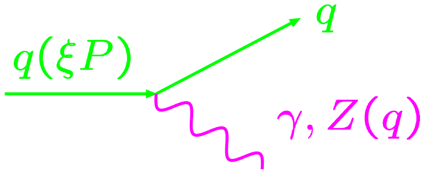

$$(\xi P + q)^2 = m_q^2 = 0$$

$$\xi = \frac{Q^2}{2P \cdot q} = x$$

(quark and proton masses neglected)

QCD:

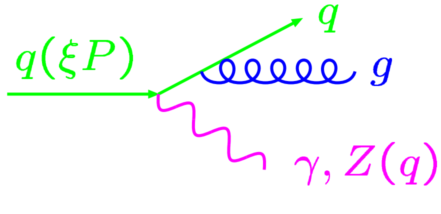

$$(\xi P + q)^2 = \mu^2 > 0$$

$$\xi = \frac{Q^2 + \mu^2}{2P \cdot q} > x$$

(multi-parton final state has non-zero invariant mass μ)

QCD Cross Sections

$$\sigma(x,Q^2) = \sum_q \int_x^1 \frac{d\xi}{\xi}\, q(\xi)\, \hat{\sigma}\left(\frac{\xi}{x},Q^2\right)$$

$$\hat{\sigma}(\frac{\xi}{x},Q^2) = \sigma_0 \Bigg\{ \delta(\frac{x}{\xi}-1) + \frac{\alpha_s}{2\pi}\left[P(\frac{\xi}{x})\ \ln\frac{Q^2}{m^2} + f(\frac{\xi}{x}) + \mathcal{O}\left(\frac{1}{Q^2}\right)\right]\Bigg\}$$

$\sigma_0\delta(z-1)$ → leading order;
→ reproduces QPM (LO).

$\frac{\alpha_s}{2\pi}P(\frac{\xi}{x})\ln\frac{Q^2}{m^2}$ → dominant $\mathcal{O}(\alpha_s)$ term;
→ has to be included to all orders since $\alpha_s \ln Q^2 = \mathcal{O}(1)$ (→ effective Q^2 dependence of PDFs, DGLAP equations, leading-log approximation).
→ $P(\xi/x) =$ QCD splitting function.
→ m^2 is infrared cutoff → factorization scale μ_f, terms of $\mathcal{O}(\ln \mu_f^2/m^2)$ are absorbed in PDFs.

$\frac{\alpha_s}{2\pi}f(\frac{\xi}{x})$ → yields corrections of the same order as the leading α_s^2 terms.

$\mathcal{O}(1/Q^2)$ → “higher twist”

The QCD Evolution Equations

DGLAP equations:

(Dokshitzer, Gribov, Lipatov, Altarelli, Parisi)

$$\frac{\mathrm{d}}{\mathrm{d}\ln Q^2}\begin{pmatrix} q^{\mathrm{S}} \\ q^{\mathrm{NS}} \\ g \end{pmatrix} = \frac{\alpha_s}{2\pi}\begin{pmatrix} P_{qq} & 0 & P_{qg} \\ 0 & P_{qq} & 0 \\ P_{gq} & 0 & P_{gg} \end{pmatrix} \otimes \begin{pmatrix} q^{\mathrm{S}} \\ q^{\mathrm{NS}} \\ g \end{pmatrix}$$

$$P_{ba} \otimes q(x,Q^2) \equiv \int_x^1 \frac{\mathrm{d}\xi}{\xi}\, q(\xi,Q^2)\, P_{ba}\left(\frac{x}{\xi}\right)$$

P_{ba} = QCD splitting function

$\propto |\mathrm{ME}|^2$ for $a(\xi) \to b(x)$

$$q^{\mathrm{S}}(x,Q^2) = \sum_q \left[q(x,Q^2) + \bar{q}(x,Q^2)\right]$$

= singlet PDF

$$q^{\mathrm{NS}}(x,Q^2) = q_i(x,Q^2) - \bar{q}_i(x,Q^2) \quad \text{or}$$

$$q_i(x,Q^2) - q_j(x,Q^2)\ (i \neq j)$$

= non-singlet PDF

(e.g. $d_v, u_v =$ valence quark PDFs)

Leading-log approximation (LLA)

- splitting functions in leading order α_s
- QPM formulae remain valid if the PDFs are solutions of the DGLAP equations

Next-to-leading-log approximation (NLLA)

- P_{ba} in next-to-leading order (α_s^2)
- additive corrections to structure functions (in particular $F_L \neq 0$)
- used in HERA analyses

Parton Distributions

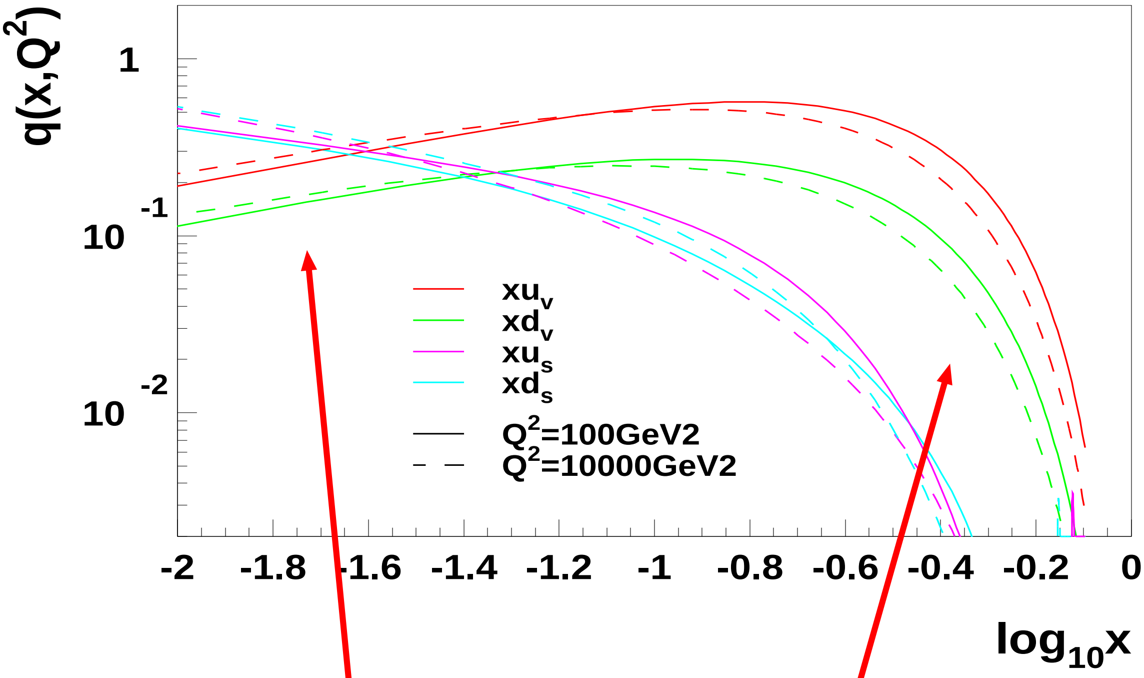

small x:
PDFs increase with Q^2

large x:
PDFs decrease with Q^2

Spatial resolution increases with growing Q^2:

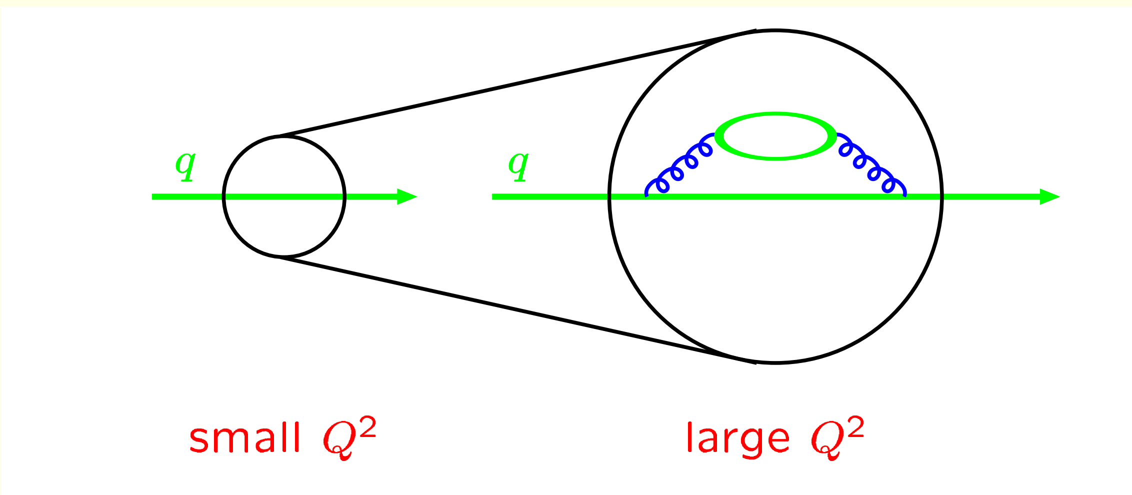

QCD Fits: Principle

Fit procedure:

- Parametrize PDFs at $Q^2 = Q_0^2$ as functions of x
- Perform QCD evolution using DGLAP equations (usually NLLA, special treatment of the heavy-quark PDFs (c, b, t))
- Calculate predictions for experimental observables (cross sections, structure functions, etc.)
- Determine PDF parameters from χ^2 fit to experimental data
- Problem: this procedure does not provide automatically the PDF uncertainties !

QCD fits performed by various theory groups: MRS(T), CTEQ, GRV

For $p = u_v, d_v, \sum_q (q + \bar{q}), g$ and also for $p = \bar{u} + \bar{d}, \bar{u} - \bar{d}, s$:

$$xp(x, Q_0^2) = A_p \, x^{a_p} \, (1 - x)^{b_p} \, P(x; c_p, \dots)$$

- x^{a_p}: characterizes PDFs at $x = 0$ (sea: $a_p < 0$, pole; valence: $a_p > 0$)
- $(1-x)^{b_p}$: characterizes PDFs at $x = 1$ ($b_p > 0$ for all PDFs)
- $P(x; c_p, \dots)$: weakly x-dependent function ("fine tuning")

QCD Fits: Data

1

NC and CC DIS data

- Fixed target experiments: measurements of structure functions (different target nuclei)
  NC: BCDMS, NMC, E665, SLAC,. . .
  CC: CCFR, CDHS(W), CHARM, BEBC, . . .
- Structure functions and cross sections from ZEUS and H1

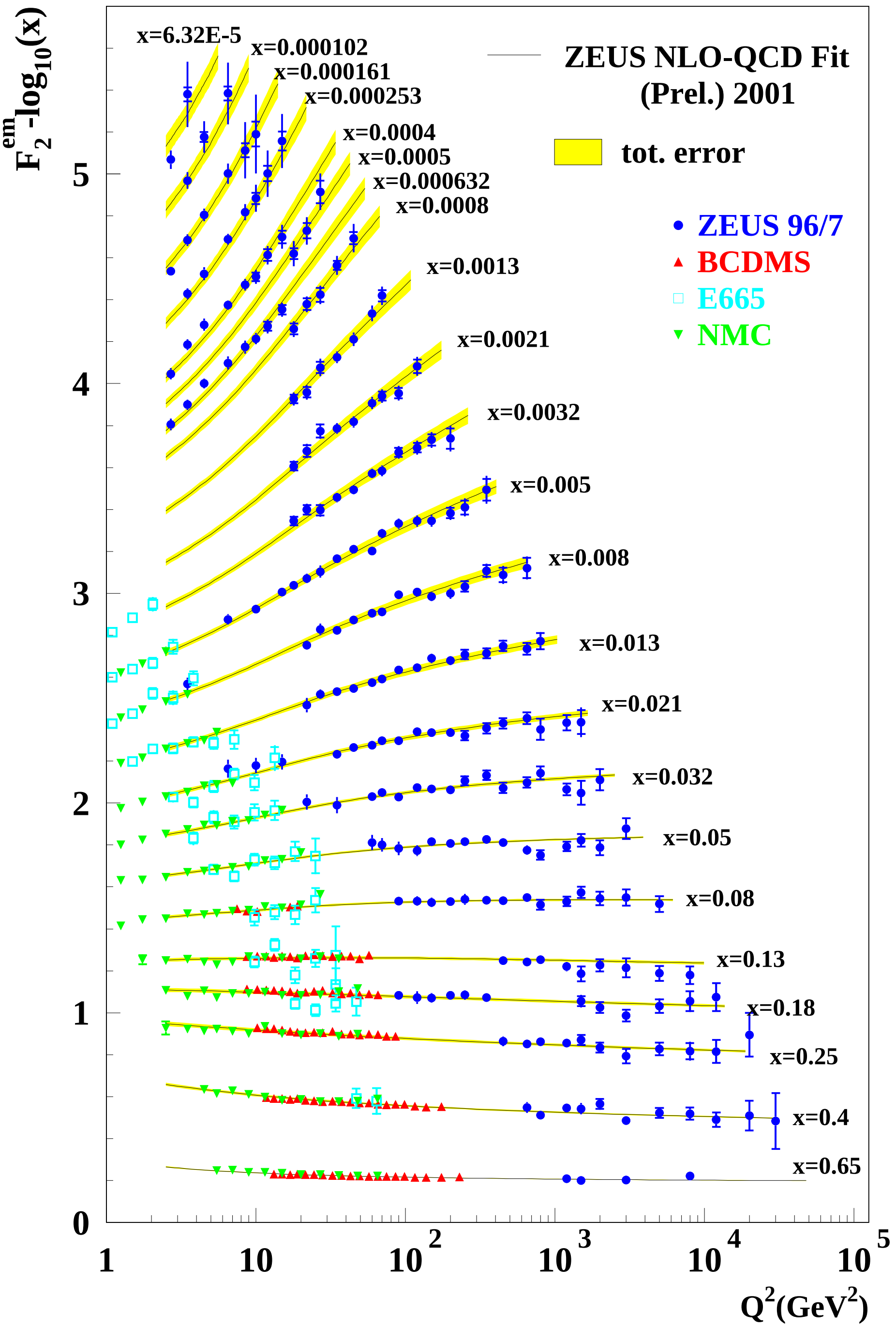

ZEUS data from 1996/97

shown fit does not use H1 data

QCD Fits: Data [2]

2

Sum rules

number of valence quarks:

$$\int_0^1 \mathrm{d}x\, u_v(x, Q_0^2) = 2 \qquad \int_0^1 \mathrm{d}x\, d_v(x, Q_0^2) = 1$$

momentum sum rule:

$$\int_0^1 \mathrm{d}x\, x \left\{ g(x, Q_0^2) + \sum_q \left[q(x, Q_0^2) + \bar{q}(x, Q_0^2) \right] \right\} = 1$$

Gottfried sum rule:

$$I_G = \int_0^1 \mathrm{d}x\, \left(\mathcal{F}_2^{\ell p} - \mathcal{F}_2^{\ell n} \right) = \frac{1}{3} + \frac{2}{3} \int_0^1 \mathrm{d}x\, (\bar{u} - \bar{d})$$

Experiment (NMC): $I_G = 0.235 \pm 0.026 \Rightarrow \bar{d} > \bar{u}$

3

Other experimental data:

reaction	subprocess	information
$p\bar{p} \to W + X$	$q\bar{q} \to W$	$u, d, u/d$
'$\bar{\nu}$'$N \to \mu^+\mu^- + X$	$\nu s \to \mu c$	s
$pp, pN \to \ell^+\ell^- + X$	$q\bar{q} \to \ell^+\ell^-$	$\bar{d}/\bar{u}$
$hh \to \gamma + X$	$qg \to q\gamma$	g
$p\bar{p} \to \text{jets} + X$	$gg \to gg$ $qg \to qg$ $qq \to qq$	$g, (q)$

The ZEUS QCD Fit

Characteristics:

By:	M. Botje, NIKHEF (DESY-99-038)
Data:	HERA: ZEUS and H1, "old" data fixed target NC: SLAC, BCDMS NMC, E665 fixed target CC: CCFR $pp, pN \to \mu^+\mu^- + X$: E866
Fit quality:	χ^2/n.d.o.f. = 1537/1557
Features:	propagation of experimental uncertainties of the input data; numerous systematic studies

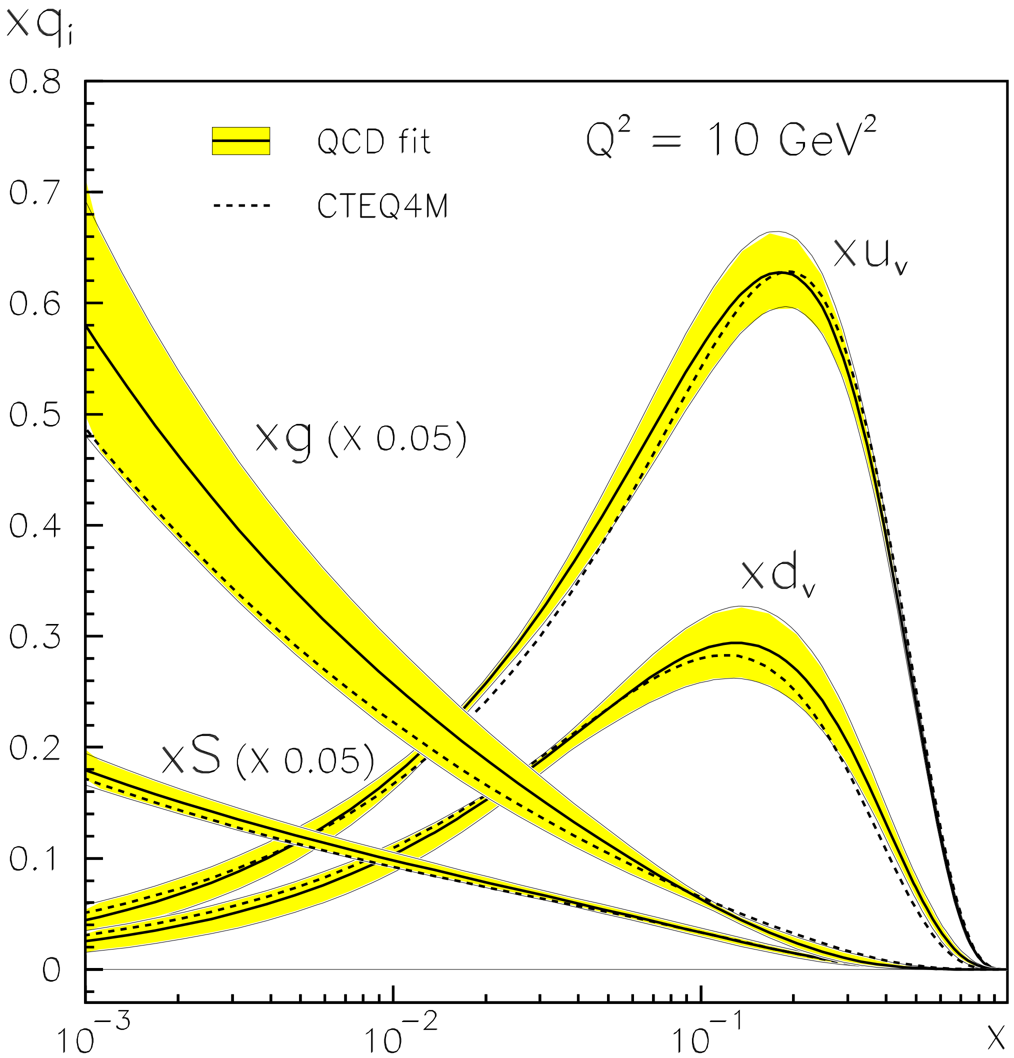

Accuracy of Cross Section Prediction

Contributions to PDF uncertainty:

- Dominant effect: statistical and systematic uncertainties of experimental data
- Further contributions from $\delta\alpha_s$, assumptions on s and the charm mass, nuclear effects
- "Total uncertainties" from ZEUS QCD fit:

$$\tilde{\sigma} = (\text{kin. factor}) \times \mathrm{d}^2\sigma/\mathrm{d}x\mathrm{d}Q^2$$

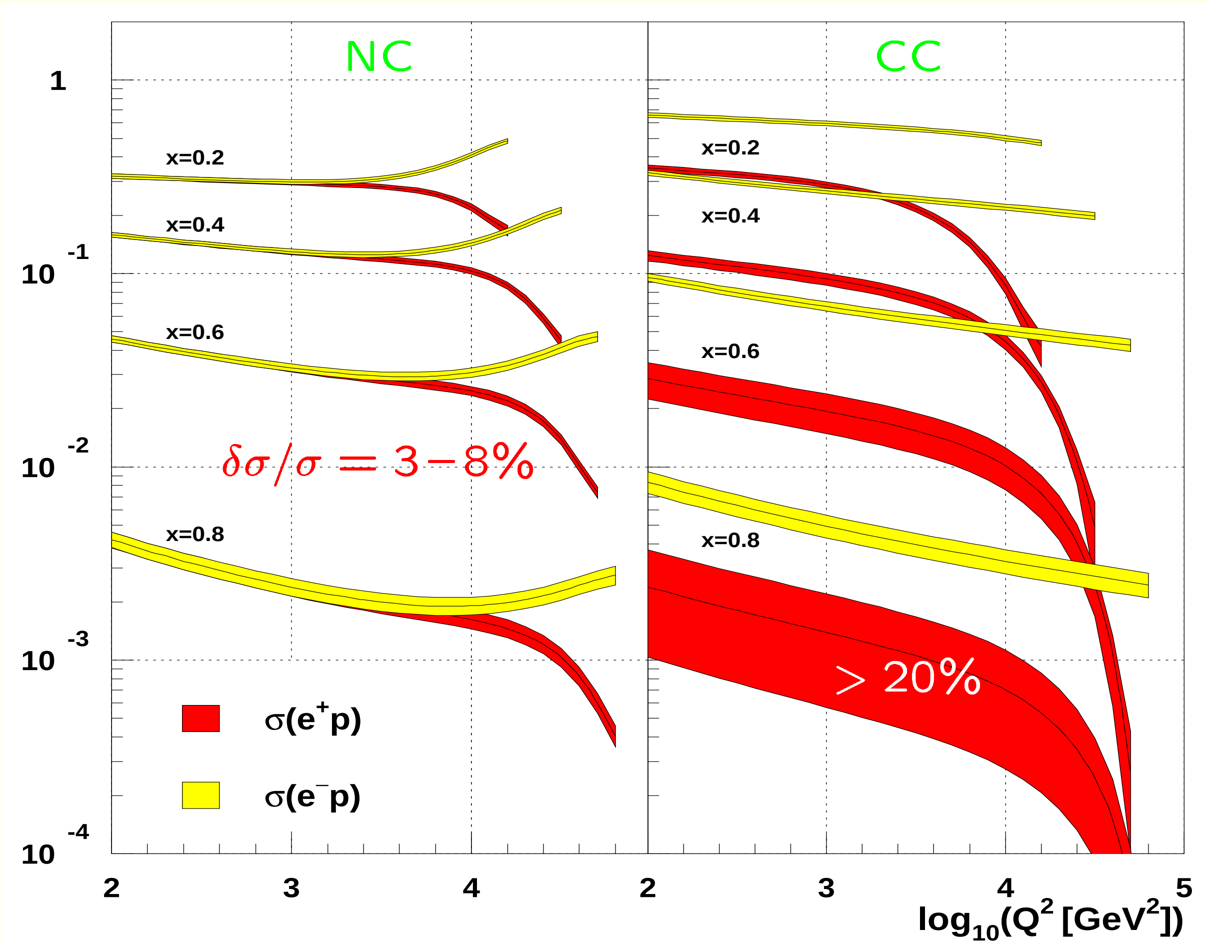

- Small (negligible) effects:
  - choice of the QCD scales μ_r and μ_f;
  - higher-twist terms $\propto 1/Q^2$;
  - errors on electroweak parameters;

Parton Distributions at High x

Experimental information on PDFs at $x \gtrsim 0.5$:

- CC DIS, '$\bar{\nu}$'p: fixes u and d separately;
  note: large exp. uncertainties
- NC DIS, proton target: fixes $4u + d$;
  NC DIS, nuclei: fixes $u + d$
  (assumption: $u^{(n)} = d^{(p)}$ and vice versa);
  note: nuclear effects large at high x
- NC DIS, $F_2^{(p)}/F_2^{(n)}$
  (comparison of proton and deuteron data):

$$R_F = \frac{\mathcal{F}_2^{(n)}}{\mathcal{F}_2^{(p)}} \xrightarrow{x\to 1} \frac{4d_v/u_v + 1}{4 + d_v/u_v}$$

precise measurements exist (NMC);
"classical" interpretation (in all standard PDFs):
data compatible with

$$R_F \to 0.25, \text{ i.e. } d_v/u_v \to 0 \text{ for } x \to 1;$$

Problem: including Fermi motion
and binding effects is non-trivial.

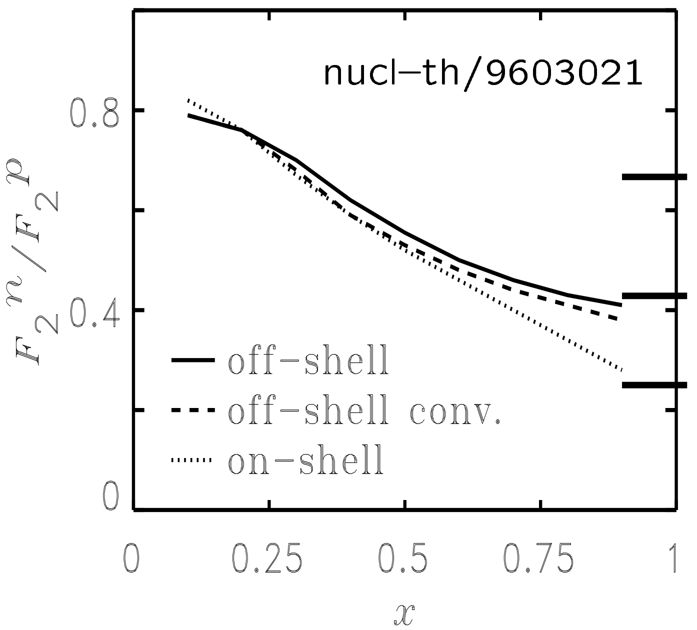

new analysis:

at large x, R_F may be larger that assumed
$\Rightarrow$
$d/u > 0$ at $x \to 1$
$\Rightarrow$
d and $\sigma_{CC}(e^+p)$ would increase by $\mathcal{O}(50\%)$ at $x = 0.5$

DIS Analyses at High Q^2

Overview:

- The crucial detector components
  - Calorimeter
  - Tracking chambers
  - Luminosity measurement
  - Trigger
- Monte Carlo simulation
- Analysis methods
  - Electron identification
  - Kinematic reconstruction
  - Energy calibration
  - Corrections
- Cross section measurement
  - Event selection
  - Some distributions
  - Determination of cross sections

The ZEUS Calorimeter

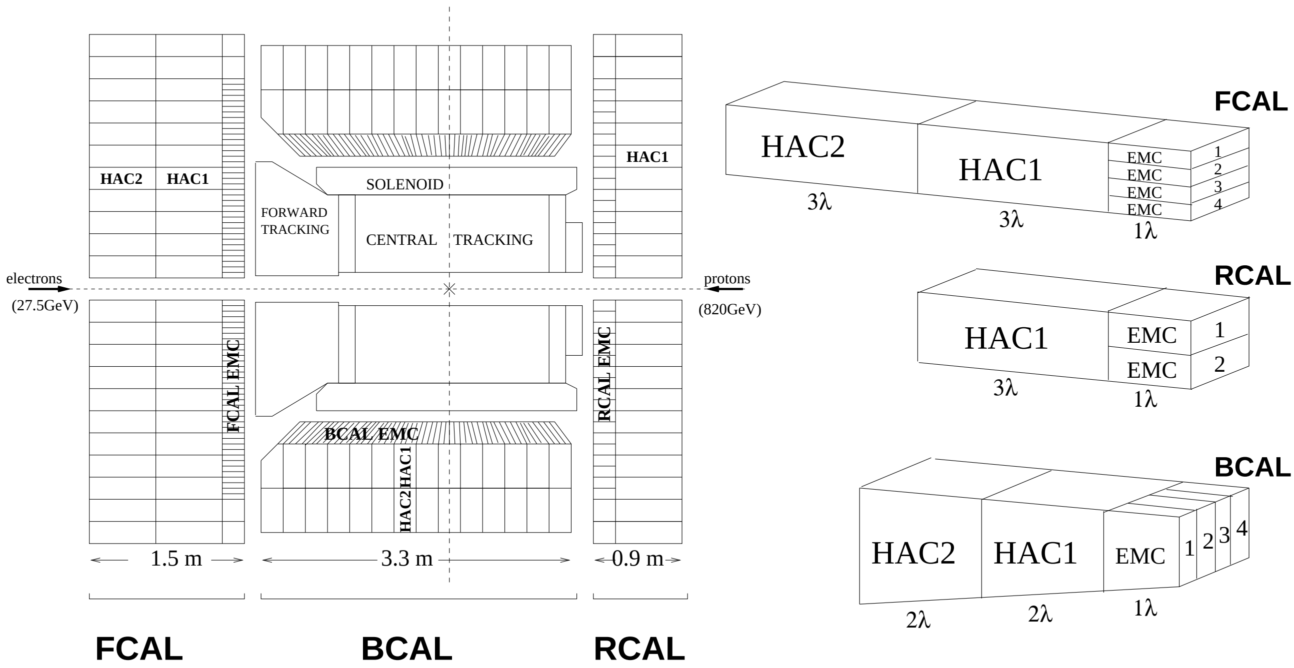

Design:

- Sampling calorimeter
  Absorber: depleted uranium (layers of 3.3 mm)
  Active: scintillator
- Segmentation:
  "towers" of about $20 \times 20\,\mathrm{cm}^2$, 2/3-fold longitudinal division (5918 cells)
- Readout: via wave-length shifting light guides to 2 PMs/cell
- Acceptance:
  99.8% of 4π
- No B-field

Parameters:

- Energy resolution:
  elm.: $\Delta E/E = 18\%/\sqrt{E}$
  had.: $\Delta E/E = 35\%/\sqrt{E}$
  (test beam conditions)
- Time measurement:
  $\Delta t/t \lesssim 1$ ns for energy deposits $\gtrsim 5$ GeV
- Compensation:
  $e/h = 1 \pm 0.01$ ($p > 5$ GeV)
- Measurement of θ_e:
  $\Delta\theta \approx 3$ mrad

The H1 Calorimeter

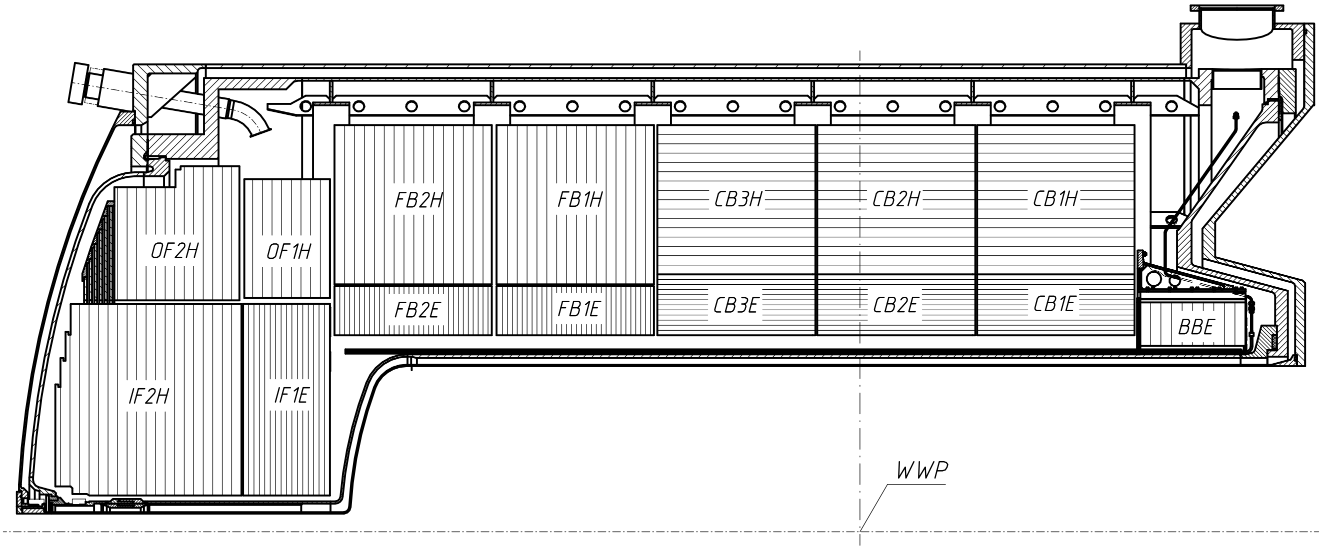

Design:

- Liquid-argon calorimeter
  Absorber:
  lead (electrom. part)
  steel (had. part)
- Segmentation:
  readout cells of ca. $50-2000\,\text{cm}^2$, (4-6)-fold longitudinal division (44352 cells)
- Readout:
  Ionisation charge in Ar produces signal at HV electrodes
- Acceptance:
  $4^\circ \lesssim \theta \lesssim 154^\circ$;
  complementing calorimeters:
  SPACAL (rear),
  FPLUG (forward)
- $B = 1.15\,\text{T}$

Parameters:

- Energy resolution:
  elm.: $\Delta E/E = 12\%/\sqrt{E}$
  had.: $\Delta E/E = 50\%/\sqrt{E}$
  (test beam conditions)
- Time measurement:
  $\Delta t/t = \mathcal{O}(100\,\text{ns})$
- No compensation:
  $e/h \approx 1.3$
- Measurement of θ_e:
  $\Delta\theta \approx 3\,\text{mrad}$

ZEUS: Central Drift Chamber

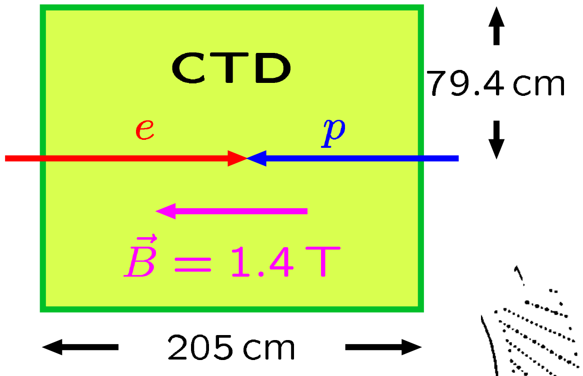

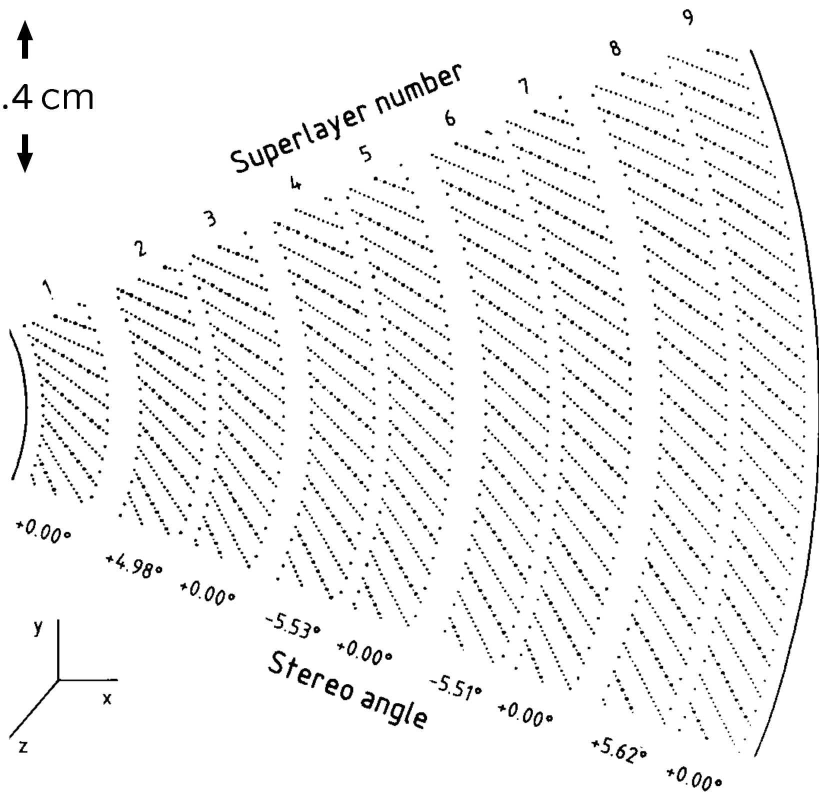

Design:

- Drift chamber with 9 "superlayers" (SL) with 8 layers of signal wires each. 4 SLs are "stereo layers"
- Lorentz angle $\approx 45°$
- Acceptance: $15° \lesssim \theta \lesssim 164°$ (≥ 2 SLs)
- Resolution: ca. 200 µm in $(r\phi)$, ca. 1 mm in Z (stereo layers)

Track reconstruction:

- Momentum resolution: $\Delta p_t/p_t = 0.0058\, p_t \oplus 0.0065 \oplus 0.0014/p_t$ (for tracks in 9 SLs, p_t in GeV)
- Ionisation ($\mathrm{d}E/\mathrm{d}x$): accuracy $\sim 8\%$
- Time measurement: not used
- Comparison to CAL: $\Delta E/E \approx \Delta p_t/p_t$ for central e with 10 GeV

H1: Tracking Chambers

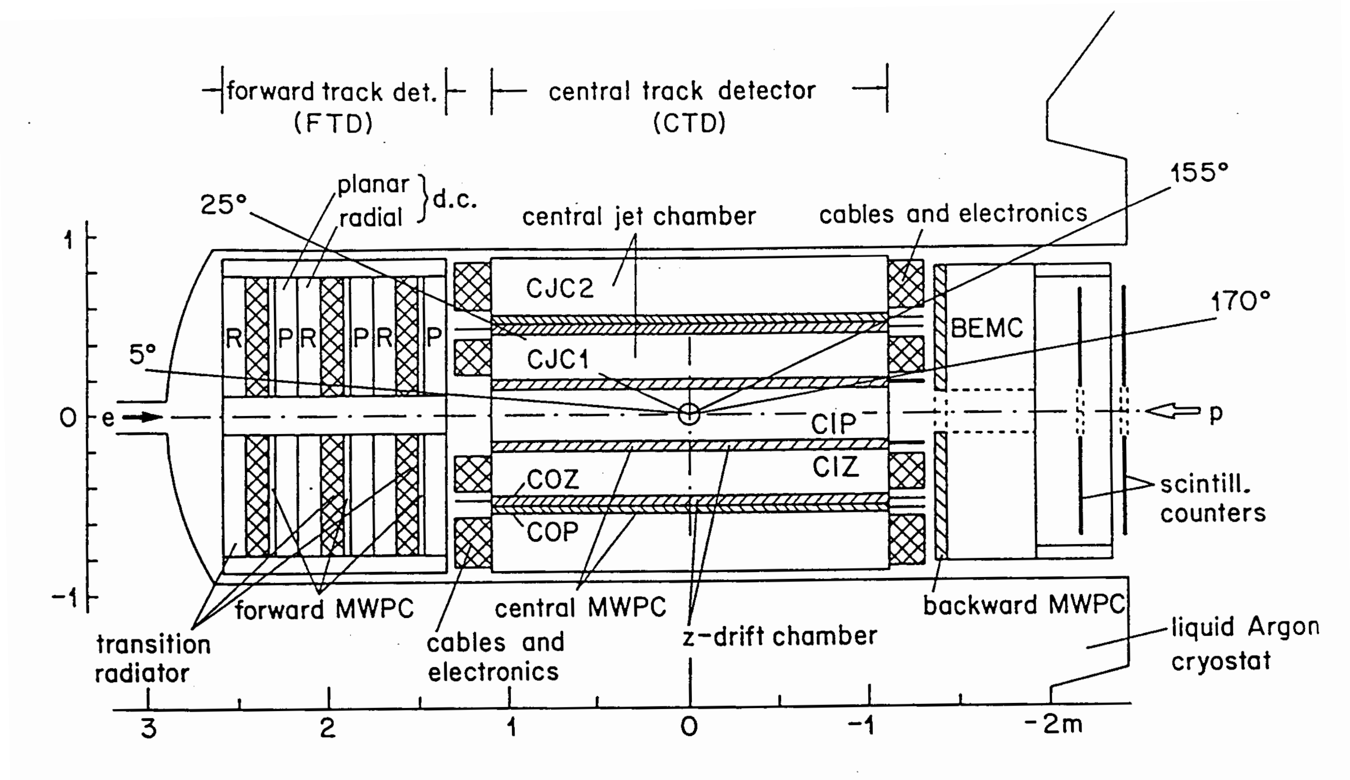

Design:

- Central part (CTD):
  jet chambers
  (56 layers of signal wires in beam direction)
  drift chambers
  (azimuthal wires for Z measurement)
  proportional chambers
  (for trigger)
- Forward part (FTD):
  (drift chambers, MWPCs, radiators for transition radiation)
- Acceptance:
  $25^\circ \lesssim \theta \lesssim 155^\circ$ (CTD)
  $5^\circ \lesssim \theta \lesssim 25^\circ$ (FTD)
- Resolution:
  ca. 200 µm $\perp$ wires,
  ca. 3 – 4 cm $\parallel$ wires

Track reconstruction:

- Momentum resolution:
  CTD: $\Delta p_t/p_t = 0.009\, p_t(\text{GeV}) \oplus 0.015$
  FTD: $\Delta p_t/p_t = \mathcal{O}(10\%)$
  for $p_t = 1$ GeV
- Ionisation ($\mathrm{d}E/\mathrm{d}x$):
  accuracy $\sim 7\%$
- Time measurement:
  $\Delta t \approx 1.6$ ns (trigger)
- Comparison to LAr:
  $\Delta E/E \approx \Delta p_t/p_t$
  for central e with 6 GeV

Luminosity Measurement

Measurement principle:

Reaction:	$ep \to ep\gamma$ (Bethe–Heitler process); cross section known to about 0.5%
Detection :	dedicated external calorimeters to detect e and/or γ ZEUS: lead–scintillator calorimeter H1: fully absorbing Čerenkov crystal hodoscopes

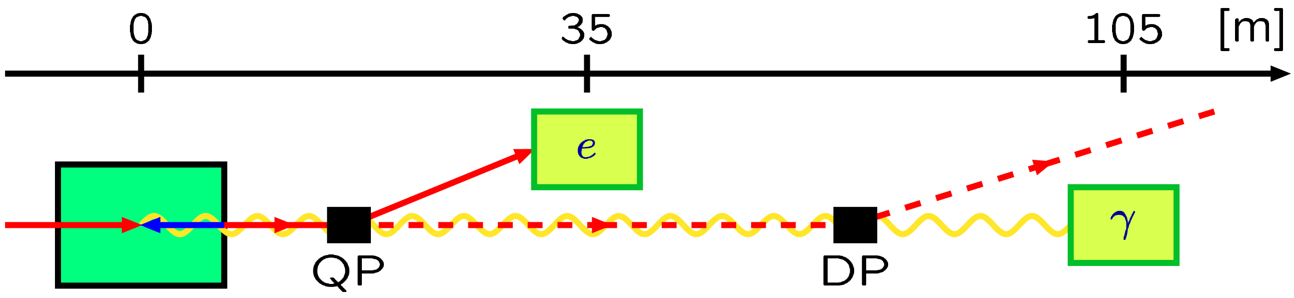

Systematic Uncertainties:

Acceptance:	requires precise knowledge of beam position, beam line geometry and detector response
Background:	bremsstrahlung, synchrotron radiation; subtraction using unpaired bunches
Pile-Up:	multiple γ/e from one bunch crossing, currently negligible
Satellites:	beam fragments outside bunches, contribute to luminosity signal but not (not fully) to ep data
Overall Uncertainty:	ZEUS: $\Delta\mathcal{L}/\mathcal{L} = 1.6\%$ (γ only) H1: $\Delta\mathcal{L}/\mathcal{L} = 1.5\%$ (e and γ)

Trigger

Typical rates:	bunch collisions	10.4 MHz
	detector signals	$\mathcal{O}$(100 kHz)
	ep reactions	$\mathcal{O}$(200 Hz)
	NC DIS, $Q^2 > 1000\,\text{GeV}^2$	$\approx$ 0.03 Hz
	CC DIS, $Q^2 > 1000\,\text{GeV}^2$	$\approx$ 0.0003 Hz
	data recording	max. 10 Hz
Tasks:	$\Rightarrow$ background reduction	
	$\Rightarrow$ selection of particular ep reaction types	

$\mathcal{O}$(100 kHz)

ZEUS: FLT
H1: Level-1 (CL1)

hardware logic

data storage in pipelines
for 4.4/2.5 μs (ZEUS/H1)
data: energy sums,
track candidates,. . .

$<$ 1 kHz

ZEUS: SLT
H1: Level-2+3

transputers and hardware logic

more precise calculations
H1: hardware-based neural-net
data: more detail, e.g.
time information

$<$ 100 Hz

ZEUS: TLT
H1: Level-4

workstation cluster

simplified offline software
data: reconstructed objects
(electron identification,
tracks, jets, etc.)

5 − 8 Hz

Monte Carlo Simulation

Event generators

- Leptons and partons from "hard subprocess":
  - corresponding to known or hypothesized cross sections
  - DIS radiative corrections included: γ radiation, electroweak 1-loop diagrams (DJANGO/HERACLES)
- Parton cascade:
  - color dipole model (ARIADNE)
  - LEPTO/MEPS as systematic check
- Hadronisation:
  - Lund string model (JETSET)

↓

Detector simulation

- Interaction of reaction products with detector
  - simulated by GEANT
  - takes into account shower development, ionisation, decays etc. (partly parametric)
  - not simulated by GEANT: signal production in active volumes, electonics, etc.
  - full simulation requires precise knowledge of detector geometry and response
- Trigger simulation

↓

Reconstruction

- ... as for experimental data

Electron Identification

Task:
identification of the scattered electron in NC DIS events

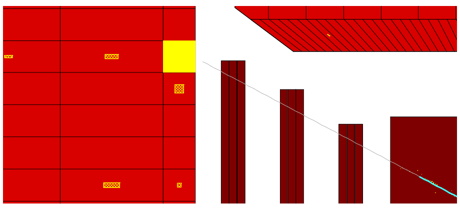

Signal:
- energy concentrated in electromagnetic calorimeter
- narrow shower
- matching track
- isolated

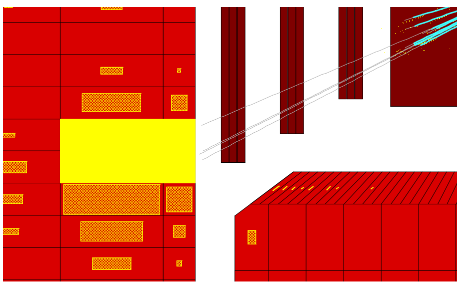

Background:
- jets:
  hadronic energy,
  extended showers,
  several tracks
- photons:
  like e, but no track

Implementation:

Variables:	clustering of calorimeter cells; hadr. energy fraction, shower topology, track/calorimeter matching (E/p, angle), isolation
Algorithms:	cuts, software-based neural nets
Problems:	e with low energy, candidates beyond tracking acceptance
Result:	efficiency and remaining background depend on E' range
	high Q^2: efficiency $\gtrsim$ 90 − 95%, almost background-free

Kinematic Reconstruction (NC)

4 independent quantities to determine
2 independent variables:

$$\begin{aligned} E' &= \text{energy of scattered electron} \\ \theta_e &= \text{angle of scattered electron} \\ (P_t)_{\text{had}} &= \text{hadronic transverse momentum} \\ \cos\gamma_{\text{had}} &= \frac{(P_t)^2_{\text{had}} - (E-P_z)^2_{\text{had}}}{(P_t)^2_{\text{had}} + (E-P_z)^2_{\text{had}}} \\ &= \cos(\text{hadronic angle}) \end{aligned}$$

$(P_t)_{\text{had}}$ and $(E-P_z)_{\text{had}}$ are calculated from vertex position and vectorial sums over all calorimeter clusters not belonging to electron.

$\Rightarrow$ several reconstruction algorithms !

1. Use both angles: θ_e and γ_{had}
   (double-angle method, DA)

   + independent of calorimeter energy scale
   − susceptible to radiative effects (ISR = γ radiation from incoming e)
   • used by ZEUS

2. Use angle and energies: θ_e, E', $\Sigma = (E-p_Z)_{\text{had}}$
   ($e\Sigma$ method)

   + stable in entire kinematic region
   − sensitive to calorimeter energy scale
   • used by H1

Kinem. Reconstruction (NC) [2]

Resolutions:

- ZEUS, $Q^2 \gtrsim 400$ GeV^2:
  $\Delta Q^2_{DA}/Q^2_{DA} \approx$ 5%
  $\Delta y_{DA}/y_{DA} \approx$ 5%
  $\Delta x_{DA}/x_{DA} \approx$ 9 − 12%
- H1: similar values, depend on uncertainty of calorimeter energy scale

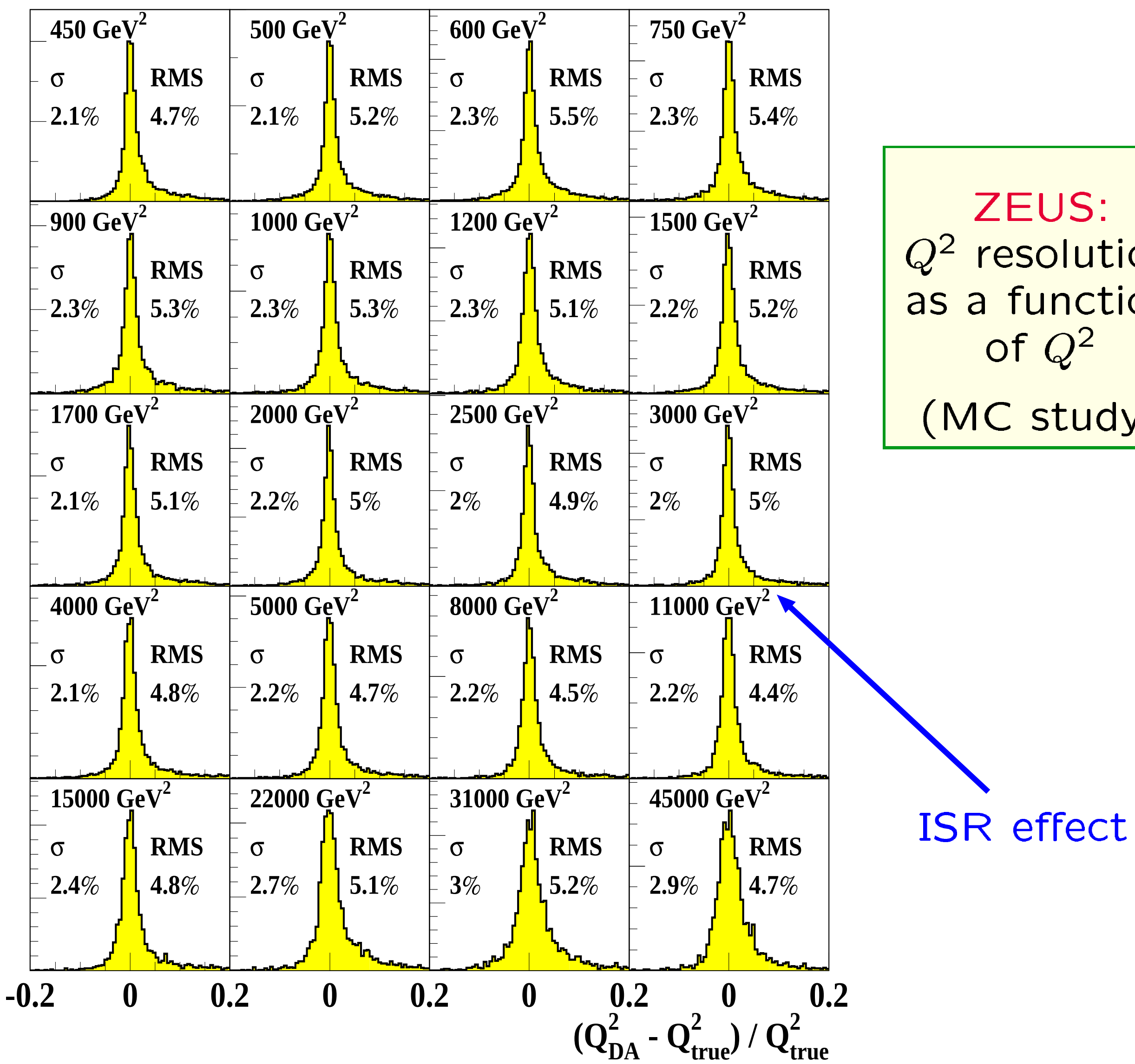

ZEUS:
Q^2 resolution as a function of Q^2

(MC study)

Kinematic Reconstruction (CC)

We only have the hadronic quantities
$(P_t)_{\text{had}}$ and $(E - P_z)_{\text{had}}$

3

Jacquet–Blondel method (JB)

$$y_{\text{JB}} = \frac{(E - P_z)_{\text{had}}}{2E_e}$$

$$Q^2_{\text{JB}} = \frac{(P_t)^2_{\text{had}}}{1 - y_{\text{JB}}}$$

$$x_{\text{JB}} = \frac{Q^2_{\text{JB}}}{y_{\text{JB}}\, s}$$

– sensitive to calorimeter energy scale
– instable at small y ($E - P_z$ small) and at large y (denominator of Q^2_{JB})
– sensitive to ISR
+ only possibility for CC analyses

Resolutions:

- ZEUS, $P_t > 50$ GeV and $y < 0.9$:

$$\Delta Q^2_{\text{JB}}/Q^2_{\text{JB}} \approx 8-20\% \oplus \frac{\delta_{\text{sca}} E_{\text{had}}}{1-y}$$

$$\Delta y_{\text{JB}}/y_{\text{JB}} \approx 8-11\% \oplus \delta_{\text{sca}} E_{\text{had}}$$

$$\Delta x_{\text{JB}}/x_{\text{JB}} \approx 20\% \oplus \delta_{\text{sca}} E_{\text{had}} \frac{2-y}{1-y}$$

($\delta_{\text{sca}} E_{\text{had}}$ = relative uncertainty of hadronic energy scale)

- H1: similar values

Correction of Detector Effects

Dominant effects:

- Absorption and secondary interactions in inactive material
- Distortion of energy flow by back-scattering (albedo) and shower development
- Calorimeter inhomogeneities
- . . .

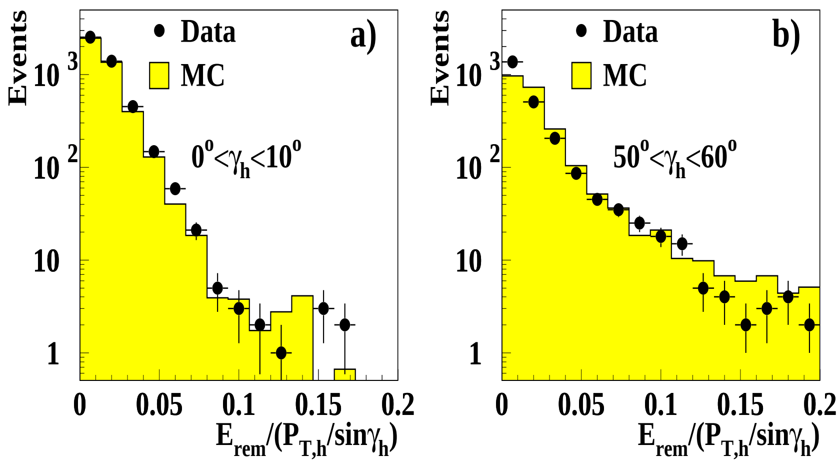

Example (ZEUS)

fraction of calorimeter energy identified as albedo and neglected

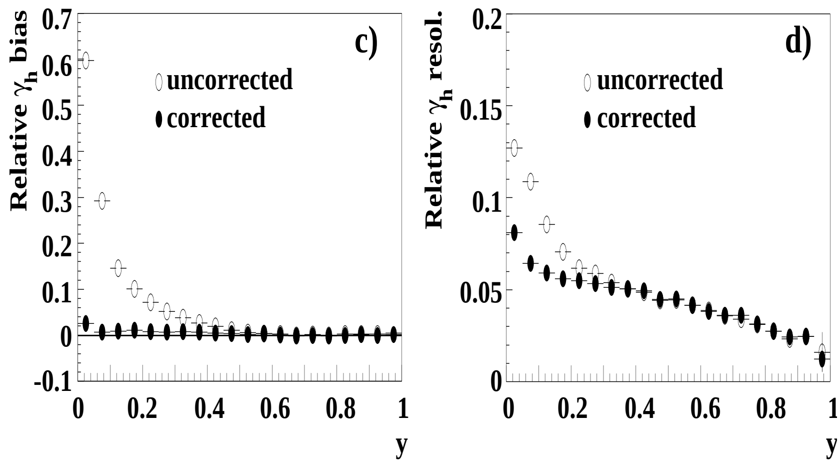

Example (ZEUS)

left:
rel. systematic offset of γ_{had}

right:
resolution of y

before/after clustering and albedo correction

Energy Calibration

Calibration methods:

- Test beam measurements
- Online:
  charge injection, uranium noise (ZEUS)
  $\Rightarrow$ time stability, homogeneity
- With ep data:
  elm.: track/calorimeter comparisons
  comparison of E' measured in calorimeter and calculated by DA method
  had.: P_t balance in NC events
  track/calorimeter comparisons (isolated hadrons)

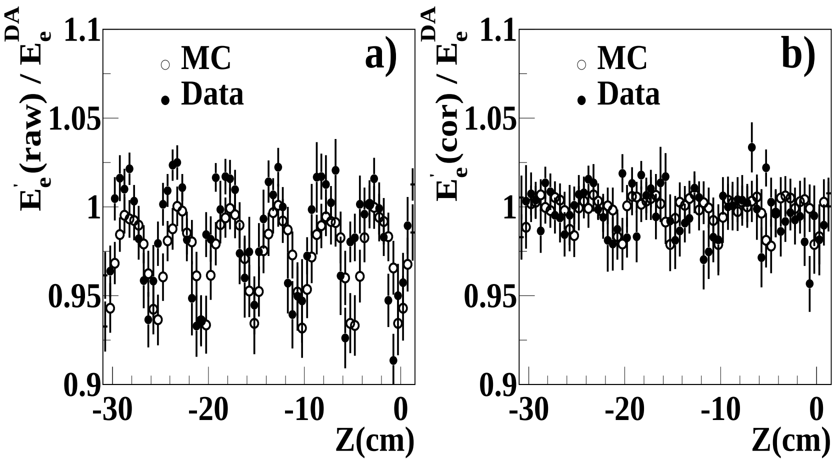

ZEUS:
$\langle E(\mathrm{CAL})/E_{\mathrm{DA}} \rangle$ as a function of the Z position before/after corrections

$\delta_{\mathrm{sca}} E_e < 2\%$

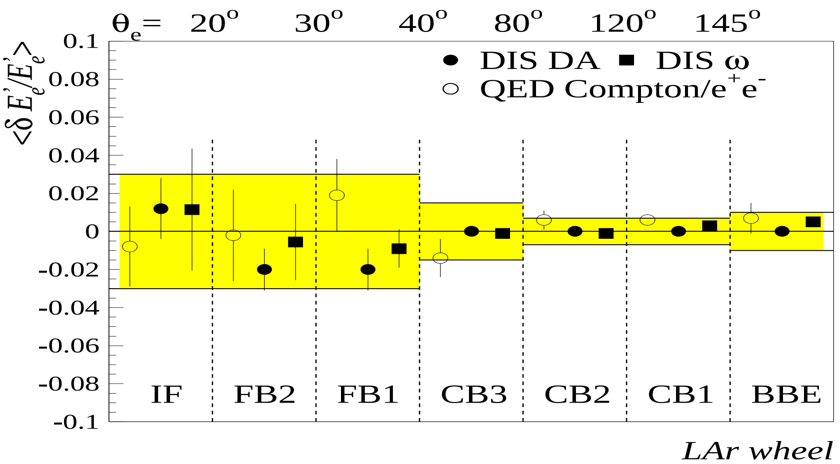

H1:
$\langle \delta E_e / E_e \rangle$ as a function of θ_e after all corrections

$\delta_{\mathrm{sca}} E_e = 0.7 - 3\%$

Backgrounds

Non-ep background

- Origin:
  - beam–gas and beam–beampipe interactions
  - cosmic particles and showers
  - halo muons
  - detector effects (spontaneous discharges etc.)
- Properties:
  - type and rate depend on beam conditions
  - not contained in MC simulation

ep background

- Photoproduction ($ep \to e$+jets):
  - reactions with two or more jets, scattered e in rear beampipe

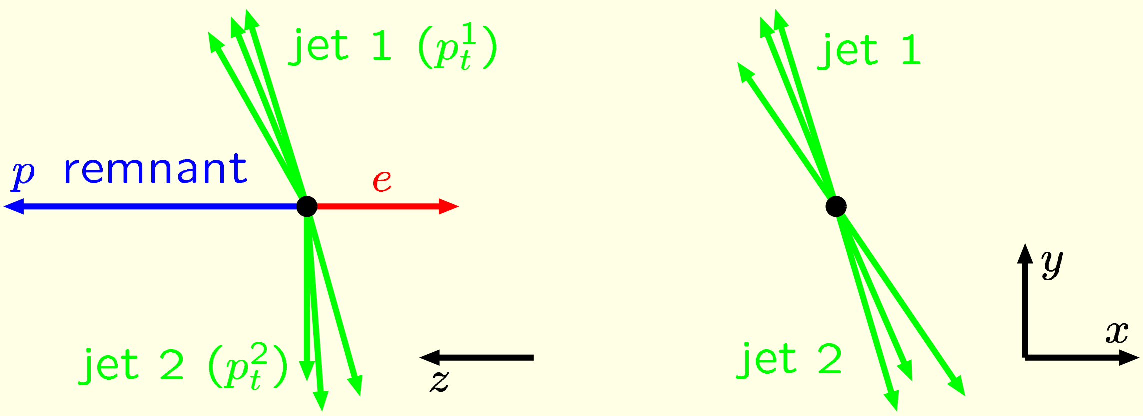

  - Danger: misidentification of jet as e ($\to$ NC) or energy mismeasurement ($P_t \approx |p_t^2 - p_t^1| \to$ CC)
- Prompt photons ($ep \to e\gamma$+jets):
  - γ can fake an e (beyond tracking acceptance, conversion)
- Lepton pair production ($ep \to e\ell^+\ell^- X$)
- W production ($ep \to eW X$)

Event Selection

NC selection:

- cuts against non-ep backgrounds
  (timing, event topology, muon identification)
- reconstructed event vertex (tracking)
  further reduces non-ep background
  provides proper kinematic reconstruction
- scattered electron
  identified, energy above threshold ($\mathcal{O}(10\,\text{GeV})$)
- longitudinal containment:

Fully detected reaction:

$$\delta = E - P_z = E'(1 - \cos\theta_e) + (E - P_z)_{\text{had}}$$
$$\stackrel{!}{=} 2E_e = 55\,\text{GeV}\ .$$

proton remnant: small contribution to δ
cut $\delta > (E - P_z)_{\text{min}}$ reduces:
– photoproduction background
– events with hard ISR

CC selection:

- cuts against non-ep backgrounds
- reconstructed event vertex
  very effective against non-ep background
  ZEUS also uses vertex estimate from CAL timing
- missing P_t
  above threshold (typically 12 GeV)
- topology cuts
  exclude e.g. events with two back-to-back jets
- visual inspection

A Background Event

Overlay of PHP event and cosmic muon produces CC candidate

photoproduction event (small E_t)

yields vertex

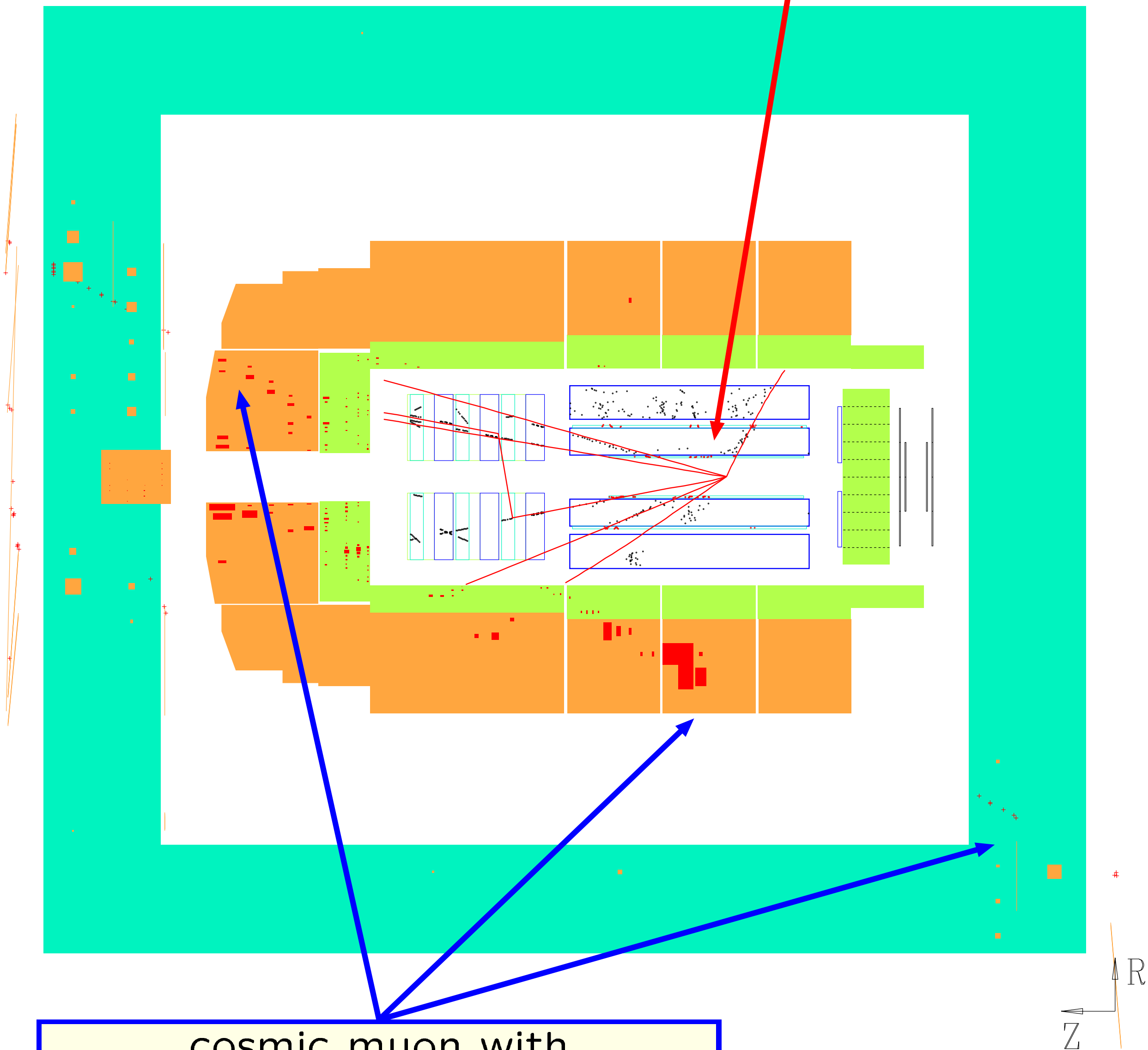

cosmic muon with associated calorimeter shower

yields P_t

Characteristic Distributions (NC)

Distributions of some NC event variables (ZEUS)
full dots: data; histograms: MC simulation

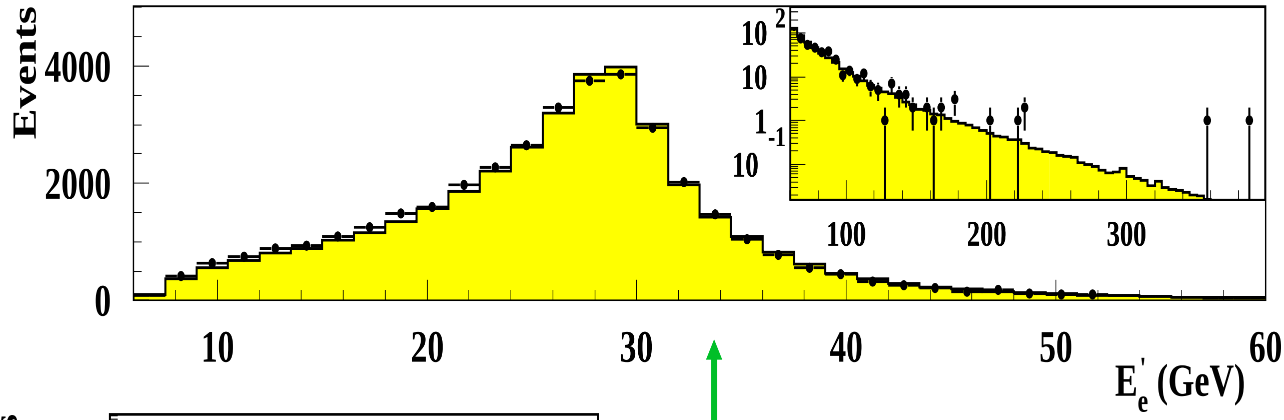

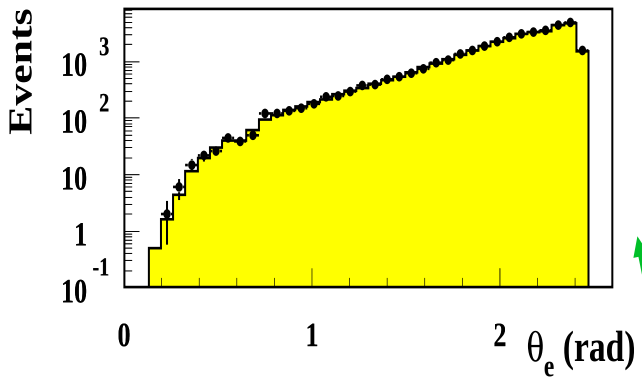

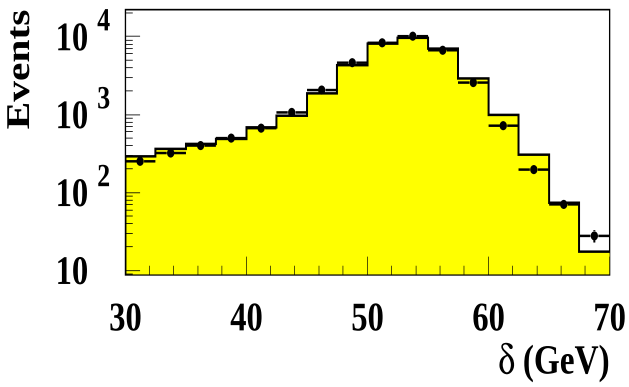

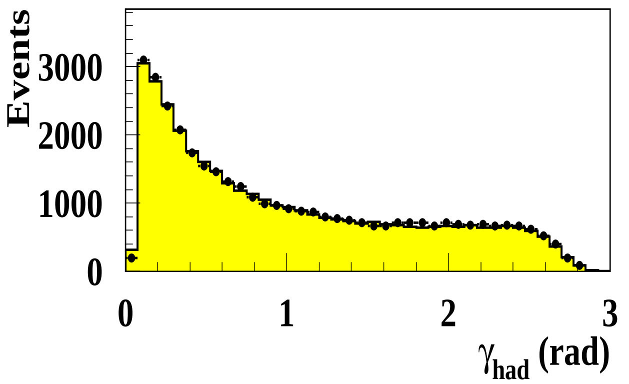

ZEUS

NC distributions

$E' =$
energy of the scattered e

$\theta_e =$
e scattering angle

$\delta = E - P_z$

$\gamma_{\text{had}} =$
hadronic angle

Measurement of Cross Sections

Ingredients:

ΔK	kinematic region, e.g. interval in x and/or Q^2
N^{obs}	number of events in ΔK
N^{bkg}	estimated number of background events in ΔK
$\mathcal{L}$	integrated luminosity
$N^{\text{obs}}_{\text{MC}}$	number of MC events in ΔK
$\mathcal{L}_{\text{MC}}$	MC luminosity
σ_{MC}	cross section ΔK used in MC simulation (including all radiative corrections)
σ_{SM}	"Born cross section", calculated using the same PDFs and the same order of pQCD as for σ_{MC}

Measured cross section

$$\sigma_{\text{meas}} = \frac{(N^{\text{obs}} - N^{\text{bkg}})/\mathcal{L}}{N^{\text{obs}}_{\text{MC}}/\mathcal{L}_{\text{MC}}}\,\sigma_{\text{MC}}$$

Includes acceptance and migration corrections;

iteration needed if resulting cross section and MC simulation don't agree.

Radiatively corrected cross section

$$\sigma_{\text{Born}} = \sigma_{\text{meas}}\,\frac{\sigma_{\text{SM}}}{\sigma_{\text{MC}}}$$

All ZEUS and H1 cross sections are radiatively corrected by this or an equivalent method.

HERA Measurements at High Q^2

Overview:

- NC and CC cross sections
  - $d\sigma/dQ^2$, $d\sigma/dx$
  - Reduced and doubly-differential cross sections
- Structure functions and PDFs
  - F_2 and xF_3
  - Valence distributions at high x
- Elektroweak aspects
  - Helicity structure of CC scattering
  - W mass and Fermi constant

$d\sigma^{NC}/dQ^2$ (e^+p)

$$\frac{d\sigma}{dQ^2} = \int_{x_{\min}}^{x_{\max}} \frac{d^2\sigma}{dx\,dQ^2}dx$$

$x_{\min} = Q^2/(s\,y_{\max})$ and $x_{\max} = \min[1, Q^2/(s\,y_{\min})]$

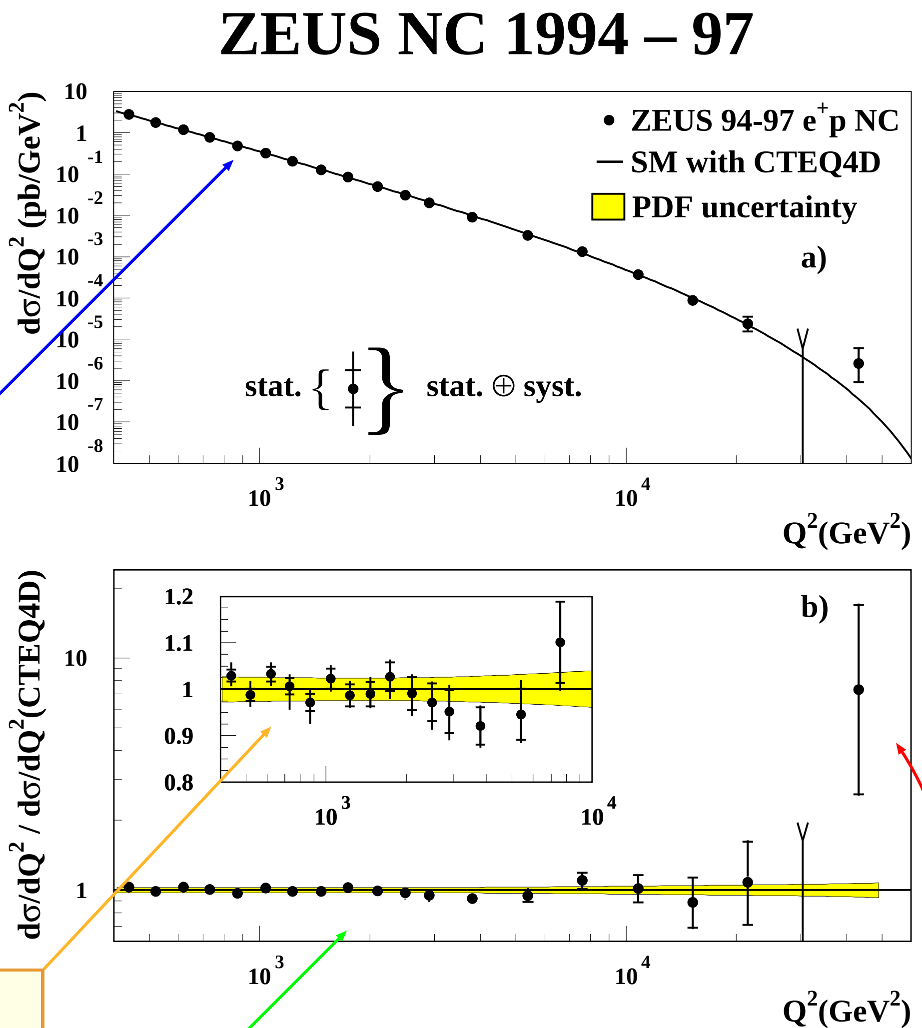

$Q^2 \ll M_Z^2$:
$d^2\sigma/dx dQ^2 \propto 1/Q^4$

yellow band = PDF uncertainty: $\sim 3-7\%$, increases with Q^2

good agreement with SM prediction for $Q^2 \lesssim 2 \times 10^4$ GeV^2

event excess at highest Q^2? (“HERA high-Q^2 excess”)

$d\sigma^{NC}/dx \;\; (e^+p)$

$$\frac{\mathrm{d}\sigma}{\mathrm{d}x} = \int_{Q^2_{\mathrm{min}}}^{Q^2_{\mathrm{max}}} \frac{\mathrm{d}^2\sigma}{\mathrm{d}x\mathrm{d}Q^2}\mathrm{d}Q^2$$

$Q^2_{\mathrm{min}} = x\, y_{\mathrm{min}}\, s$ and $Q^2_{\mathrm{max}} = x\, s$

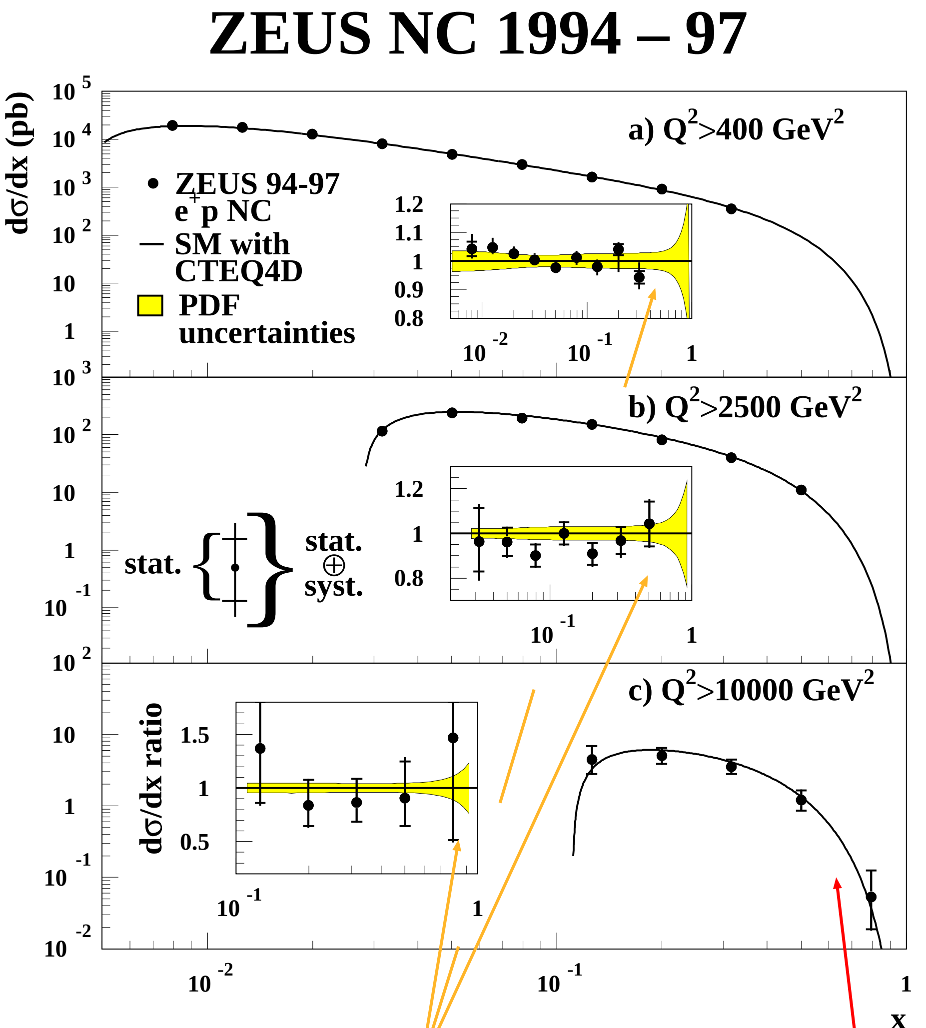

Good agreement of exp. data and SM prediction confirms PDF parm's

large PDF uncertainty at high x

high-Q^2 excess not visible in $\mathrm{d}\sigma/\mathrm{d}x$ (integration over $Q^2 > 10^4$ GeV^2)

$\tilde{\sigma}^{NC}\ (e^- p)$

$$\tilde{\sigma}_{\mathrm{NC}} = \frac{xQ^4}{2\pi\alpha^2[1+(1-y)^2]}\,\frac{d^2\sigma^{ep\to eX}}{dx\,dQ^2}$$

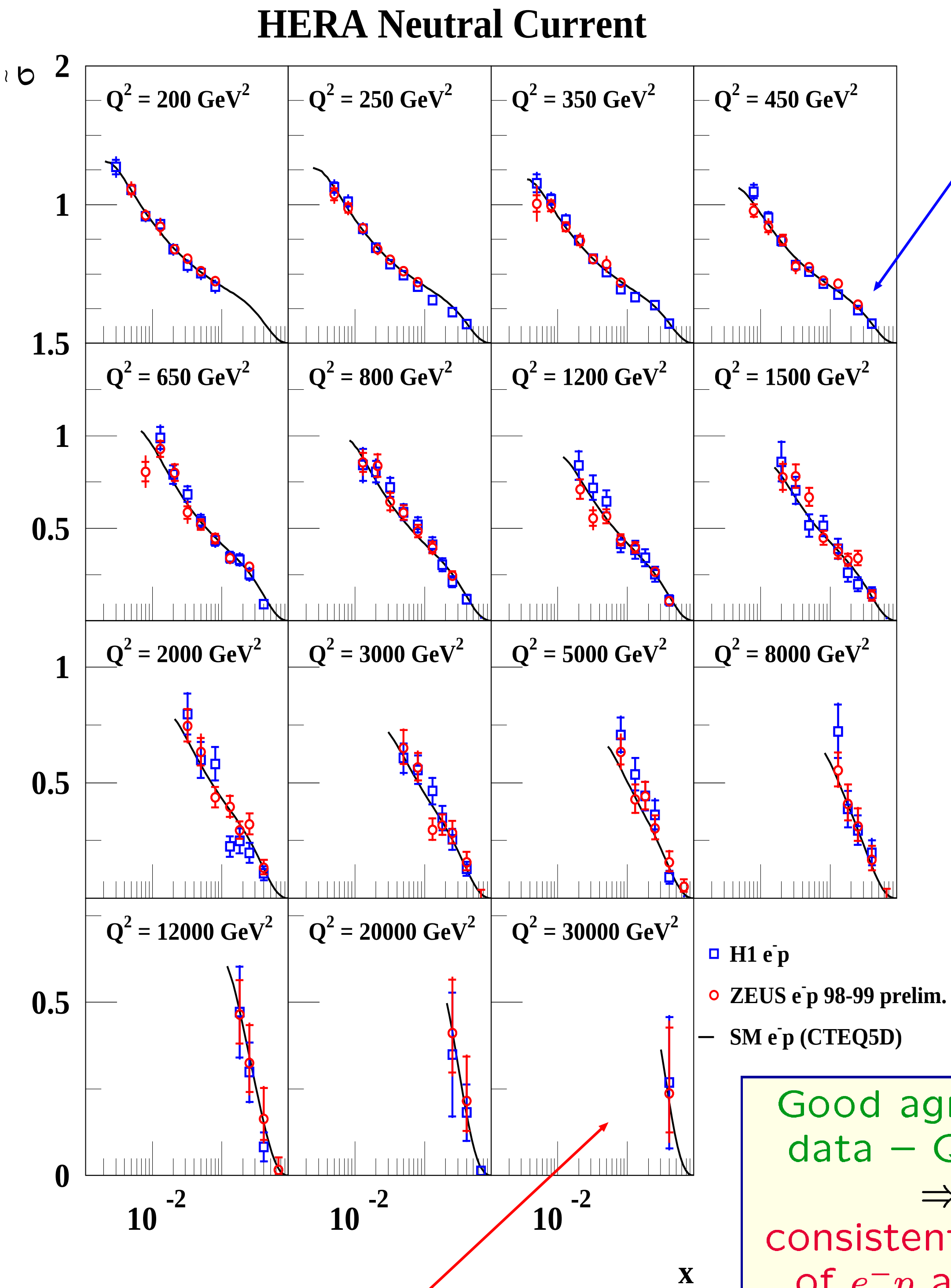

$q_v(x, Q^2)$

Good agreement data – QCD fit

$\Rightarrow$

consistent picture of e^-p and e^+p reactions

no high-Q^2 excess in e^-p

$$F_2^{em}$$

$$\tilde{\sigma}_{\rm NC} = F_2^{\rm em}\,(1+\delta_Z)\,(1-\delta_3-\delta_L)\,(1+\delta_r)$$

$\delta_Z =$ correction for Z contribution to F_2
$\delta_{3,L} =$ corrections for xF_3 and F_L terms
$\delta_r =$ radiative corrections

from SM calculation

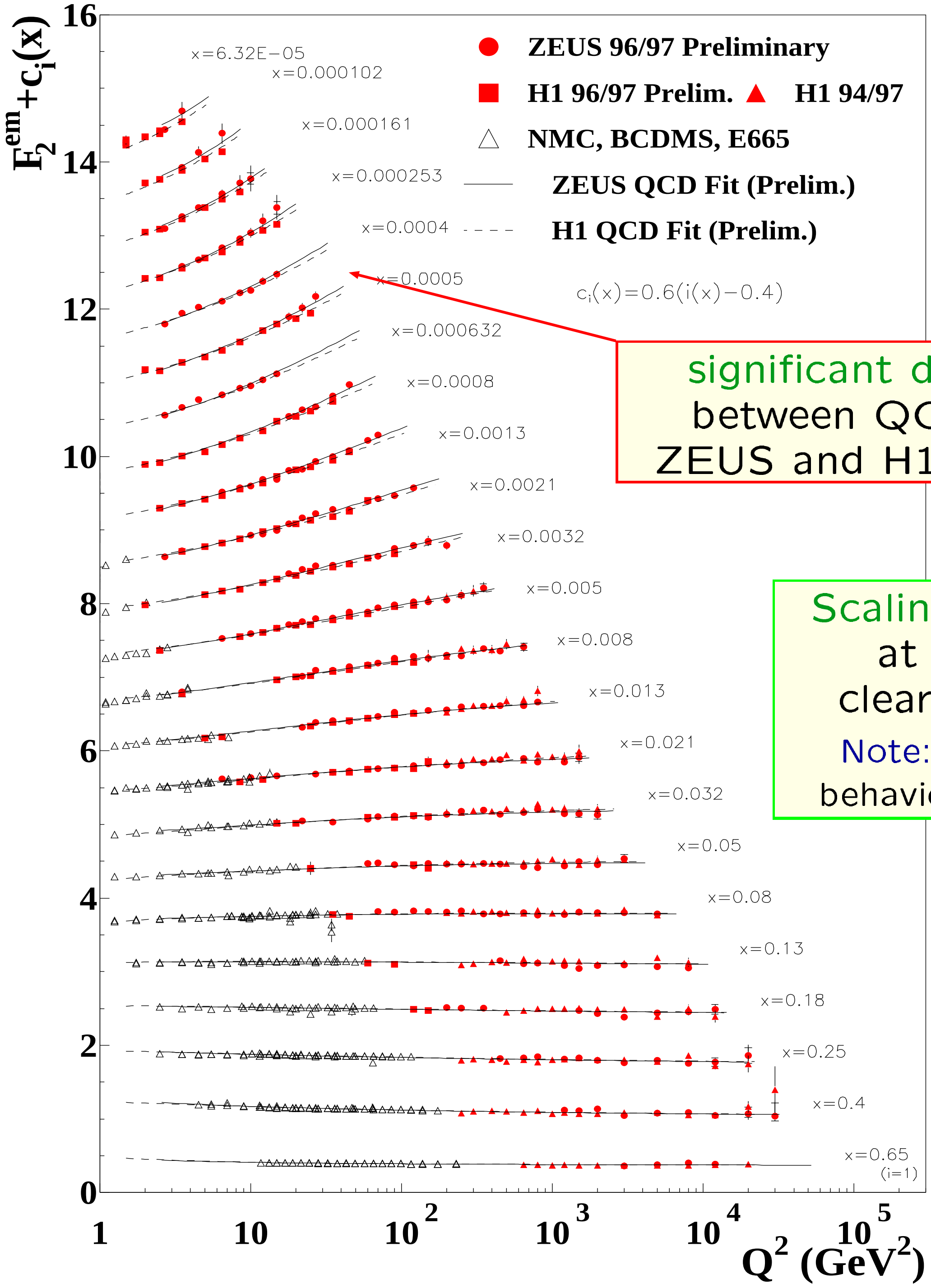

significant differences between QCD fits by ZEUS and H1 at small x

Scaling violation at small x clearly visible.
Note: plot hides behavior at large x

$d\sigma^{NC}/dQ^2$ (Comparison e^+p/e^-p)

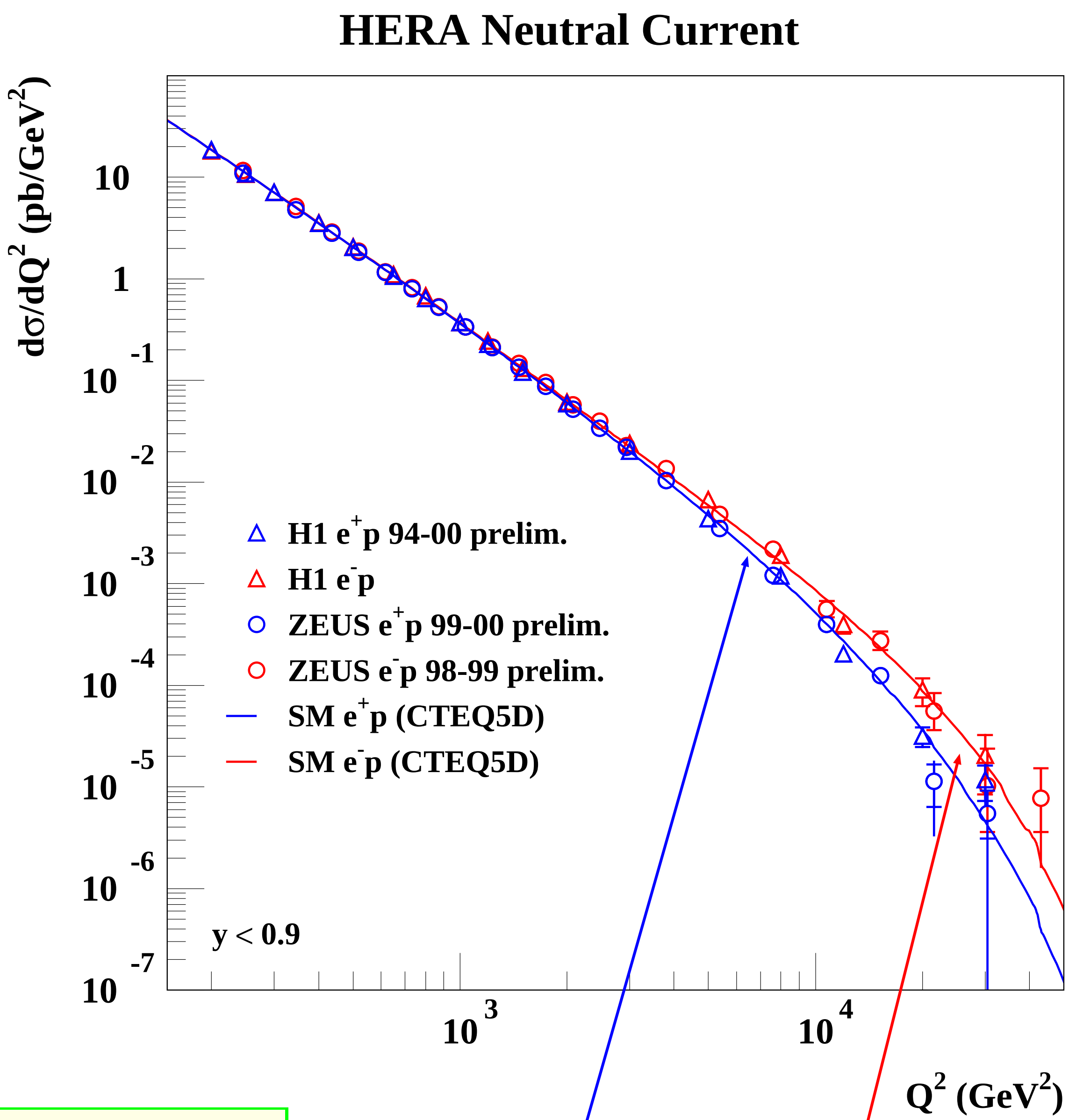

Good agreement between ZEUS and H1 in the whole Q^2 range

e^+p data are corrected to $\sqrt{s} = 318$ GeV

difference
$d\sigma/dQ^2(e^-p) - d\sigma/dQ^2(e^+p)$
caused by xF_3 term (Z exchange)

$d\sigma^{NC}/dx$ (e^+p and e^-p) for $Q^2 > 1000$ GeV^2 and $Q^2 > 10\,000$ GeV^2

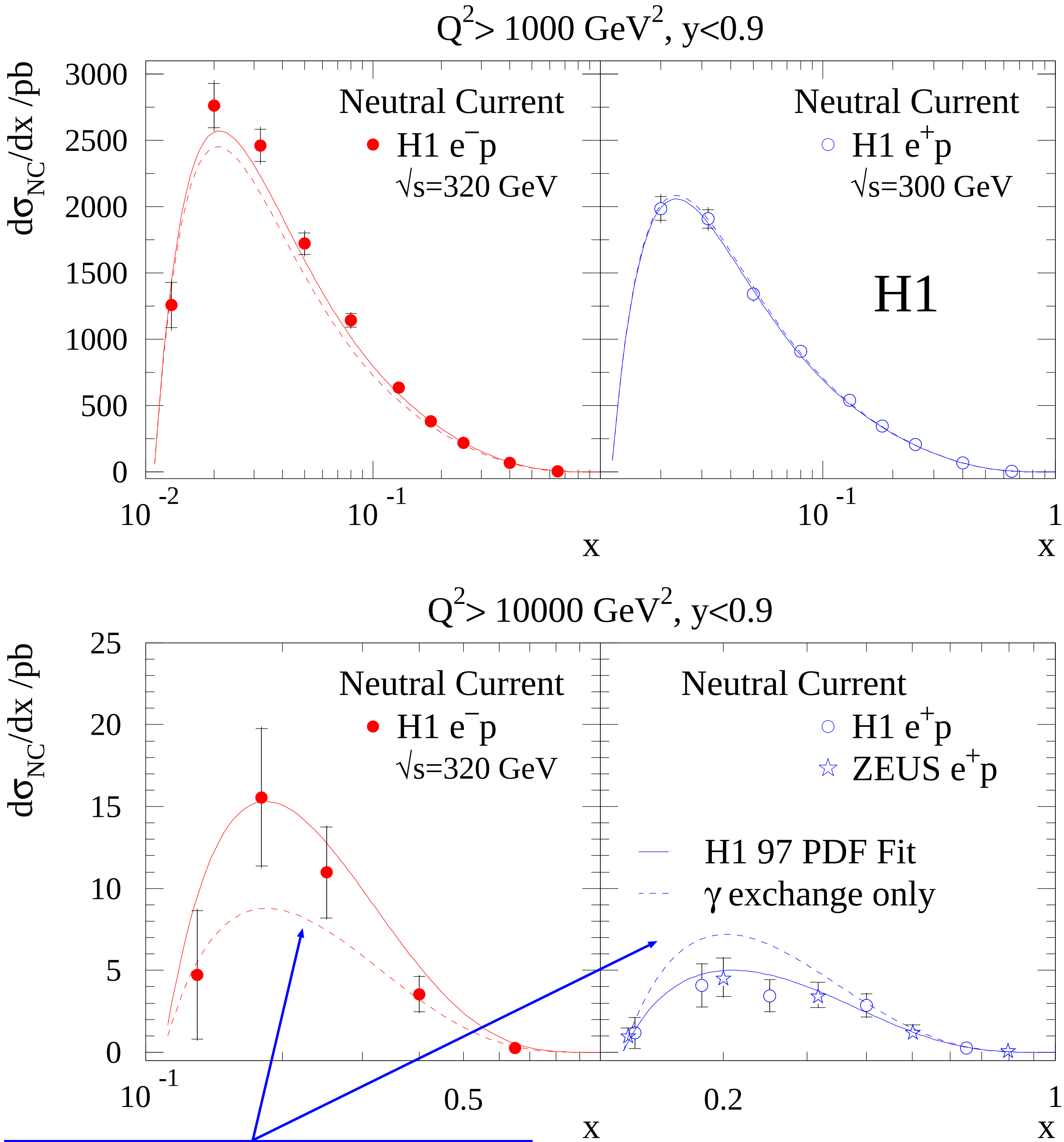

dashed lines:
"SM" expectation for
γ exchange only
($M_Z \to \infty$);
$\sigma^\gamma(e^-p) > \sigma^\gamma(e^+p)$ because of s

Data are sensitive to contribution from Z exchange

$\tilde{\sigma}^{NC}$ (Comparison e^+p/e^-p)

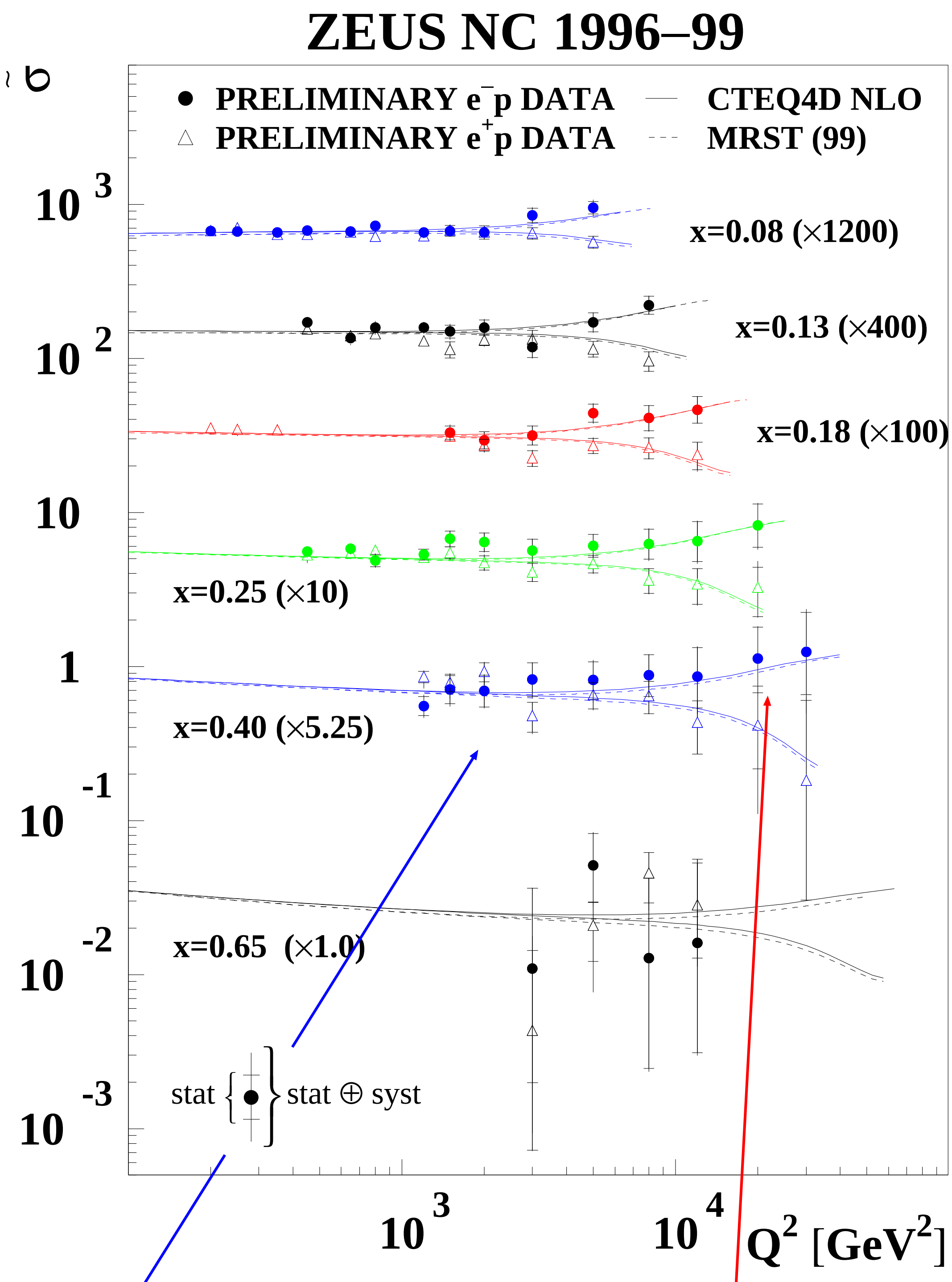

small $Q^2 \ll M_Z^2$:
$\tilde{\sigma}^{NC}(e^+p) \approx \tilde{\sigma}^{NC}(e^-p)$,
independent of x

large $Q^2 \gtrsim M_Z^2$:
significant xF_3 terms;
precision sufficient for
measurement of
$\tilde{\sigma}^{NC}(e^+p) - \tilde{\sigma}^{NC}(e^-p)$

$xF_3(x, Q^2)$ (ZEUS)

$$xF_3(x,Q^2) = \left(\frac{Y_-^{300}}{Y_+^{300}} - \frac{Y_-^{318}}{Y_+^{318}}\right)^{-1} \left(\tilde{\sigma}_{\mathrm{NC}}^{e^-p,\,318} - \tilde{\sigma}_{\mathrm{NC}}^{e^+p,\,300}\right) - \Delta F_L$$

$$Y_\pm^{\sqrt{s}\,[\mathrm{GeV}]} = 1 \pm (1-y)^2 \text{ with } y = Q^2/xs$$

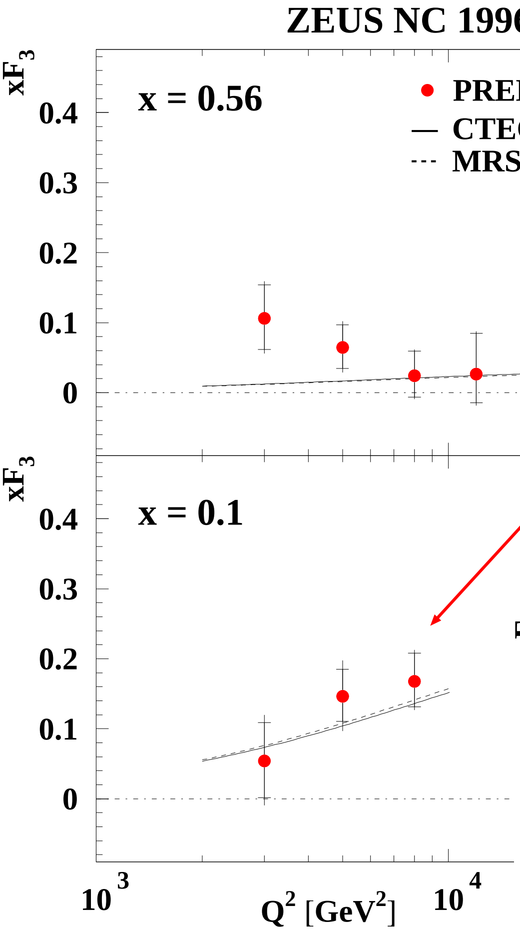

Q^2 dependence:
dominated by propagator term $\propto Q^2/(Q^2+M_Z^2)$;
in addition sensitive to singlet QCD evolution

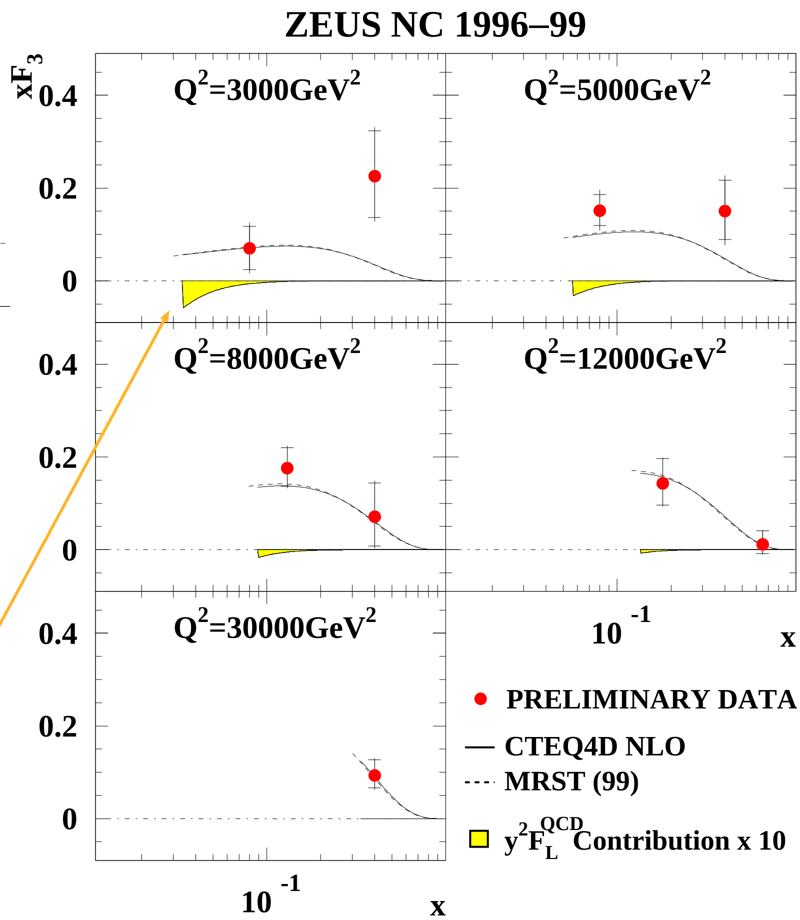

x dependence:
sensitive to valence quark distributions

F_L correction currently negligible

$d\sigma^{CC}/dx\ (e^+p)$

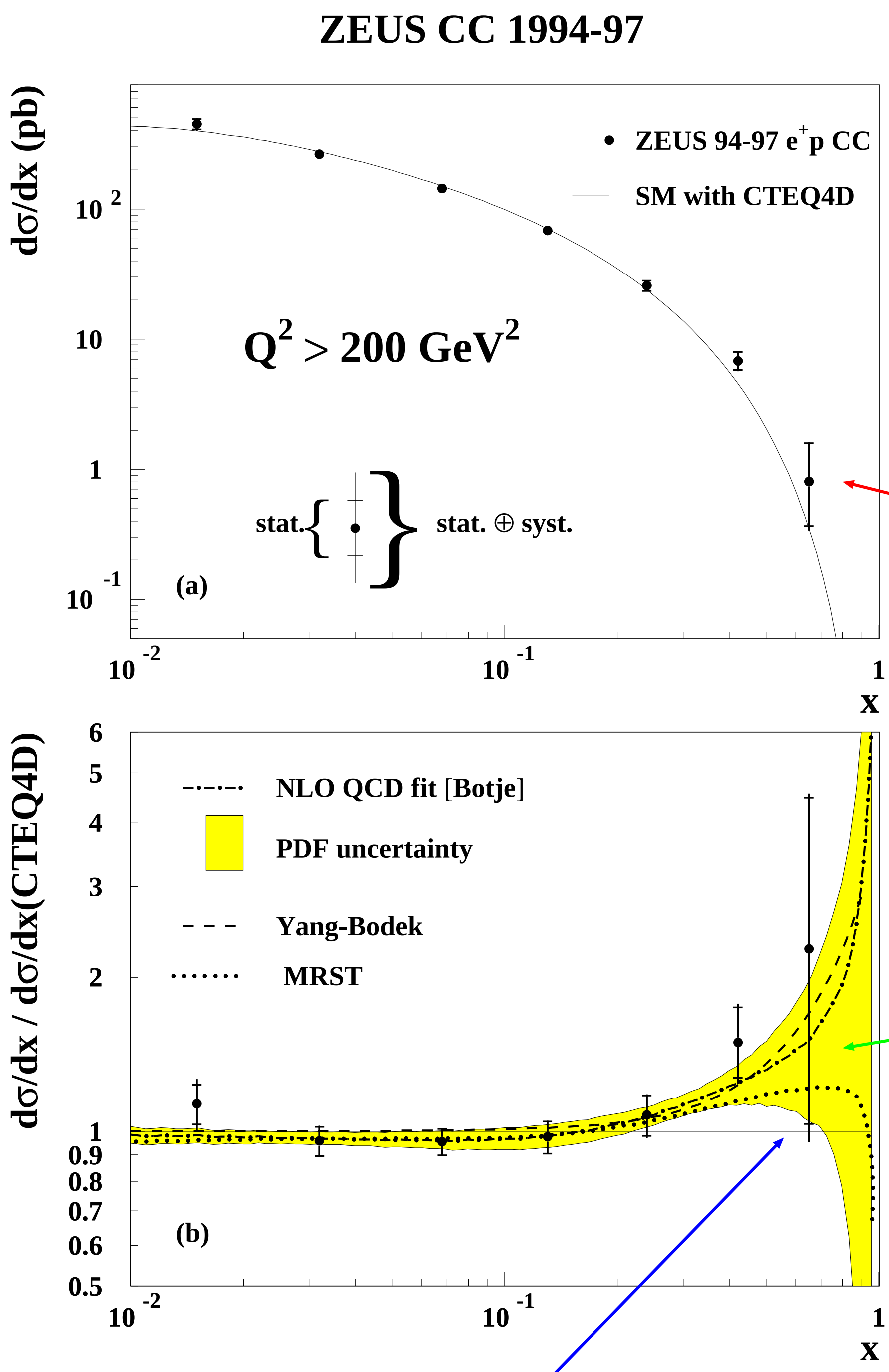

e^+p:
$d\sigma/dx$
at high x
dominated by
$d_v(x, Q^2)$

"high-x excess":
moderately significant event excess
at $x \gtrsim 0.3$

PDF uncertainty "diverges" at high x

QCD fits yield different behavior of d/u at $x \to 1$:

ZEUS	$d/u \propto (1-x)^{-c} \to \infty$
Bodek–Yang	$d/u \to 0.2$ (boundary condition)
MRST	$d/u \propto (1-x)^{+c'} \to 0$

$d\sigma^{CC}/dx \;\; (e^- p)$

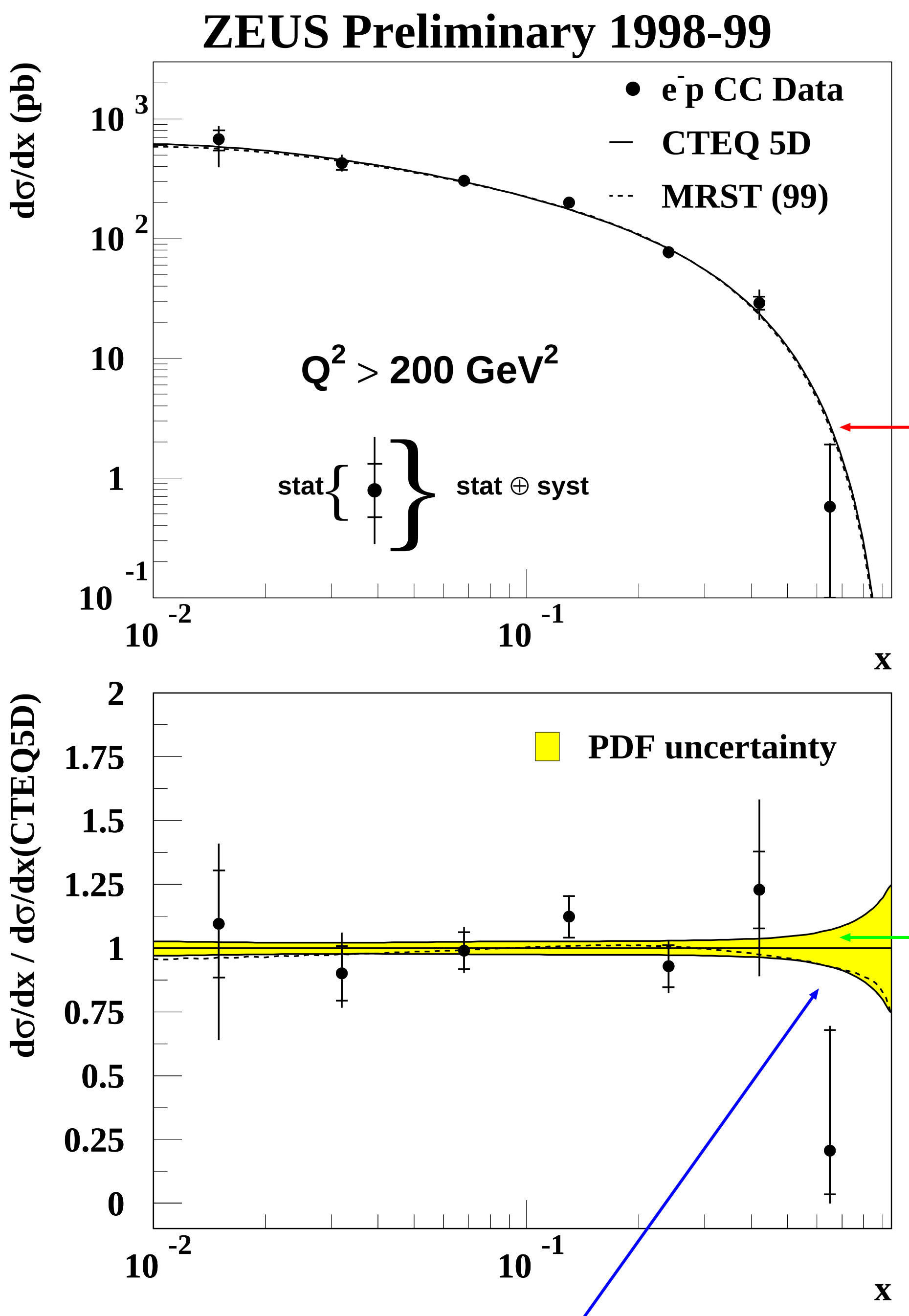

$e^- p$:
dσ/dx
at high x
dominated
by $u_v(x, Q^2)$

no "high-x excess":
possibly
small
negative
deviation
at $x \gtrsim 0.3$

PDF
uncertainty
is stable
at high x
[at small Q^2,
$u(x, Q^2)$ is
known more
precisely than
$d(x, Q^2)$]

moderate variations of
u distribution in different
QCD fits

$d\sigma^{CC}/dQ^2$ (Comparison e^+p/e^-p)

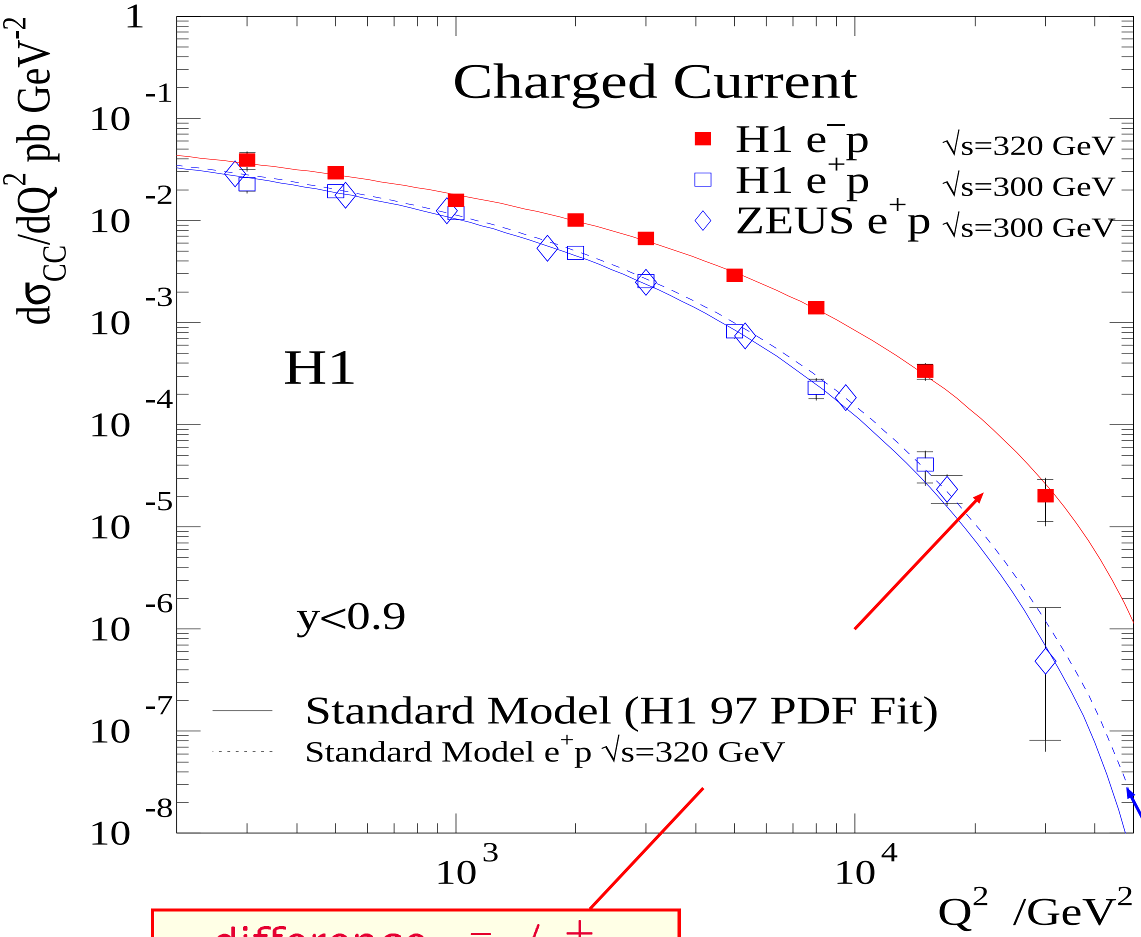

difference e^-p/e^+p increases with Q^2 ($>$ factor 10 at $Q^2 \gtrsim 20\,000$ GeV^2)

difference $\sqrt{s} = 300/318$ GeV is small

Q^2 dependence of dσ/dQ^2:

- PDF values in integration region $x \in [x_{\text{min}} = Q^2/s; 1]$
  (x dependence of PDFs is dominant, but Q^2 dependence also contributes)
- "Helicity factor": 1 for e^-q, $e^+\bar{q}$; $(1-y)^2$ for $e^-\bar{q}$, e^+q
  $y = Q^2/xs$, integration region: $y > Q^2/s$
- W propagator term $\propto [M_W^2/(Q^2 + M_W^2)]^2$

$\tilde{\sigma}^{CC}\ (e^+p)$

$$\tilde{\sigma}_{CC} = \frac{2\pi x}{G_F^2}\left(\frac{Q^2+M_W^2}{M_W^2}\right)^2 \frac{d^2\sigma_{CC}}{dx\,dQ^2}$$

$$= \begin{cases} (1-y)^2(d+s) + (\bar{u}+\bar{c}) & \text{for } e^+p \\ (u+c) + (1-y)^2(\bar{d}+\bar{s}) & \text{for } e^-p \end{cases}$$

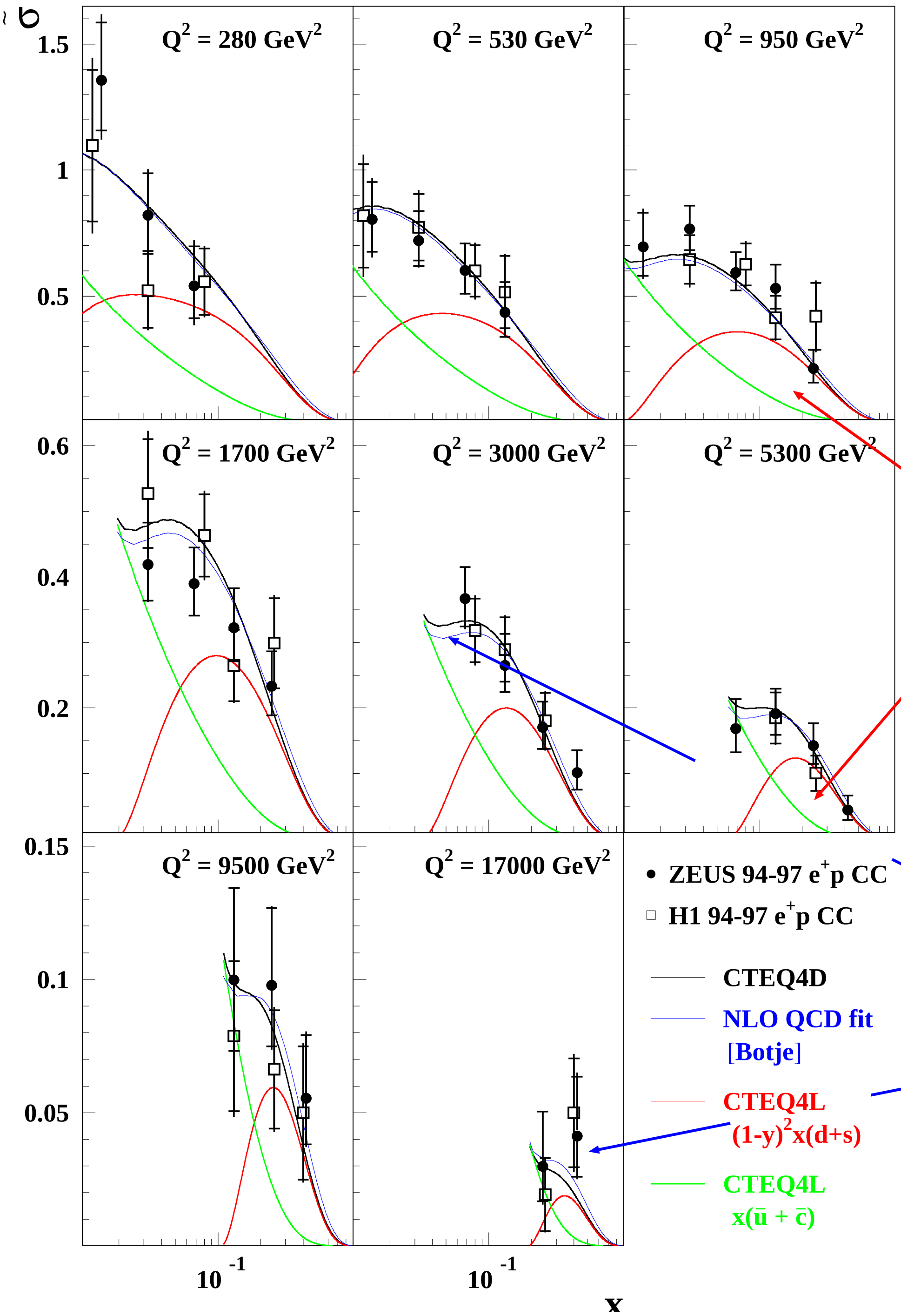

Good agreement ZEUS/H1

for $x \gtrsim 0.2$: $(1-y)^2(d+s)$ dominates

visible differences ZEUS fit/ CTEQ4

$\tilde{\sigma}^{CC}\ (e^- p)$

$$\tilde{\sigma}_{CC} = \frac{2\pi x}{G_F^2}\left(\frac{Q^2+M_W^2}{M_W^2}\right)^2 \frac{d^2\sigma_{CC}}{dx\,dQ^2}$$

$$= \begin{cases} (1-y)^2(d+s) + (\bar{u}+\bar{c}) & \text{for } e^+p \\ (u+c) + (1-y)^2(\bar{d}+\bar{s}) & \text{for } e^-p \end{cases}$$

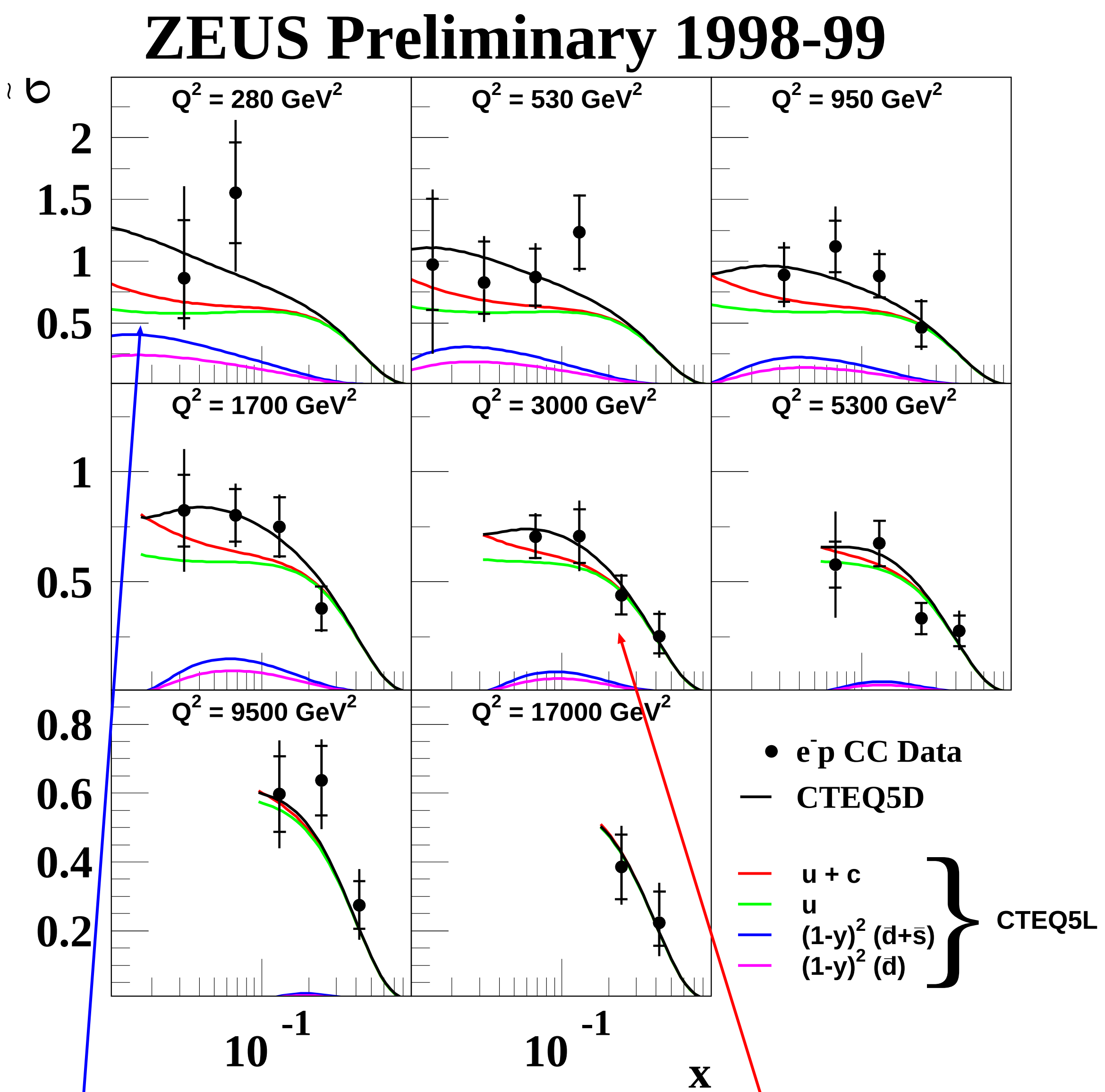

for $x \lesssim 0.1$: considerable contributions from c and $\bar{s}$

for $x \gtrsim 0.2$: u dominates (no $(1-y)^2$ -suppression)

Valence Distributions

$$xu_v(x,Q^2) = \tilde\sigma(x,Q^2)\Big|_{\mathrm{exp}} \cdot \left.\frac{xu_v(x,Q^2)}{\tilde\sigma(x,Q^2)}\right|_{\mathrm{SM}} \qquad (\text{NC: } e^\pm p,\ \text{CC: } e^- p)$$

$$xd_v(x,Q^2) = \tilde\sigma(x,Q^2)\Big|_{\mathrm{exp}} \cdot \left.\frac{xd_v(x,Q^2)}{\tilde\sigma(x,Q^2)}\right|_{\mathrm{SM}} \qquad (\text{CC: } e^+ p)$$

> 0.7

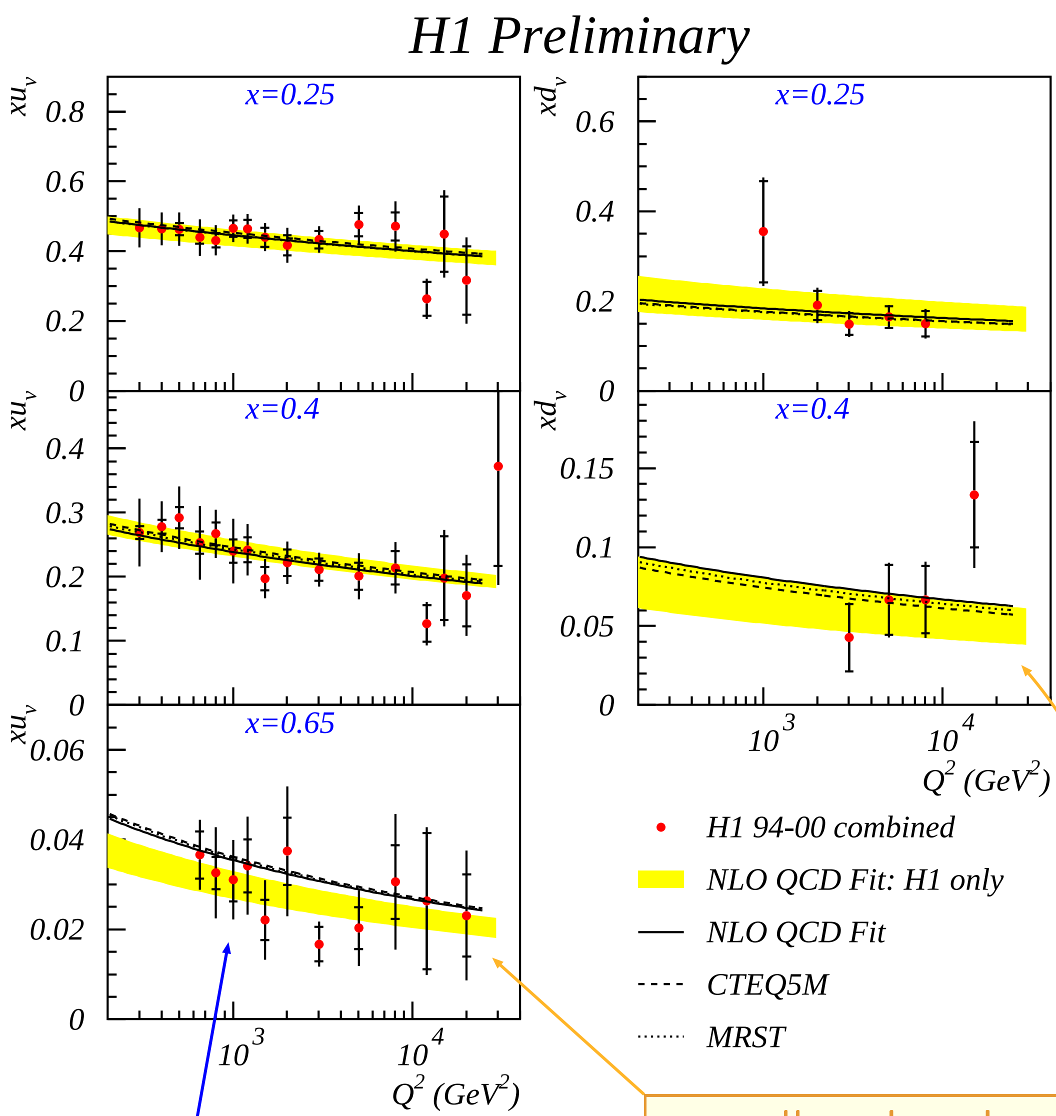

$u_v(x{=}0.65, Q^2)$:
in H1 fit $\sim 17\%$ smaller
than in standard PDFs;
significant? ZEUS?

yellow band:
QCD fit to
H1 data
with $Q^2 > 20$ GeV^2

$\tilde{\sigma}^{CC}$ as a Function of $(1-y)^2$

y dependence of $\tilde{\sigma}_{CC}$ determined by helicity structure of eq CC scattering:

$e^- q$
$e^+ \bar{q}$

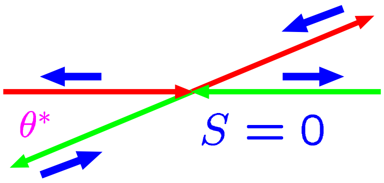

isotropic scattering
$\tilde{\sigma} \propto 1$

$e^+ q$
$e^- \bar{q}$

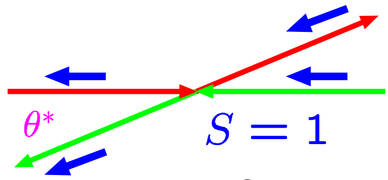

amplitude $\propto \cos^2(\theta^*/2)$
$\tilde{\sigma} \propto (1-y)^2$

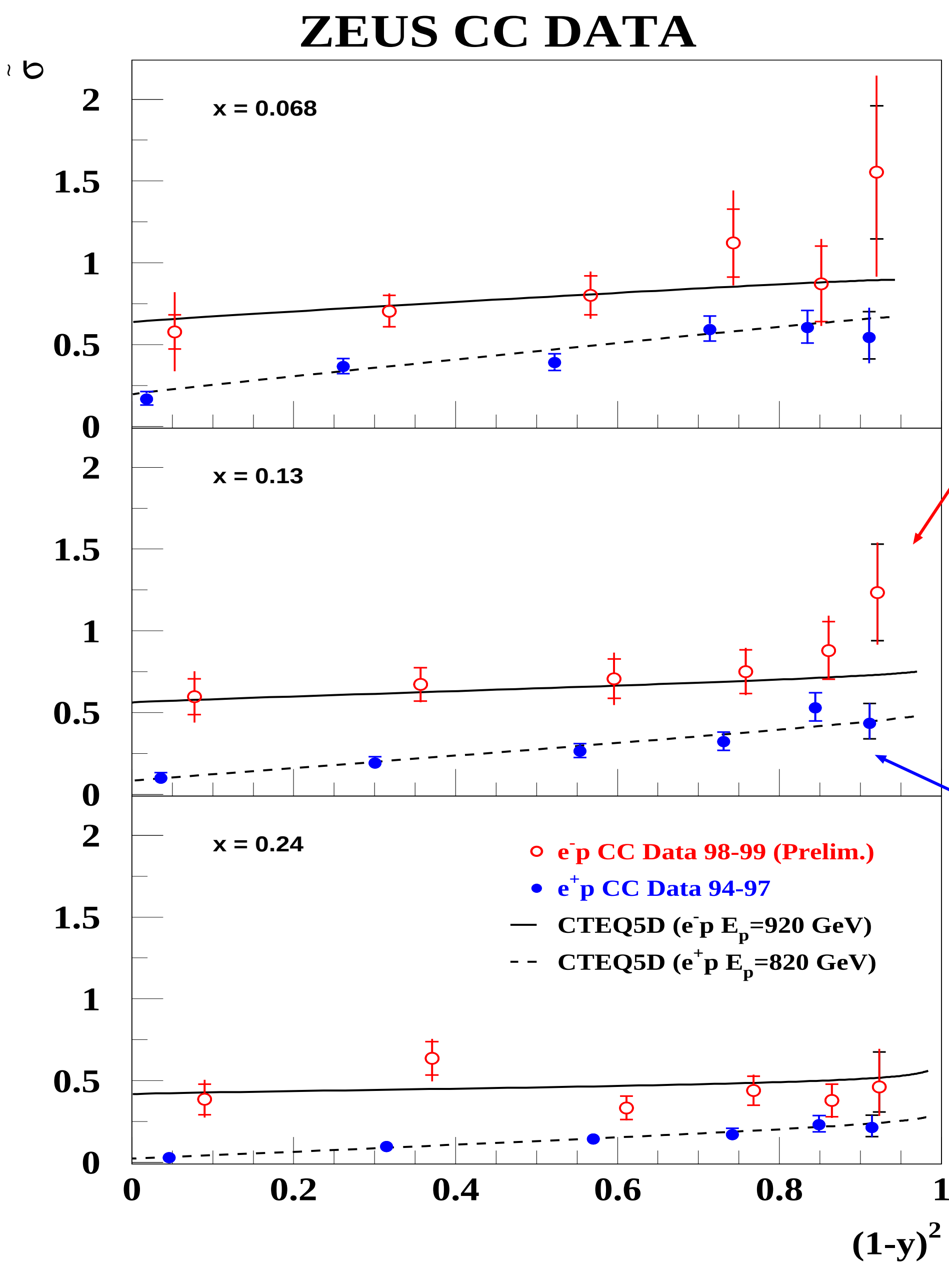

$e^- p$:
dominated by
$u_v(x, Q^2)$

$e^+ p$:
dominated by
$(1-y)^2 d_v(x, Q^2)$

Determination of M_W and G_F

$$\frac{d^2\sigma_{CC}}{dx dQ^2} \propto {G_F}^2 \left(\frac{1}{1+Q^2/{M_W}^2}\right)^2 \Rightarrow$$ Fit to CC data yields G_F and M_W as independent parameters

ZEUS result: 1σ confidence region includes SM point.

Comparison with SM relation:

$$G_F = \frac{\pi\alpha}{\sqrt{2}} \times \frac{M_Z^2}{M_W^2(M_Z^2 - M_W^2)} \frac{1}{1-\Delta r}$$

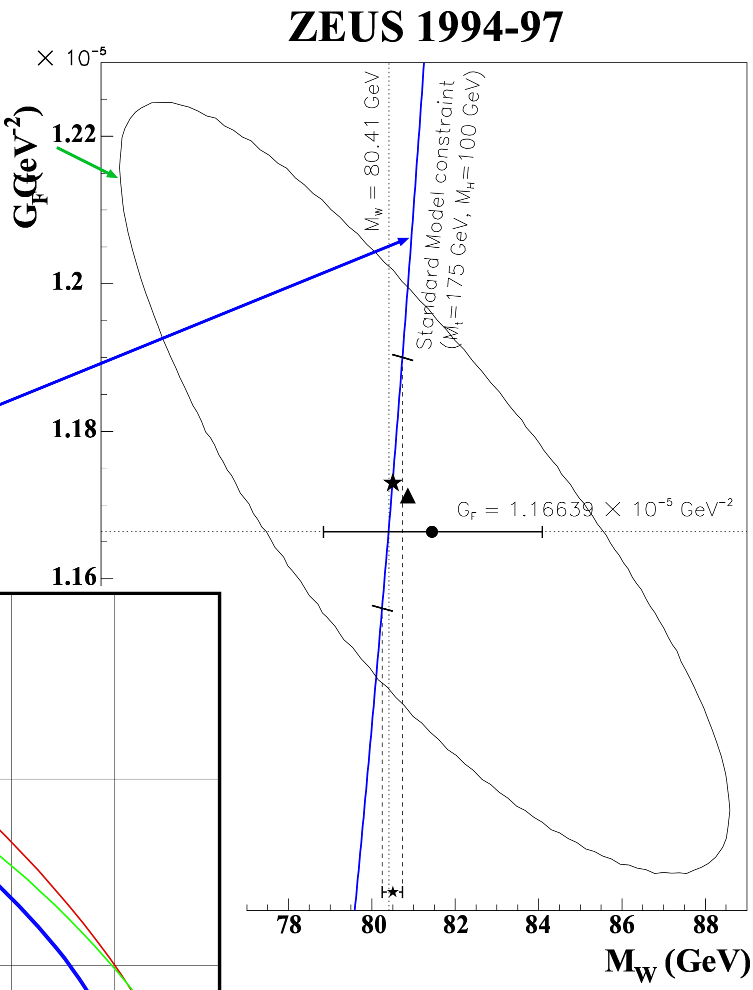

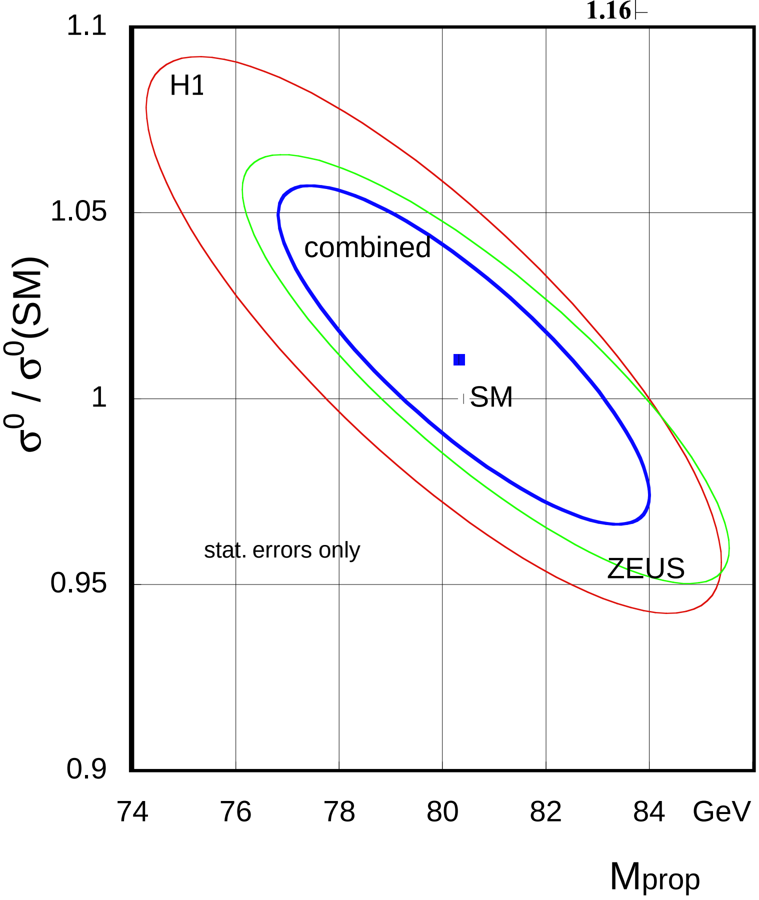

comparison with H1: $\Delta\chi^2 = 1$ confidence regions

Summary

The differential cross sections for e^-p and e^+p NC and CC scattering have been measured at HERA in the region $Q^2 \lesssim 30\,000\,\mathrm{GeV}^2$

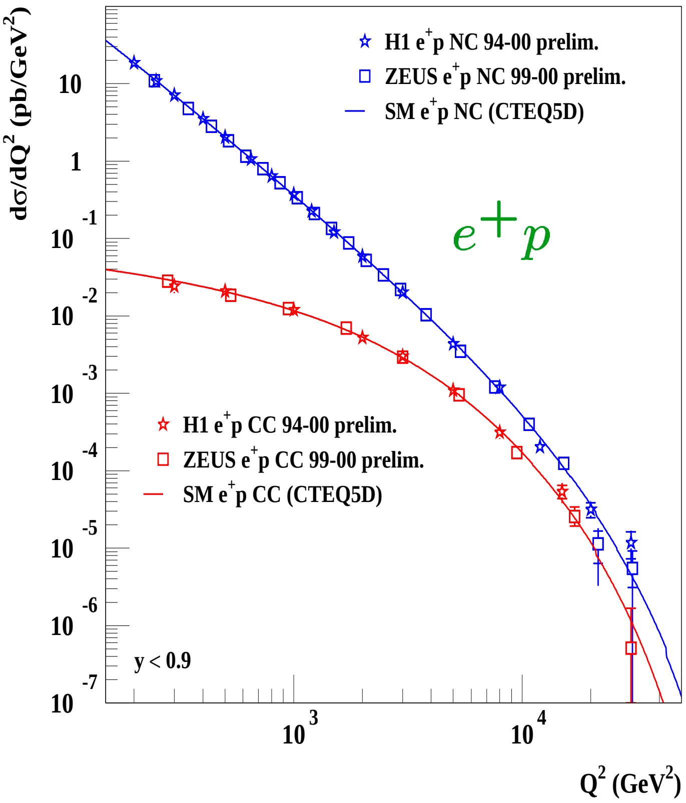

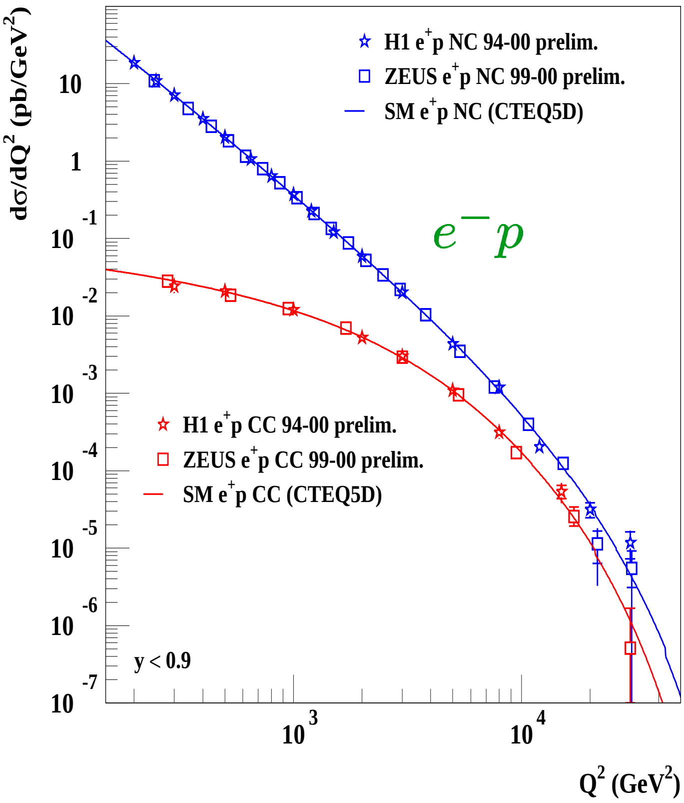

For $Q^2 \lesssim 20\,000\,\mathrm{GeV}^2$: excellent agreement with predictions (SM plus QCD fits to fixed target data)

Small deviations at high Q^2 and x ...

have caused a lot of excitement but are probably due to statistical fluctuations and high-x PDF effects. New physics?

Search for "New Physics"

Overview:

- The "HERA high-Q^2 effect"
- eq resonances
  - Leptoquarks
  - R_P-violating squarks
- Lepton flavor violation
  - Direct production of lepton flavor violating states
  - Exclusion limits at high masses
- Excited fermions
- Contact interactions
- Extra dimensions
- Events with lepton and $\not{P}_t$
  - The H1-ZEUS puzzle
  - Anomalous top production

The H1 Events at High Q^2

First results of the DIS analyses 1996/97:

- First high-statistics data at $Q^2 \gtrsim 10\,000\ \mathrm{GeV}^2$
- Unexpected excess of events at high x and Q^2
- Triggered a lot of excitement and activities

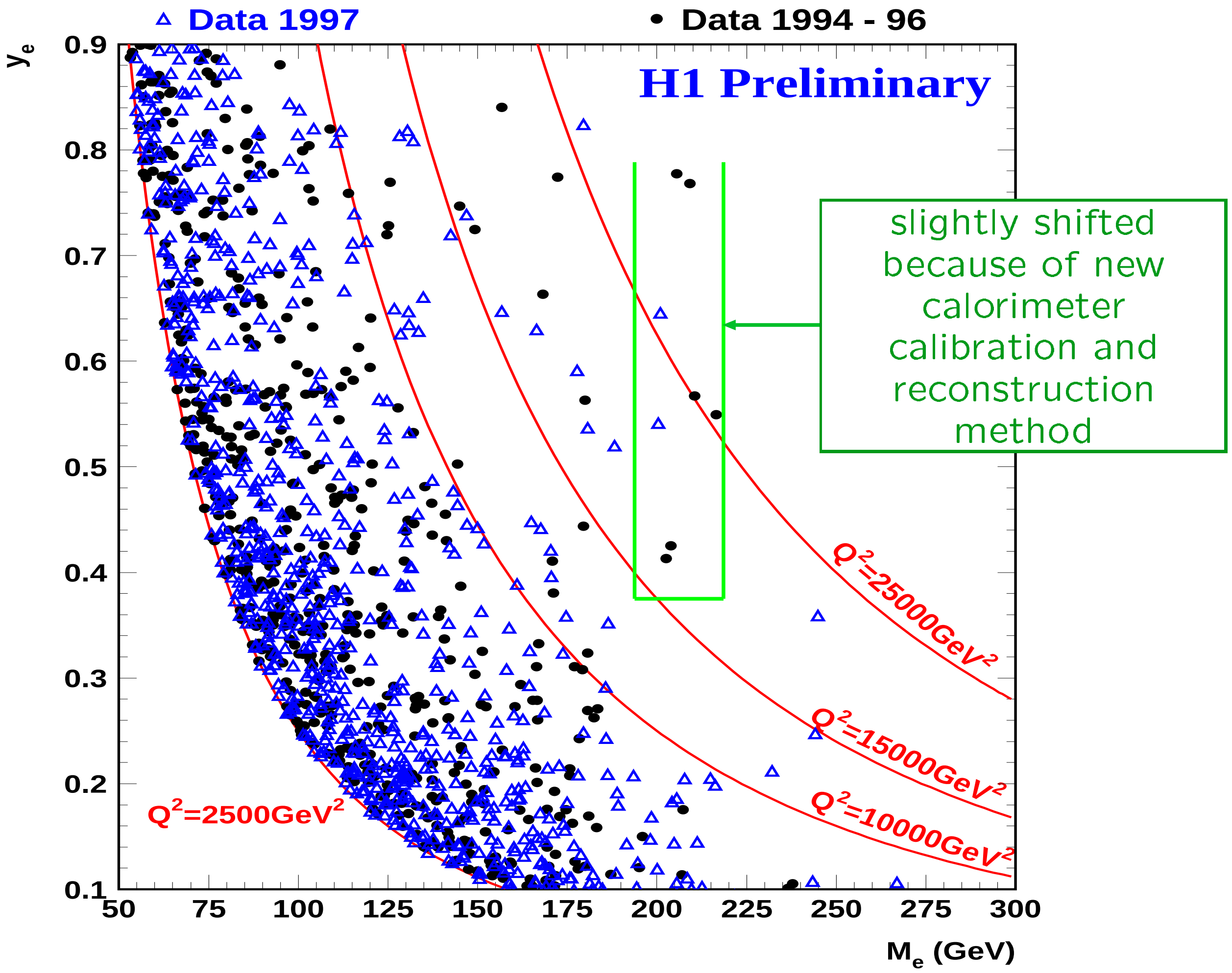

Event numbers:

kinematic region	1994–96 obs.	1994–96 MC	1994–97 obs.	1994–97 MC
$187.5 < M_e < 212.5$ GeV and $y_e > 0.4$	7	0.95 ± 0.18	8	3.01 ± 0.54
$x_e > 0.55$ and $y_e > 0.25$	1	0.45 ± 0.18		
$Q_e^2 > 35\,000\ \mathrm{GeV}^2$	0	0.08 ± 0.04		

The ZEUS Events at High Q^2

. . . and in the ZEUS data?

- ZEUS also observes event excess, but not at exact same place
- Note: ZEUS and H1 use(d) different kinematic reconstruction methods

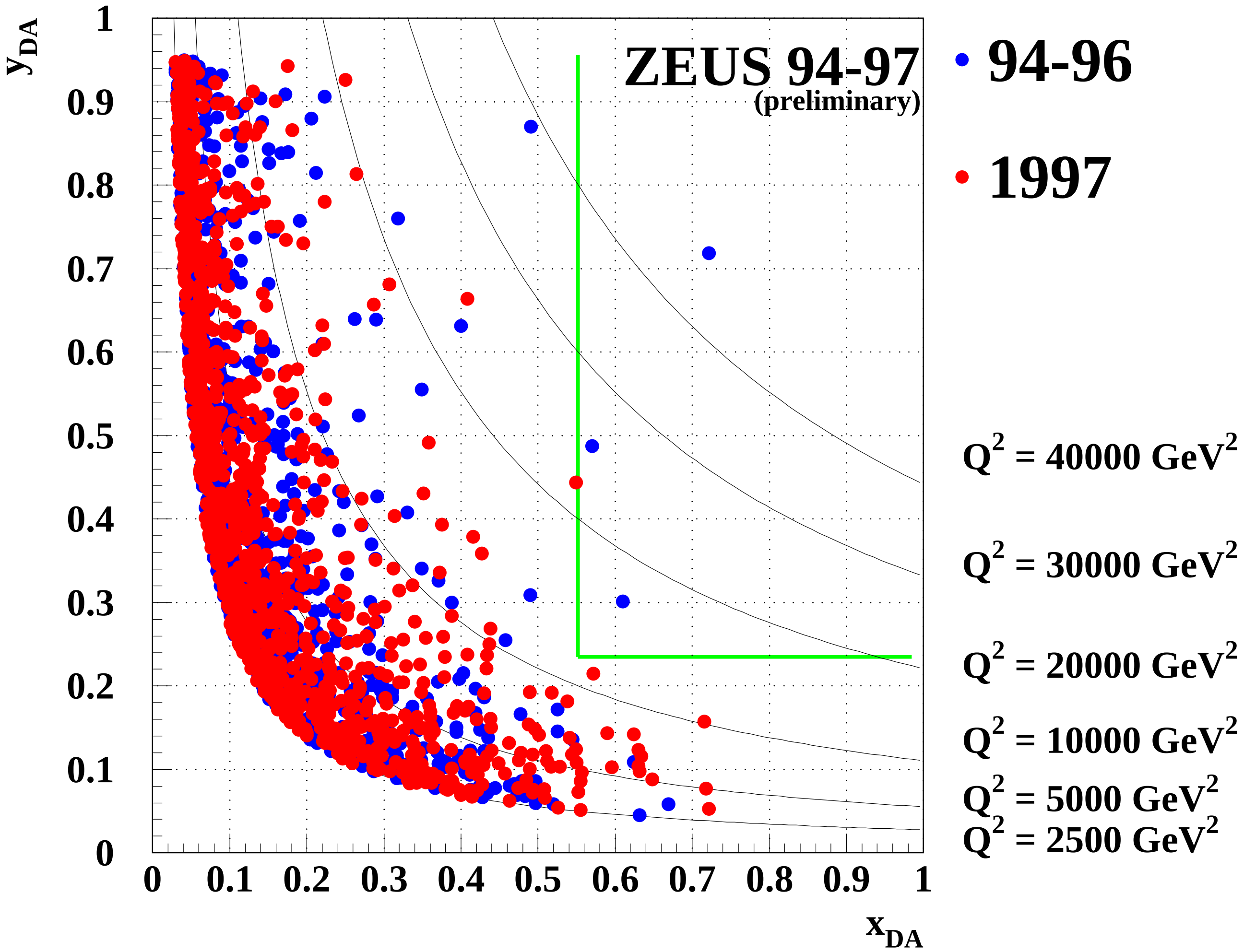

Event numbers:

kinematic region	1994–96 obs.	1994–96 MC	1994–97 obs.	1994–97 MC
$x_{DA}>0.55$ and $y_{DA}>0.25$	4	0.91 ± 0.18	4	1.90
$Q^2_{DA}>35\,000$ GeV^2	2	0.15 ± 0.05	2	0.34
$187.5<M_{DA}<212.5$ GeV and $y_{DA}>0.4$	2	1.75 ± 0.14		

Speculations and Questions

What could it be?

- Statistical fluctuation?
- eq resonance ?
  - would such a signal be compatible with other experiments?
  - leptoquark or squark?
  - are mass values of H1 ($M_e \approx 200$ GeV) and of ZEUS ($M_{\mathrm{DA}} = \sqrt{s x_{\mathrm{DA}}} \approx 225$ GeV) compatible?
  - does the y distribution look like a LQ decay?
- Contact interaction?

Significance analyses:

- Poisson: $p = p(N_{\mathrm{obs}}, N_{\mathrm{MC}}; M_e)$
- What is the smallest p in the whole kinematic region ?
- MC: how frequently occurs a "smaller smallest p" ? H1: 0.9%, ZEUS: 6% .

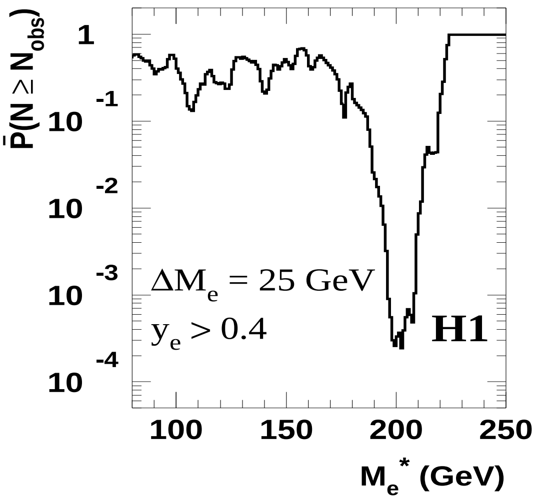

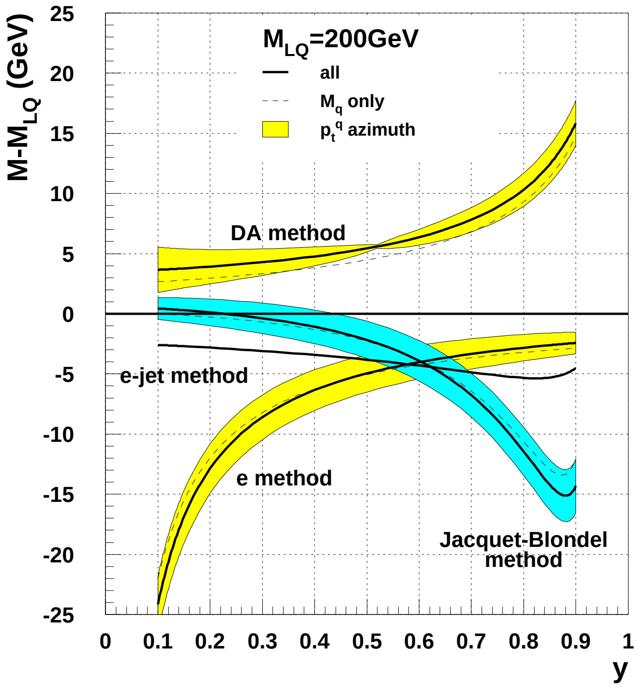

Mass of a eq resonance:

- $M = \sqrt{xs}$ for free, massless partons
- QCD radiation affects different reconstruction methods differently

Leptoquark Production at HERA

What are leptoquarks (LQs) ?

- States with Yukawa coupling λ to e and q
- $\mathrm{SU}(3)_c \times \mathrm{SU}(2)_{\mathrm{L}} \times \mathrm{U}(1)_{\mathrm{Y}} \Rightarrow$
  14 multiplets per flavor combination (BRW)
  - fermion number $F = 0, 2$ (coupling to e^+q, e^-q),
  - spin $S = 0, 1$ (scalar/vector),
  - weak isospin T,
  - chirality of coupling (L, R)

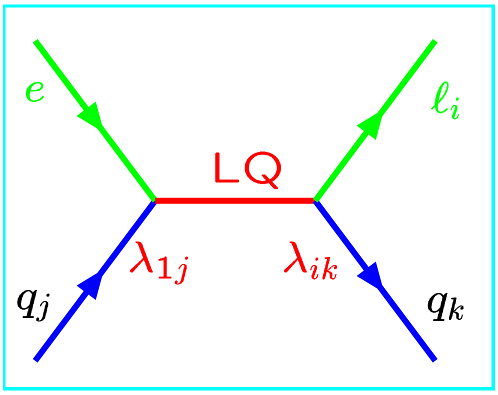

$\sigma(ep \to \mathrm{LQ} + X \to eq + X)$

$$\frac{d\sigma^{\mathrm{LQ}}}{dy} = \frac{\pi\lambda^2}{4s}\,\mathrm{BR}(\mathrm{LQ} \to eq)\; q(x, \mu^2_{\mathrm{LQ}}) \times \begin{cases} 1 & (S = 0) \\ 6(1-y)^2 & (S = 1) \end{cases}$$

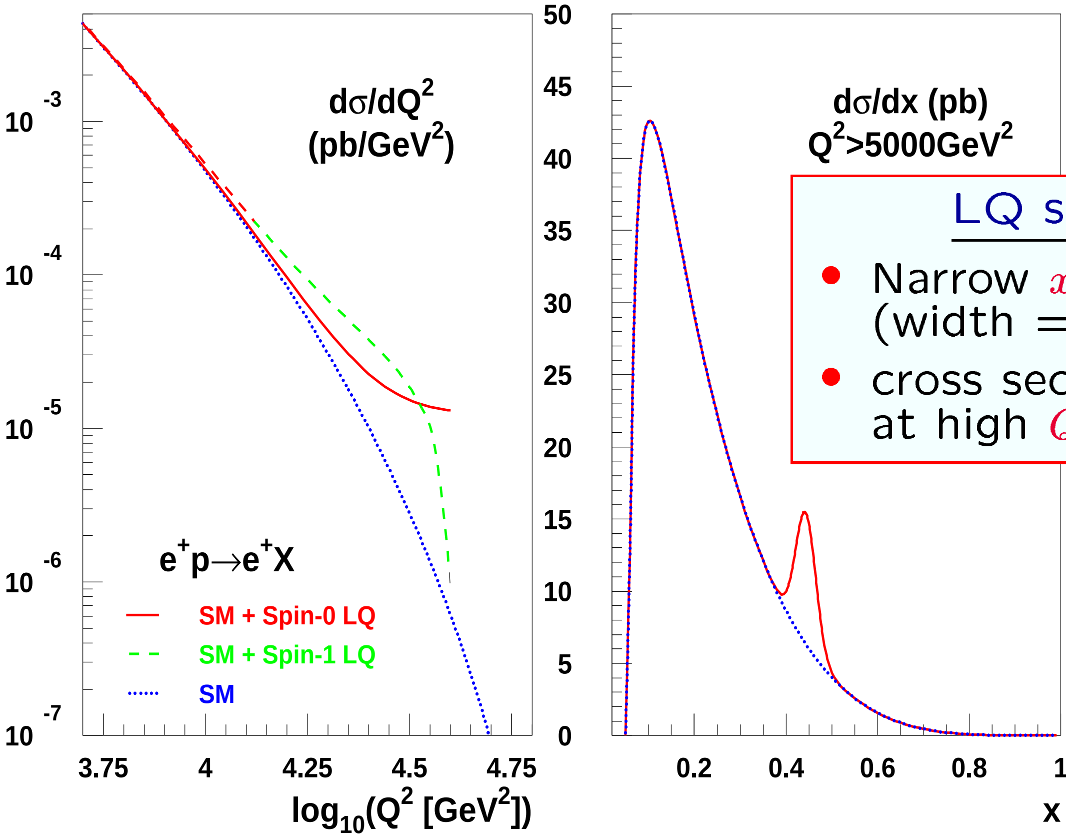

LQ signal

- Narrow x resonance (width = exp. resol.)
- cross section increase at high Q^2

Exclusion Limits from TeVatron

$\sigma(p\bar{p} \to \mathrm{LQ}\,\overline{\mathrm{LQ}}\;X) \propto \Big|$ 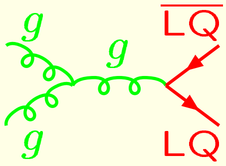 $+$ 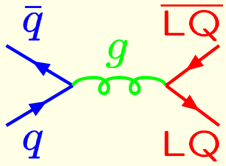 $+ \ldots \Big|^2$

$\sigma(p\bar{p} \to \mathrm{LQ}\,\overline{\mathrm{LQ}}\;X \to eeqq\;X) \propto \mathrm{BR}(\mathrm{LQ} \to eq)^2$

$\sigma(p\bar{p} \to \mathrm{LQ}\,\overline{\mathrm{LQ}}\;X)$ independent of λ_{1j}

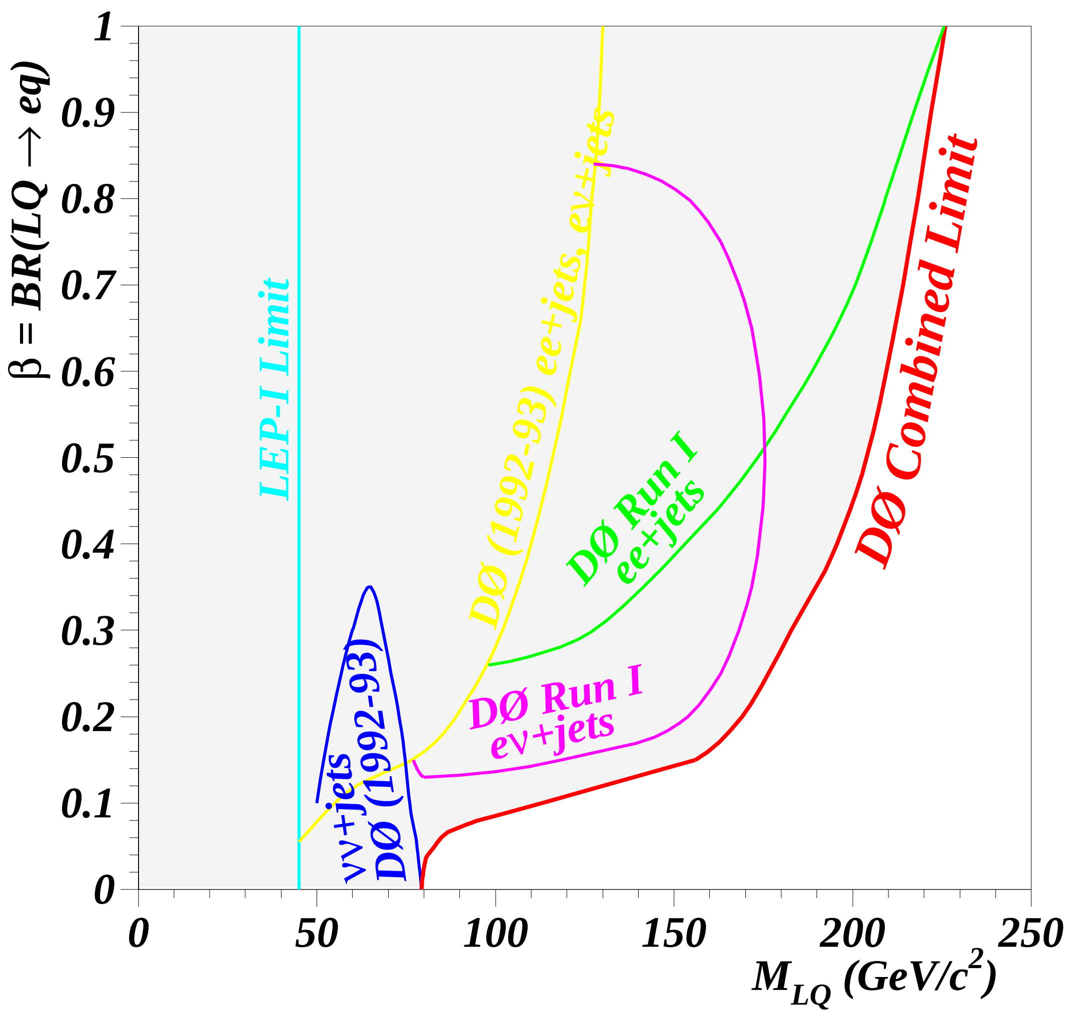

TeVatron: lower limits on LQ mass (95% C.L.)			
LQ Spin	$\beta = 1$ DØ	$\beta = 1$ CDF+DØ	$\beta = 1/2$ DØ
$S = 0$	225 GeV	242 GeV	204 GeV
$S = 1$	298 GeV	—	270 GeV

HERA (e+Jet) Mass Spectra

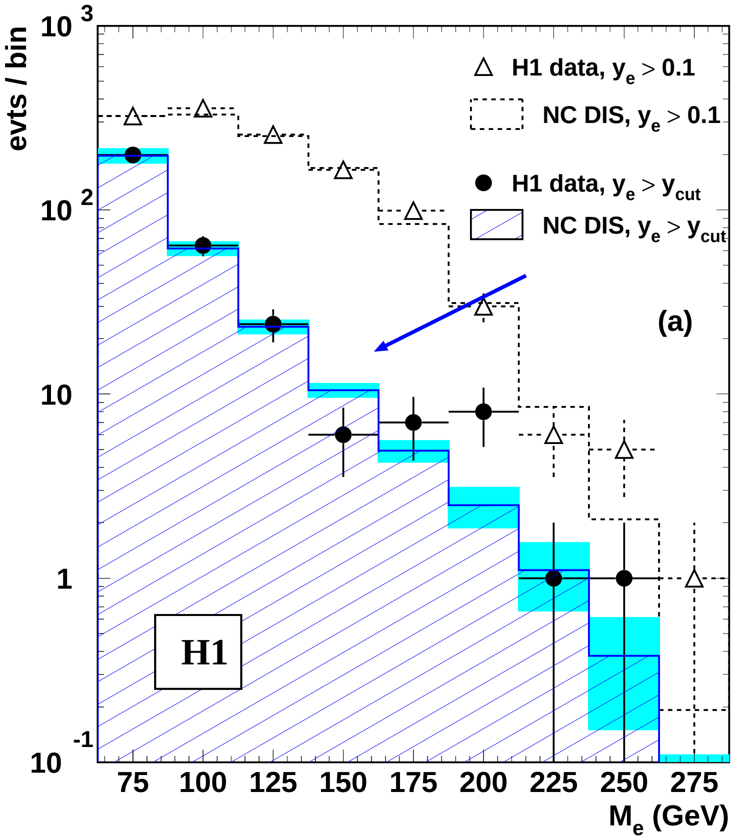

H1:

- Distribution of $M_e = \sqrt{x_e s}$ for $y > y_{\mathrm{cut}}$
- y_{cut} optimized for LQ search

ZEUS:

- M_{ej} without y cut
- $\cos\theta^*$ distribution for $M_{ej} > 200$ GeV

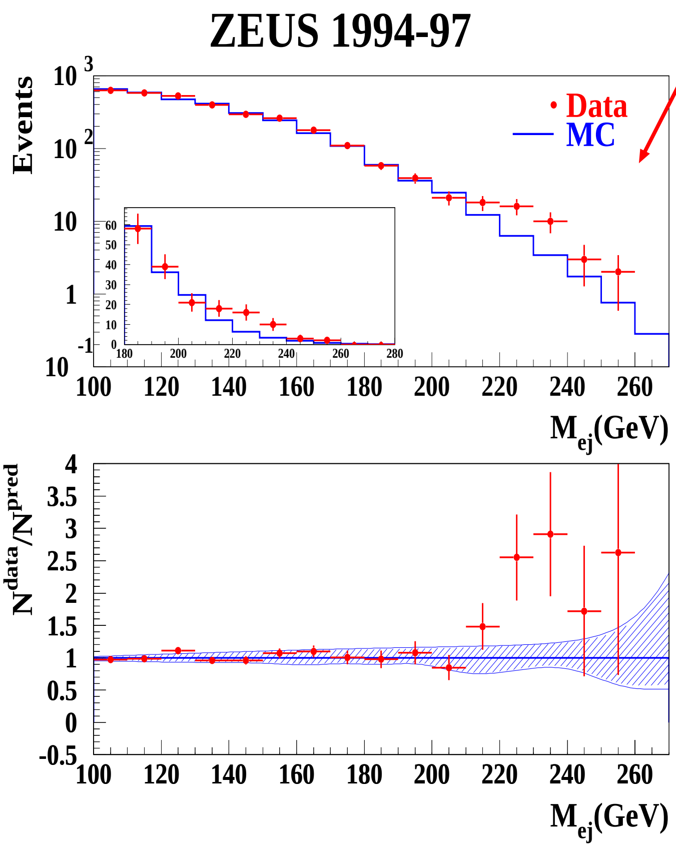

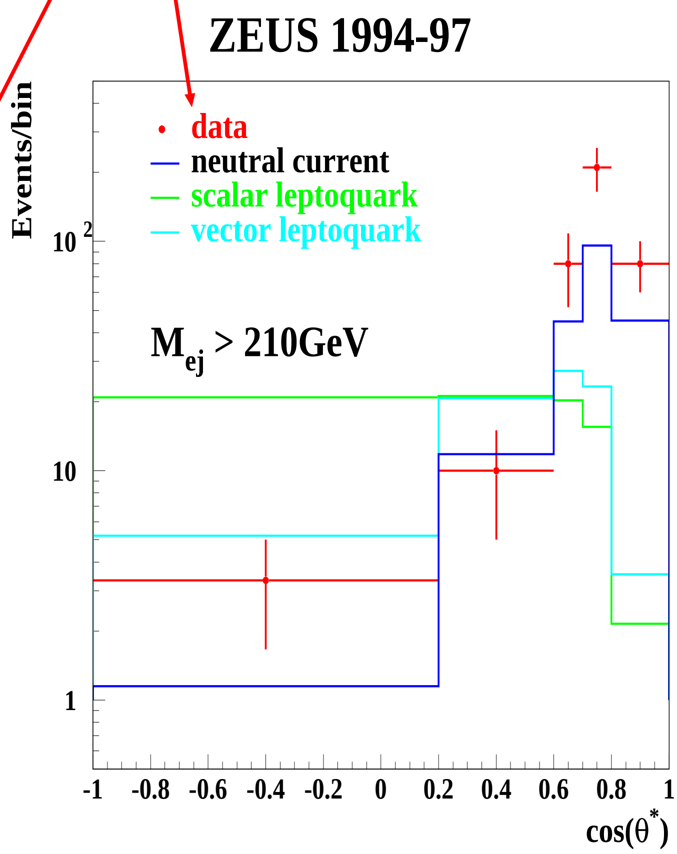

. . . . . . and in the Latest Data ?

New ZEUS event numbers:

$Q^2 > 35\,000$ GeV^2

data set	$\mathcal{L}$[pb^{-1}]	obs.	MC
1994–97 e^+p	47.7	2	0.34
1998–99 e^-p	16.2	2	1.02
1999–00 e^+p	39.2	1	0.53
$x_{DA} > 0.55, y_{DA} > 0.25$			
1994–97 e^+p	47.7	4	1.9
1998–99 e^-p	16.2	1	1.3
1999–00 e^+p	39.2	0	1.6

ZEUS:

no anomalies in the “signal regions”

H1:

no significant event excess in new e^+p data

(not shown: neither in e^-p)

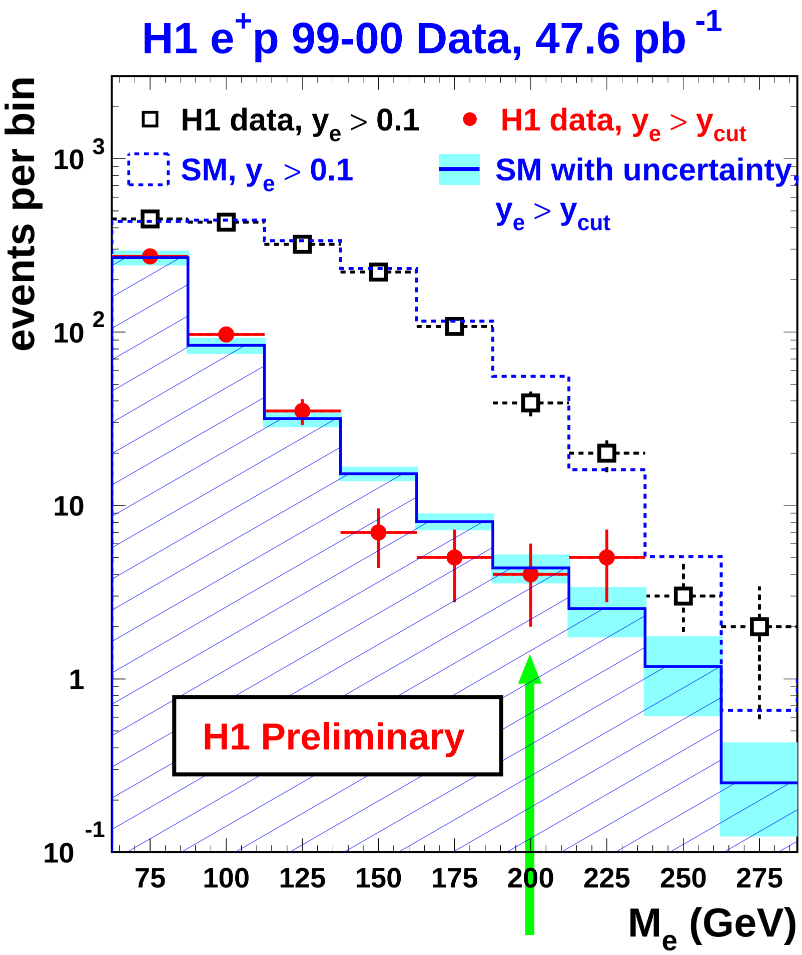

LQ Limits from HERA

No clear signal for LQ production
$\Rightarrow$
upper limits for coupling λ_{1j} as a function of M_{LQ}
assumption: LQs respect SM symmetries
and decay exclusively to eq or $\nu q'$

$F = 0$
$S = 0$

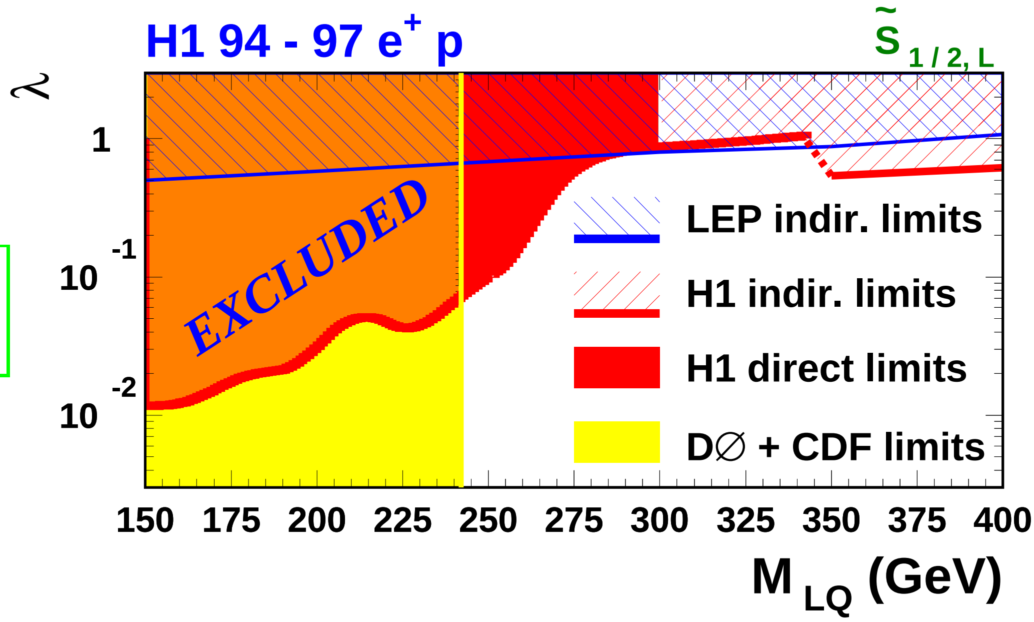

$F = 2$
$S = 0$

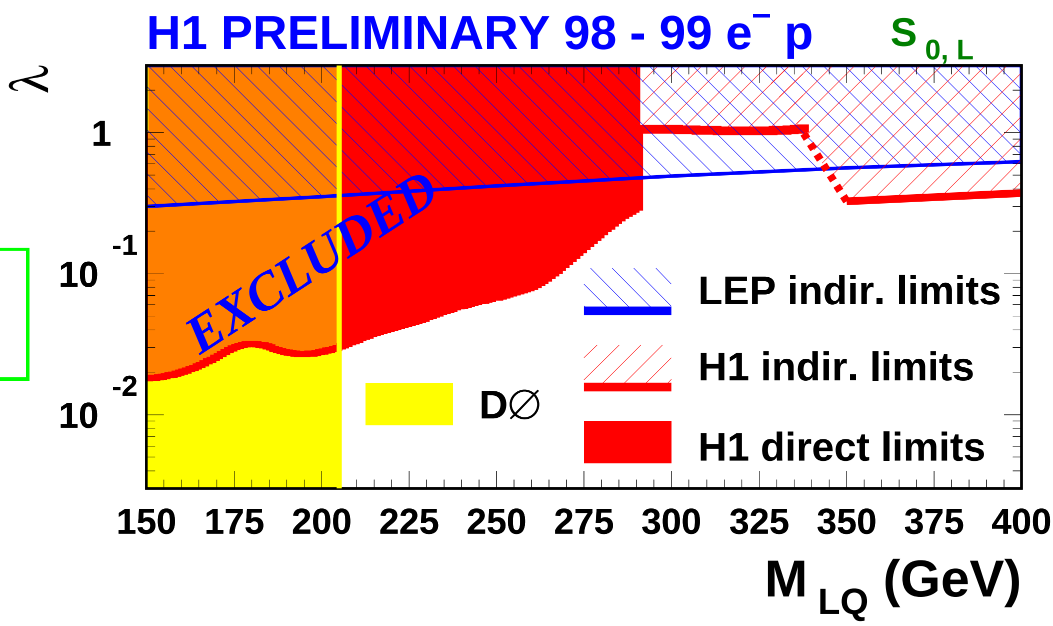

LEP: LQ exclusion limits from $eeqq$ contact interactions

LQ's with Alternative Decay Channels

If LQs have decays other than to eq or $\nu q'$
we can have $\beta_e = \mathrm{BR}(\mathrm{LQ} \to eq) \neq 1$ or 0.5

$\Rightarrow$

consider limits on β_e as functions of M_{LQ}
for fixed λ_{11} (e^+p scattering)

$F=0$
coupling
to d quark

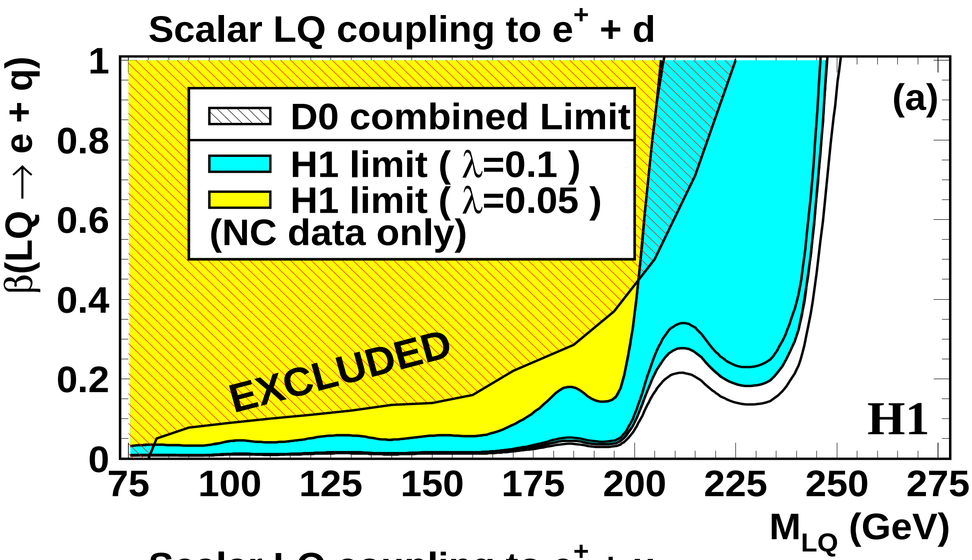

$F=0$
coupling
to u quark

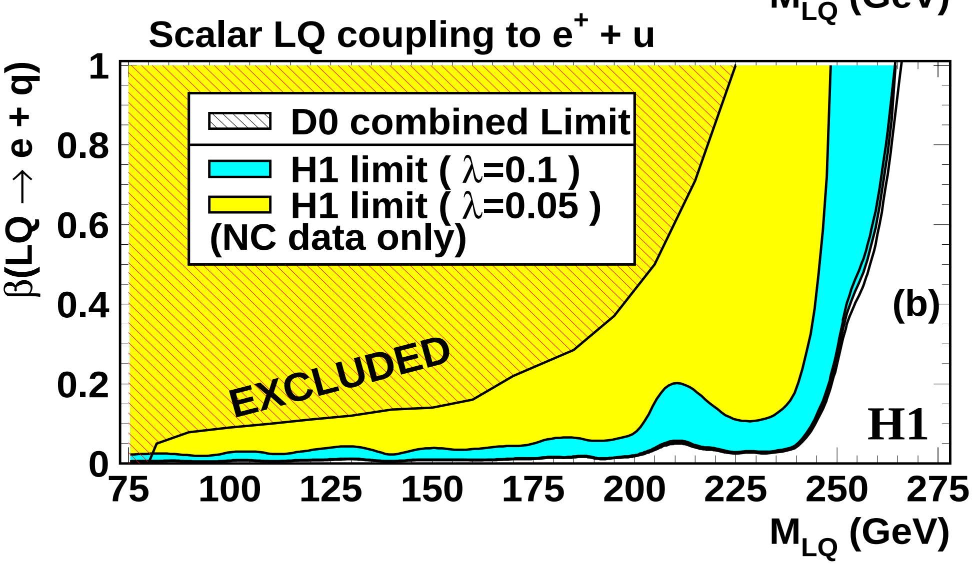

→ HERA has discovery potential at high M_{LQ} and low β_e

→ Bump at $M_{\mathrm{LQ}} \sim 210$ GeV is caused by H1 event excess

R_P-Violating Squarks

Supersymmetry (SUSY):

Each SM fermion has a bosonic partner and vice versa.

Examples:

SM	SUSY
quark q	squark $\tilde{q}$
lepton ℓ	slepton $\tilde{\ell}$
photon γ	photino $\tilde{\gamma}$
Higgs H	5 higgsinos $(h^\circ, H^\circ, A^\circ, H^\pm)$

neutral gauginos and higgsinos $\to$ neutralinos (χ°)
charged gauginos and higgsinos $\to$ charginos $(\chi^\pm)$

The R parity:

$$R_P = (-1)^{3B+L+2S} = \begin{cases} +1 & \text{for SM} \\ -1 & \text{for SUSY} \end{cases}$$

If R_P is not conserved...

– SUSY particles can be singly produced

– squarks ($\tilde{q}$) can behave like LQs with alternative decay channels (i.e. $\mathrm{BR}(\mathrm{LQ} \to eq) < 1$)

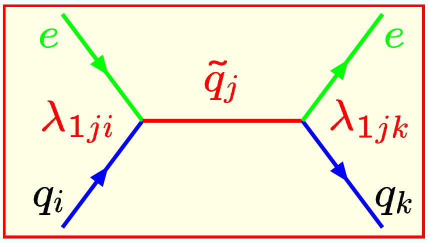

Search for R_P-Violating Squarks at HERA

Alternative decays of R_P-violating $\tilde{q}$ (examples):

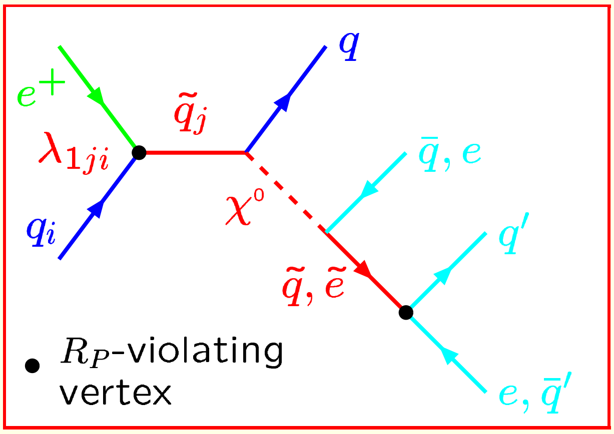

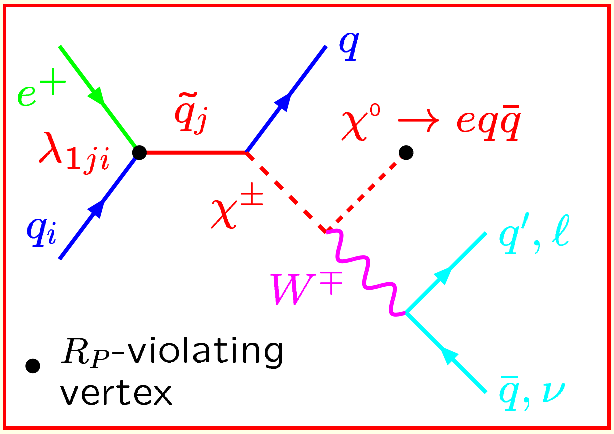

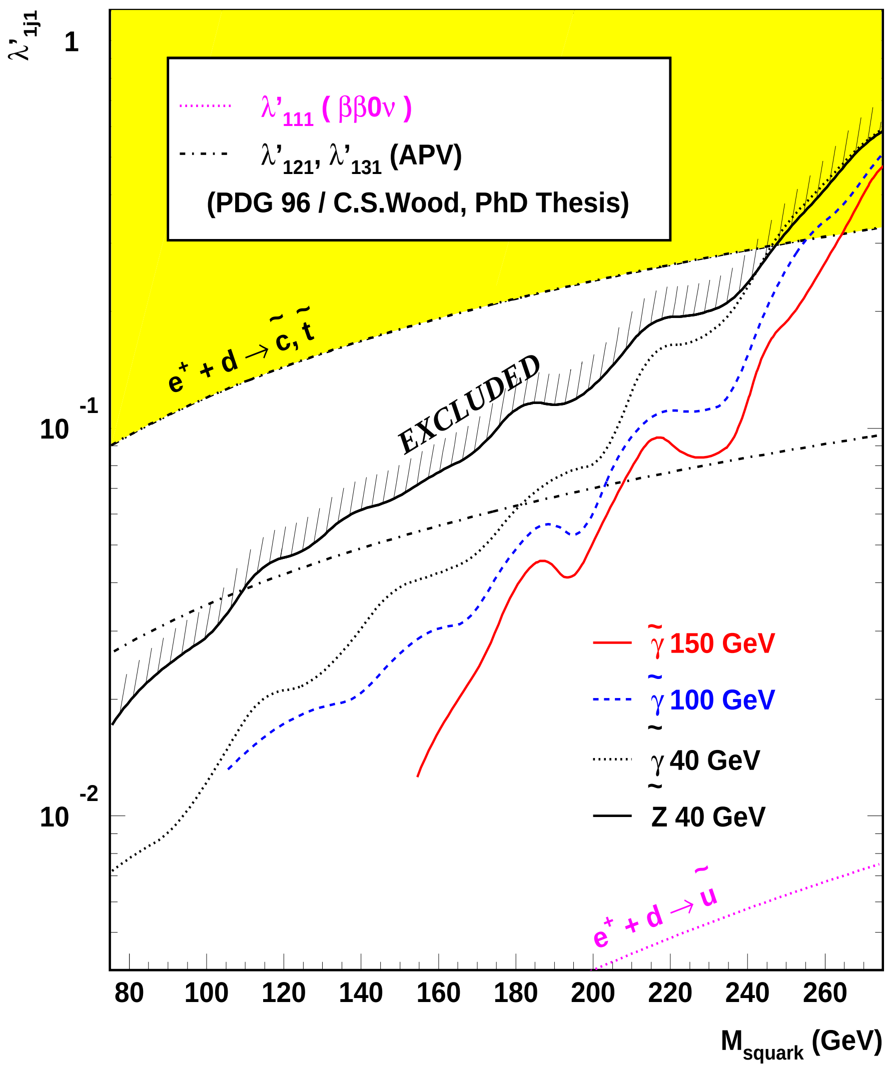

H1:

- Search for $e + n$ jets; e can be e^-.
- No event excess.
- Assumption: $\tilde{q}$ couples to $q_1 = u, d$ $\Rightarrow$ upper limits on λ_{1j1} .
- Discovery potential for $\tilde{q}_{2,3}$.

Similar results from ZEUS.

Violation of Lepton Flavor

Search for events with τ (μ) in final state;
interpretation as
$$e^+p \to \mathrm{LQ}\ X \to \tau^+q\ X$$
strong interest: lepton flavor is violated in ν sector !

H1 candidate event for $e^+p \to \tau X$;

after preselection:
$N_{\text{obs}} = 28$
$N_{\text{exp}} = 23.7 \pm 5.7$

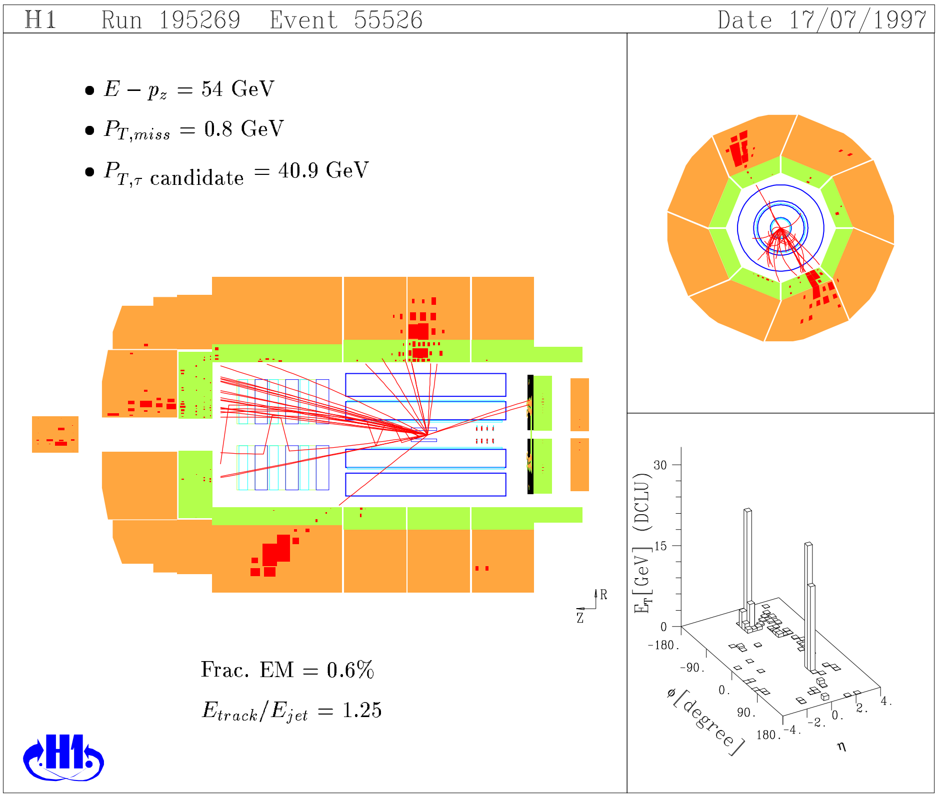

Event selection (H1):

- isolated ($\tau \to$ hadron) candidate
- $\not{P}_t > 10$ GeV in τ direction

Efficiency:

- $\sim 10\% \ldots 25\%$, increases with M_{LQ}

Result:

- no event selected

Similar analysis by ZEUS: no signal

Exclusion Limits for Lepton Flavor Violating LQs

Direct search for LQs with couplings to eq (λ_{1j}) and to τq (λ_{3j}) or μq (λ_{2j})

H1: LQ $\to \tau q$

Assumption: LQ couples only to e^+u and to τ^+q

Search for events with e+jet or τ+jet

Exclusion limits for λ_{3k} (95% C.L.) as a function of M_{LQ} at fixed λ_{11}

High HERA sensitivity in the channel $e \to \tau$

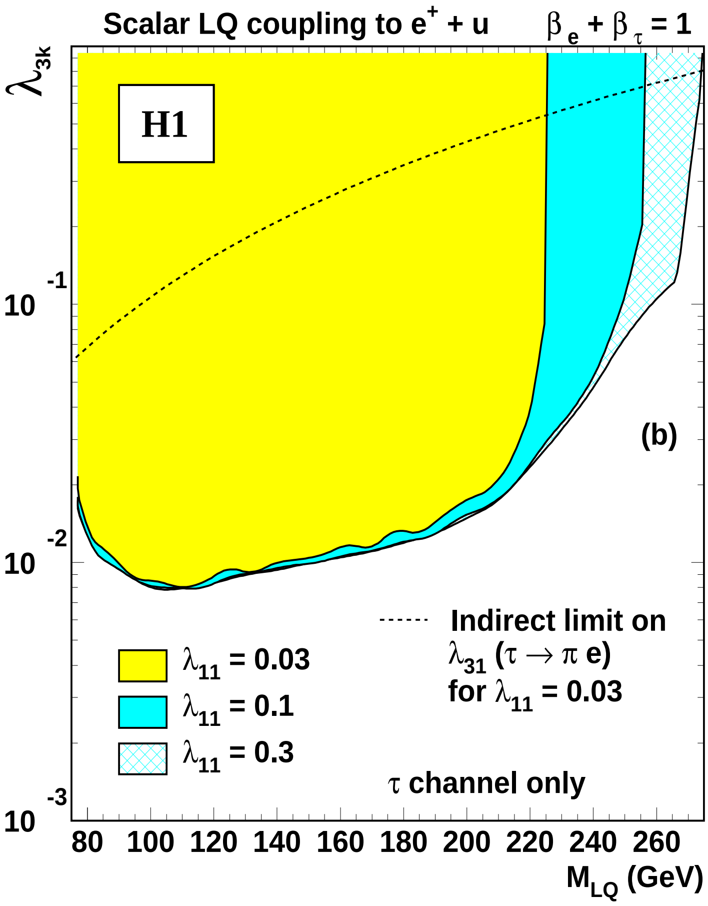

ZEUS: LQ $\to \mu q$ or LQ $\to \tau q$

Search: for events with μ + jet or τ + jet

Limits: for $\lambda_{11}\sqrt{\mathrm{BR}(\mathrm{LQ}\to\mu q)}$ and $\lambda_{11}\sqrt{\mathrm{BR}(\mathrm{LQ}\to\tau q)}$ as functions of M_{LQ}

Masses: $M_{\mathrm{LQ}} > 262-285$ GeV (95% C.L.)
$M_{\mathrm{LQ}} > 259-285$ GeV (95% C.L.)
for electromagnetic coupling strength ($\lambda^2 = 4\pi\alpha$)

Limits for LQs with $M_{\mathrm{LQ}} > \sqrt{s_{\mathrm{HERA}}}$

Indirect search for LQ's with couplings
to eq (λ_{1j}) and to τq (λ_{3j}) or μq (λ_{2j})

s and u channel exchange:

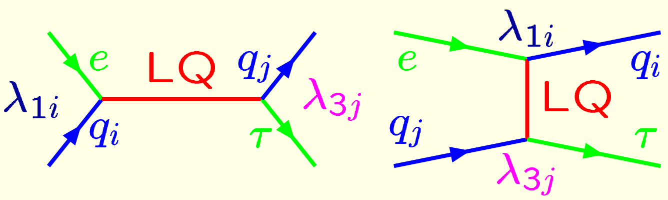

$$\sigma \propto \left(\frac{\lambda_{1i}\lambda_{3j}}{M_{\mathrm{LQ}}^2}\right)^2$$

$q_i q_j$	$S^L_{1/2}$	$S^R_{1/2}$	$\tilde{S}^L_{1/2}$	V^L_0	V^R_0	$\tilde{V}^R_0$	V^L_1
1 1	$\tau \to \pi e$ 0.0032 0.030 0.046	$\tau \to \pi e$ 0.0016 0.025 0.037	$\tau \to \pi e$ 0.0032 0.046 0.062	G_F 0.002 0.033 0.049	$\tau \to \pi e$ 0.0016 0.033 0.049	$\tau \to \pi e$ 0.0016 0.024 0.041	G_F 0.002 0.012 0.019
1 2	**0.030** 0.047	$\tau \to$K e 0.05 **0.025** 0.038	$\tau \to$K e 0.05 **0.046** 0.063	$\tau \to$K e 0.03 0.036 0.053	$\tau \to$K e 0.03 0.036 0.053	**0.026** 0.045	K $\to \pi\nu\bar{\nu}$ $2.5 \cdot 10^{-6}$ 0.012 0.021
1 3	—	B$\to \tau e$ X 0.08 **0.049** 0.065	B$\to \tau e$ X 0.08 **0.049** 0.065	B$\to l\nu$X 0.02 0.044 0.062	B$\to \tau e$ X 0.04 0.044 0.062	—	B$\to l\nu$X 0.02 0.044 0.062
2 1	0.153 **0.15**	$\tau \to$K e 0.05 0.092 0.095	$\tau \to$K e 0.05 0.105 0.12	$\tau \to$K e 0.03 0.049 0.064	$\tau \to$K e 0.03 0.049 0.064	**0.061** 0.073	K $\to \pi\nu\bar{\nu}$ $2.5 \cdot 10^{-6}$ 0.026 0.032
2 2	$\tau \to e\gamma$ 0.03 0.187 0.18	$\tau \to e\gamma$ 0.02 0.101 0.10	**0.120** 0.13	**0.061** 0.076	**0.061** 0.076	**0.102** 0.107	**0.041** 0.044
2 3	—	B$\to \tau e$ X 0.08 0.153 0.14	B$\to \tau e$ X 0.08 0.153 0.14	B$\to l\nu$X 0.02 0.102 0.112	B$\to \tau e$ X 0.04 0.102 0.112	—	B$\to l\nu$X 0.02 0.102 0.112
3 1	—	B$\to \tau e$ X 0.08 0.162 0.16	B$\to \tau e$ X 0.08 0.162 0.16	V_{ub} 0.002 0.052 0.068	B$\to \tau e$ X 0.04 0.052 0.068	—	V_{ub} 0.002 0.052 0.068
3 2	—	B$\to \tau e$ X 0.08 0.202 0.19	B$\to \tau e$ X 0.08 0.202 0.19	B$\to l\nu$X 0.02 0.073 0.083	B$\to \tau e$ X 0.04 0.073 0.083	—	B$\to l\nu$X 0.02 0.073 0.083
3 3	—	0.275 **0.23**	0.275 **0.23**	$\tau \to e\gamma$ 0.51 0.144 **0.14**	$\tau \to e\gamma$ 0.51 0.144 **0.14**	—	0.144 **0.14**

ZEUS/H1:

Upper limits on $\dfrac{\lambda_{1i}\lambda_{3j}}{M_{\mathrm{LQ}}^2}$

0.0032
limits from
rare decays etc.

0.025
best limit
from ZEUS

0.15
best limit
from H1

Excited Fermions

Fermion sub-structure

$\Leftrightarrow$ heavy excited fermion states (f^*),
couple to ground-state fermions and gauge bosons

e^*, ν^* production at HERA:

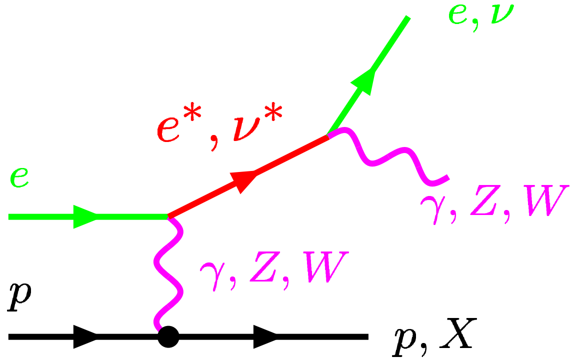

Model ($S_{f^*} = 1/2$):

(Hagiwara, Komamiya, Zeppenfeld)

$$\mathcal{L}_{ff^*} = \frac{1}{\Lambda} \cdot f_R^* \Big[f(gV)_{SU(2)_L} + f'(gV)_{U(1)_Y} + f_s(gV)_{SU(3)_C} \Big] f_L$$

Assumption at HERA:
$|f| = |f'|$ and $f_s = 0$

f^* decay	exp. signatures
$e^* \to e + \gamma$	$e + \gamma$
$e^* \to e + Z$	$e + 2$, $3e$, $e + \not{P}_t$, ...
$e^* \to \nu + W$	$\not{P}_t$ + 2jets, $e + \not{P}_t$, ...
$\nu^* \to \nu + \gamma$	$\gamma + \not{P}_t$
$\nu^* \to e + W$	e + 2jets, $2e + \not{P}_t$, ...
$\nu^* \to \nu + Z$	$\not{P}_t$ + 2jets, $2e + \not{P}_t$, ...
$q^* \to q + \gamma$	γ+jet
$q^* \to q' + W$	$e + \not{P}_t$+jet, ...

$\not{P}_t$ = missing transverse momentum

Example: Search for $e^* \to e\gamma$

Experimental signature:

– 2 isolated elm. clusters
– small hadronic p_t
– no $\not{P}_t$

Background:

QED Compton

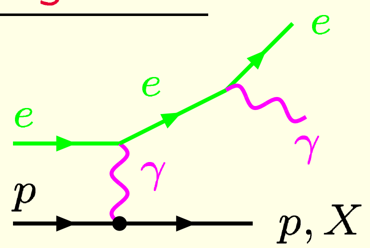

ZEUS candidate with highest $e\gamma$ mass ($M_{e\gamma}$=159 GeV)

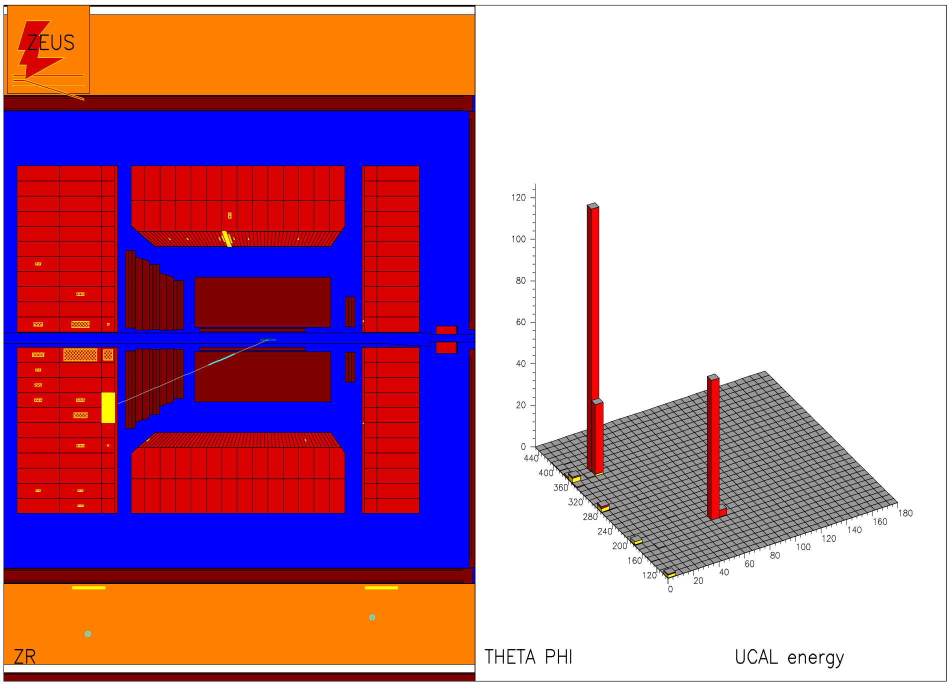

$M_{e\gamma}$ spectrum

- ● data
- ☐ SM background
- QED Compton (yellow)
- e^* (simulation) (cyan)

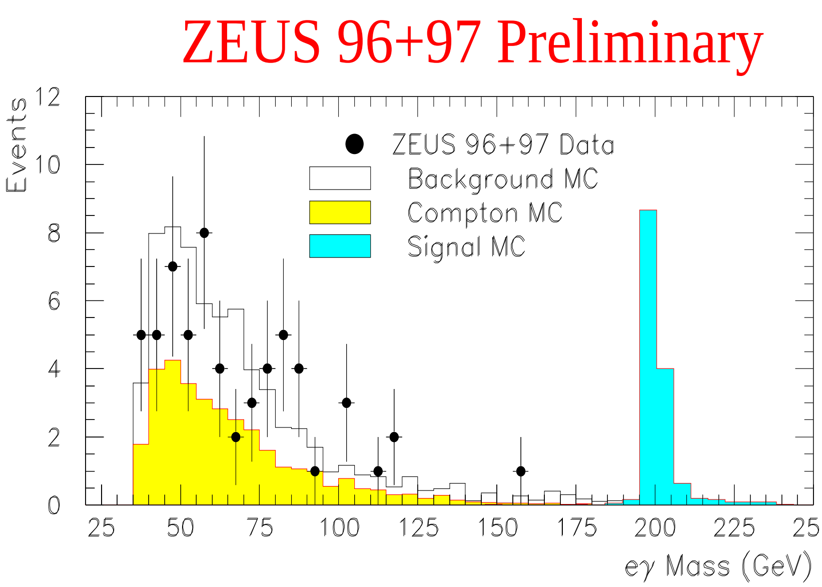

e^*, q^* and ν^* Exclusion Limits

No evidence for f^* production at HERA

$\Rightarrow$ Upper limits on $|f|/\Lambda$

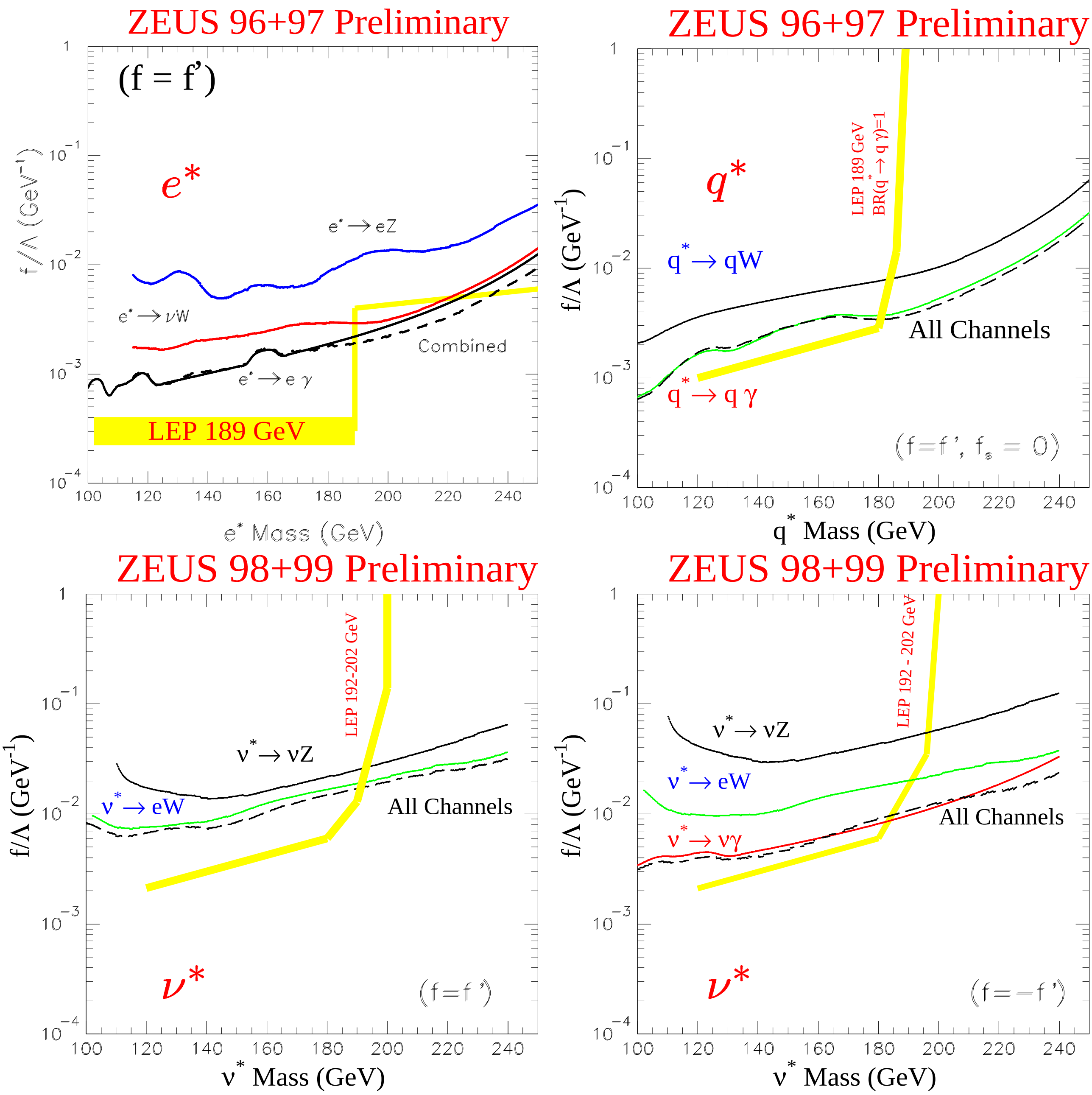

- For $M_{f^*} \lesssim \sqrt{s_{\mathrm{LEP}}}$ HERA is less sensitive than LEP, for high masses HERA sensitivity is better (similar)
- HERA provides the only limits for $M_{\nu^*} \gtrsim 200$ GeV (best ν^* limits from e^-p data).
- Similar results from H1.

Contact Interactions (CI)

CI: effective phenomenological description of processes with mass scales $\gg \sqrt{s_{\text{HERA}}}$;
historical equivalent: 4-fermion interaction

$eeqq$-CI:

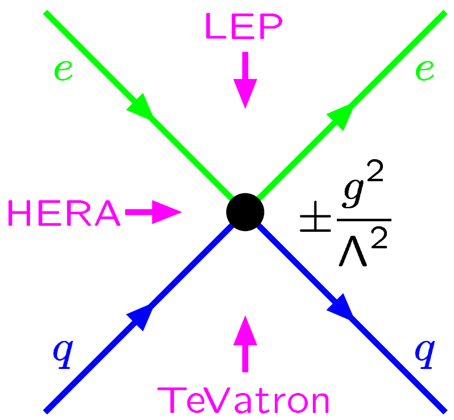

Examples of CI:

- Exchange of heavy gauge bosons
- Leptoquarks or squarks (s/u channel)
- Exchange interaction of composite leptons and quarks
- ...

Effective Lagrangian:

$$\mathcal{L} = \epsilon \frac{g^2}{\Lambda^2} \sum_{\substack{a,b=L,R \\ q=u,d}} \eta_{ab}^q (\bar{e}_a \gamma^\mu e_a)(\bar{q}_b \gamma_\mu q_b)$$

- Interference with SM (constructive or destructive).
- Linear combinations of the $\eta_{ab}^q \Rightarrow$ "CI scenarios".
- $\epsilon = \pm 1$; $\eta_{ab}^q = 1, 0$; g^2/Λ determines CI strength
- If there are $eeqq$ CI, they modify several cross sections simultaneously:
  - $\rightarrow$ NC-DIS (HERA);
  - $\rightarrow$ $e^+e^- \rightarrow q\bar{q}$ (LEP);
  - $\rightarrow$ $p\bar{p} \rightarrow e^+e^- + X$ (TeVatron).

Search for CI Signatures

HERA: Search for deviations from SM expectation for $d\sigma/dQ^2$ (H1) or for the event distributions $d^2N_{obs}/dx\,dQ^2$ (ZEUS).

Modification of $d\sigma_{NC}/dQ^2$ by CI:

- CI-SM interference ($\propto \pm Q^2/\Lambda^2$)
- pure CI contribution ($\propto Q^4/\Lambda^4$)
- cross section increases at high Q^2
- different statistical analysis methods

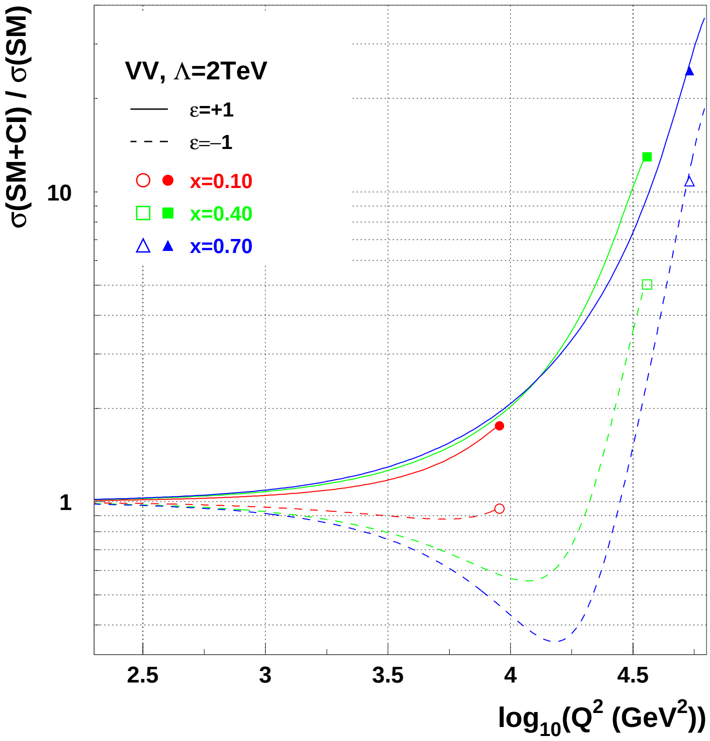

Most important result from low-energy experiments:

measurement of the "weak charge" (Q_W) of the Cs nucleus (atomic parity violation, APV)

$$\Delta^{CI}Q_W = \frac{2Z+N}{\sqrt{2}G_F}\frac{4\pi\epsilon}{\Lambda^2}\left(\eta^u_{LL}+\eta^u_{LR}-\eta^u_{RL}-\eta^u_{RR}\right) + \frac{Z+2N}{\sqrt{2}G_F}\frac{4\pi\epsilon}{\Lambda^2}\left(\eta^d_{LL}+\eta^d_{LR}-\eta^d_{RL}-\eta^d_{RR}\right)$$

experimental result: $\Delta^{exp}Q_W = 1.28 \pm 0.46$

- APV: 2.8σ effect
- APV effect and limits are beyond HERA sensitivity
- at HERA: search for parity-conserving CI

Limits on CI Mass Scales

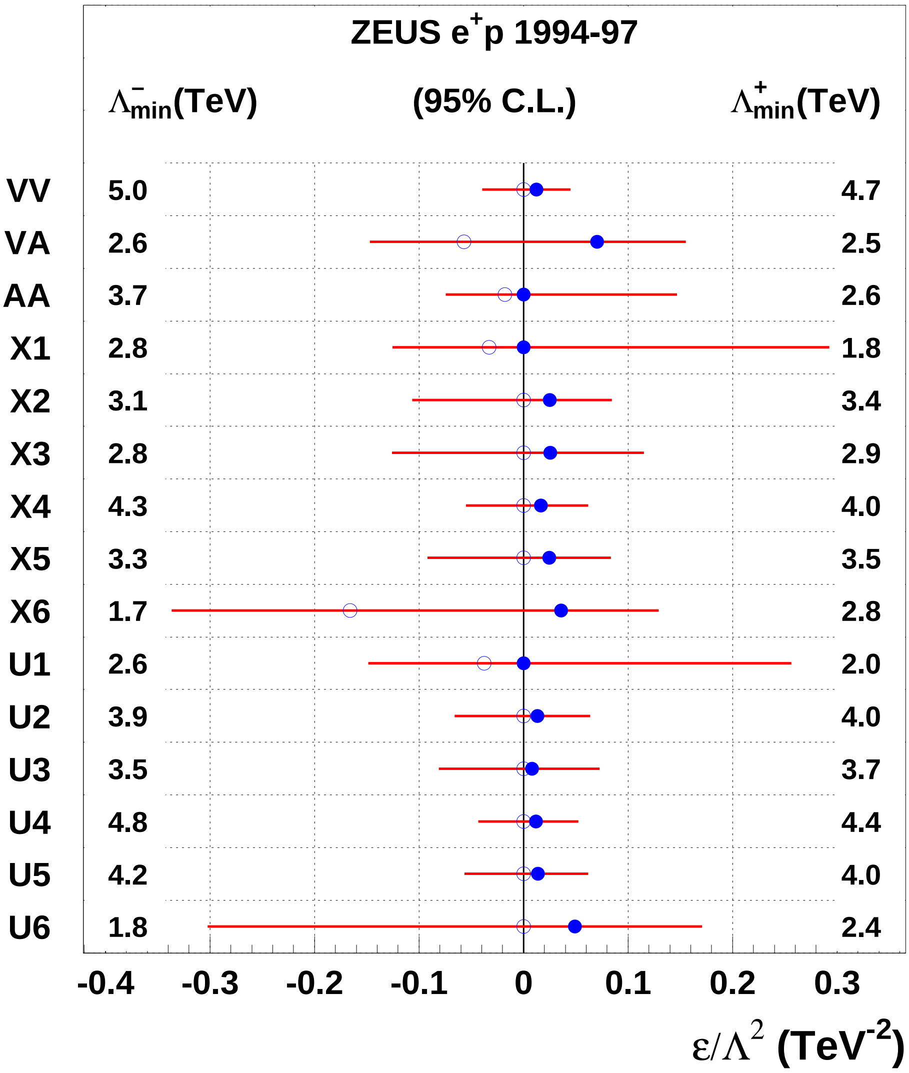

ZEUS:

separate statistical analysis for $\epsilon = +1$ and $\epsilon = -1$.

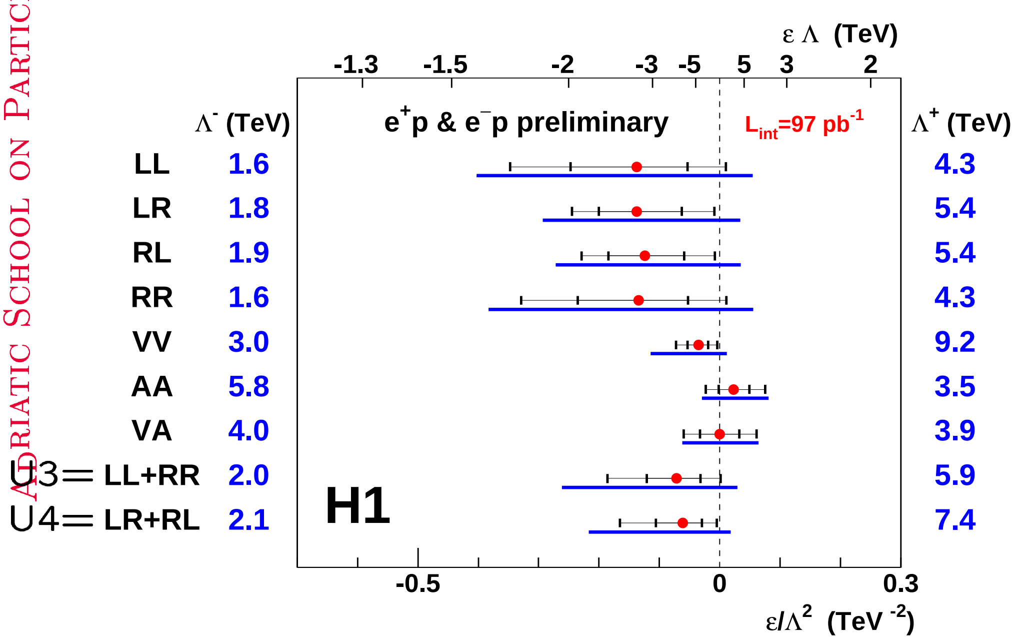

H1:

common confidence region for $\epsilon = +1$ and $\epsilon = -1$.

Extra Dimensions

Theoretical Scenario:

- Gravitons live in $4+n$ dimensions (size R_S), all other particles constrained to 4 dimensions
- $\Rightarrow$ Violation of Newton's law for $r \lesssim R_S$
  $\Rightarrow$ Characteristic gravitation mass scale M_S:
  $$R_S^n M_S^{2+n} \sim 1/G_N = M_P^2$$
- $n = 2$ ($R_S = \mathcal{O}(100\,\mu\text{m})$, $M_S = \mathcal{O}(\text{TeV})$) is possible
- "Projections" of the gravitons to 4 dimensions couple to massive particles with strength $\propto \lambda_s/M_S^4$
  $\Rightarrow$ CI-type modification of $\sigma(ep)$

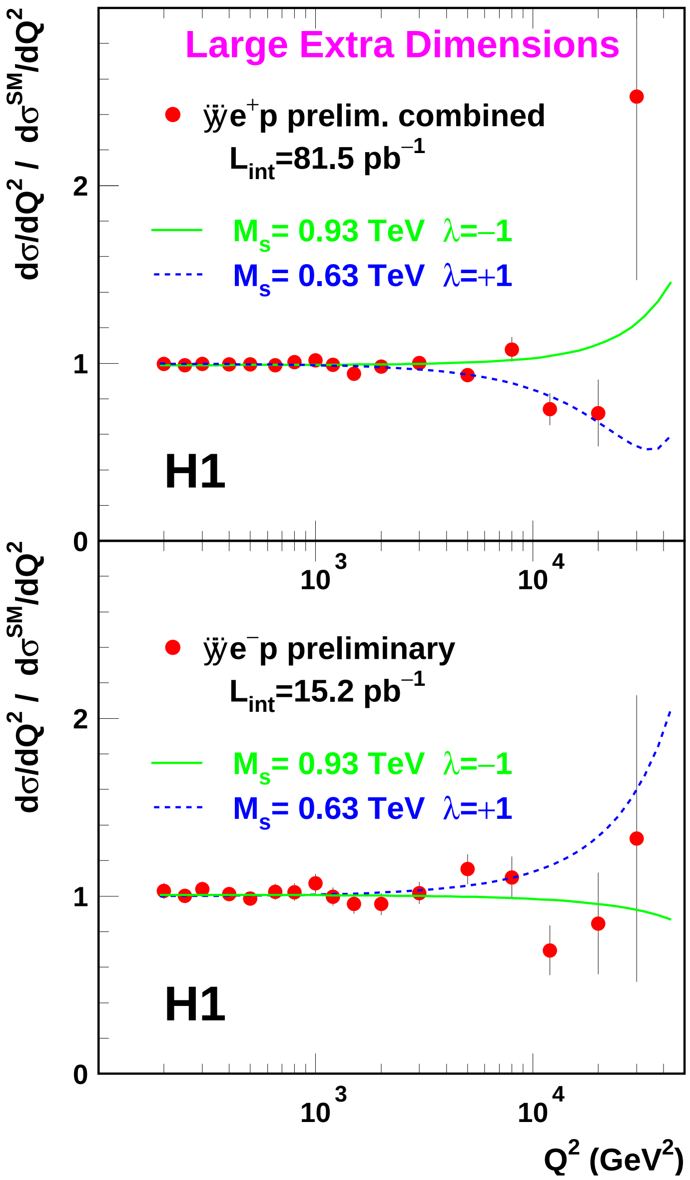

H1 limits:

No evidence for extra dimensions.

Exclusion limits at 95% C.L.:

$M_S > 0.93\,\text{TeV}$
$(\lambda_S = +1)$

$M_S > 0.63\,\text{TeV}$
$(\lambda_S = -1)$

Events with Leptons and $\not{P}_t$

Event signatures:

- Isolated lepton (μ or e) with high p_t
- Large missing transverse momentum $\not{P}_t$, not in lepton direction
- Hadronic jet with moderate to large p_t

$e^+p \to \mu^+X$

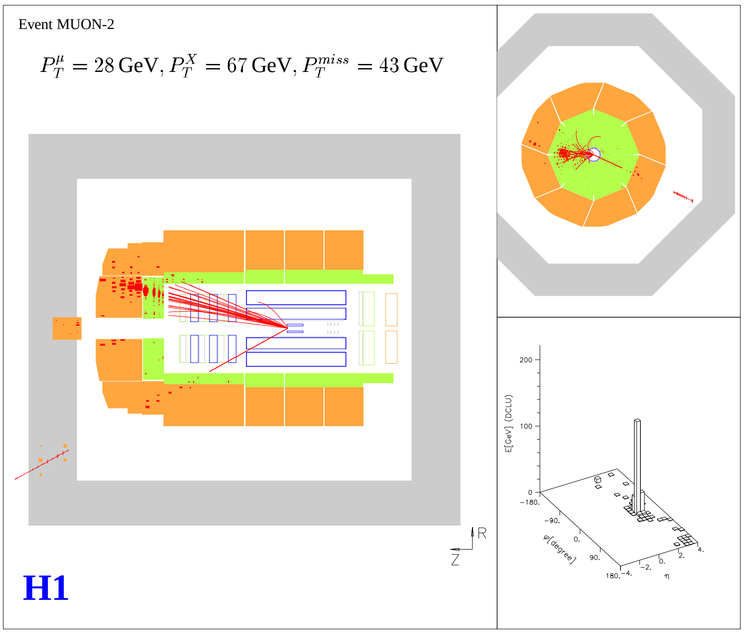

SM Reactions:

$$ep \to W + \text{jet} + X$$
$$\to \ell\nu_\ell + \text{jet} + X$$
$$ep \to \ell^+\ell^- + X$$

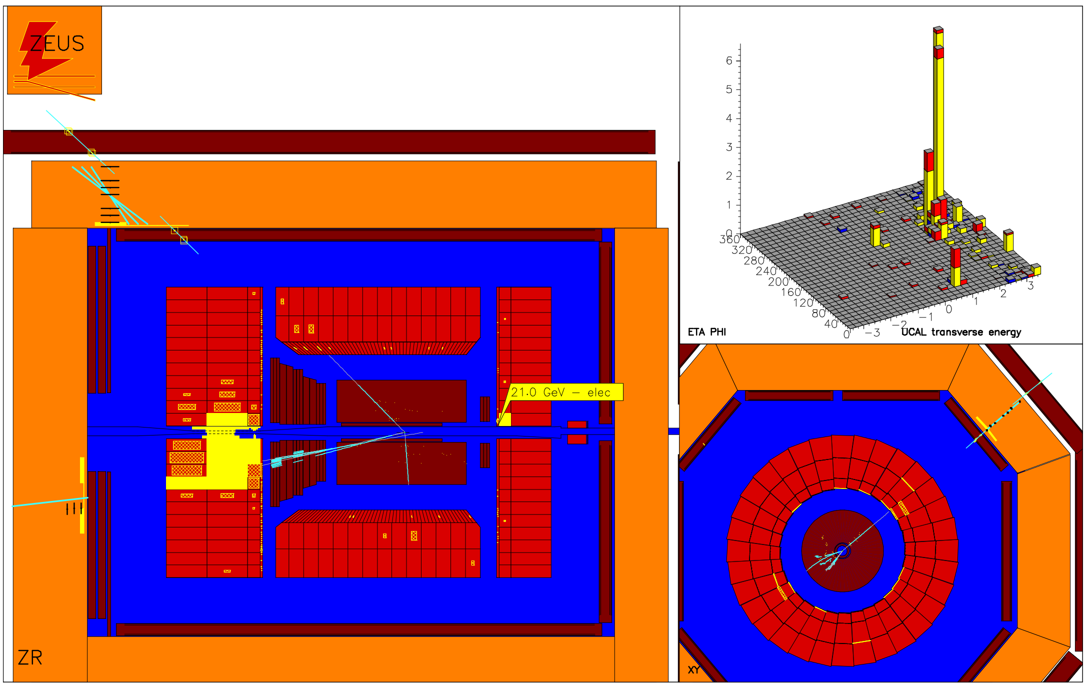

The ZEUS/H1 Puzzle

Inconsistent observations by H1 and ZEUS ?

H1:
- Significant excess of "$\not{P}_t$+lepton events";
- many of these with large hadronic transverse momentum P_t^X
- only in e^+p data (doesn't mean much)

ZEUS:
- Number of $\not{P}_t$+lepton events consistent with expectation
- no event excess at high P_t^X

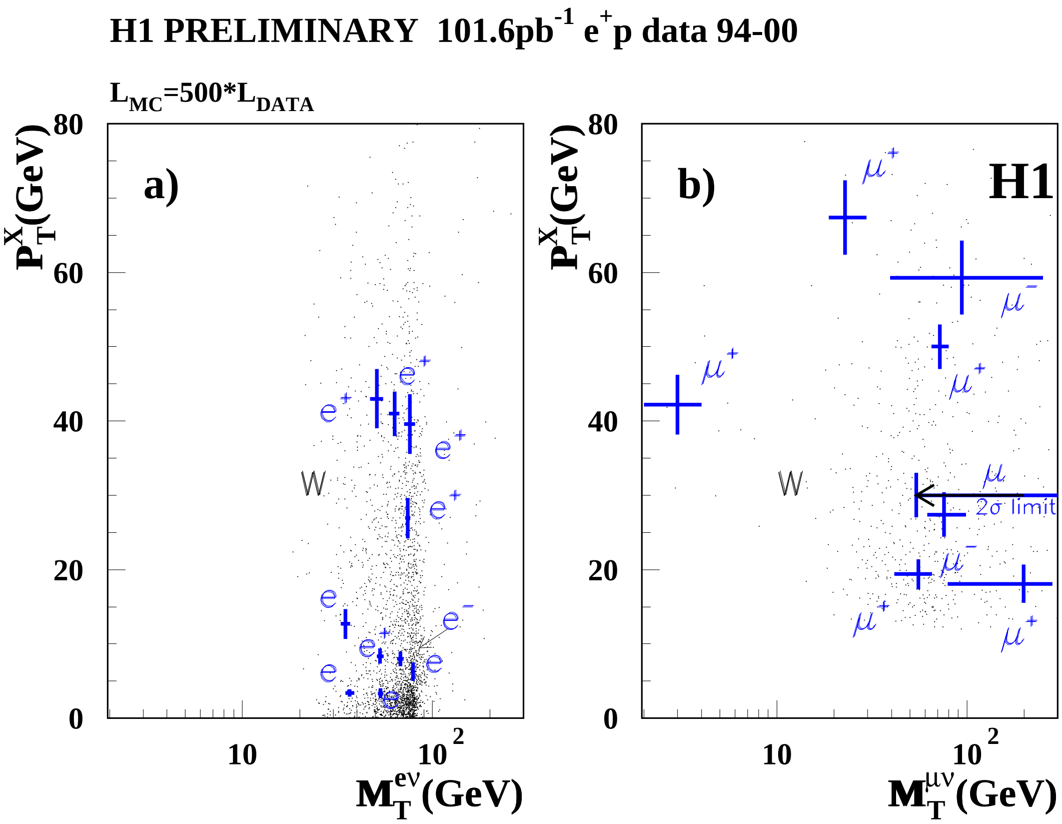

Event numbers:

		e obs.	e exp.	μ obs.	μ exp.
P_T^X>25 GeV	H1	4	1.29	6	1.54
	ZEUS	1	1.14	1	1.29
P_T^X>40 GeV	H1	2	0.41	4	0.58
	ZEUS	0	0.46	0	0.50

Top Production

Top production at HERA?

H1:	•	5 $\not{P}_t$+lepton events are compatible with top production (1.5 expected)
ZEUS:	•	no evidence for top production
Theory:	•	top production cross section at HERA is tiny in SM.
	•	Possible: anomalous $tu\gamma$ coupling (e.g. in models of dynamic fermion mass generation, see e.g. hep–ph/9901411)

HERA sensitivity competitive if tqZ coupling is small

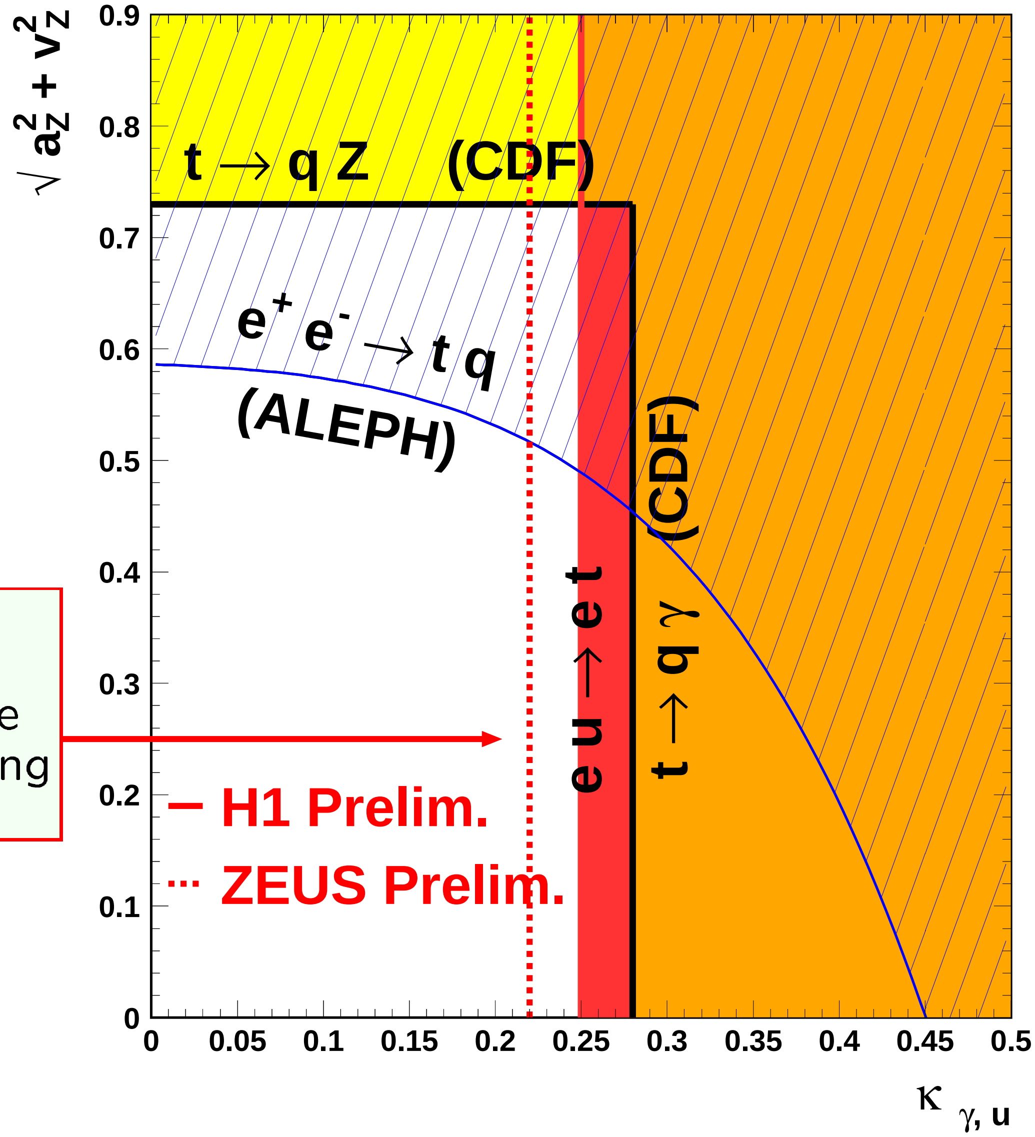

Outlook

The future of HERA

- We are at the end of an upgrade shutdown
  - new interaction zones $\rightarrow$ increased luminosity ($\mathcal{O}(100-150\,\text{pb}^{-1}/\text{year})$)
  - longitudinal e polarization
  - detector upgrades & improvements
- Data taking 2002–2005 (or longer?)
  - improved statistics, refined measurements of low-cross-section processes (e.g. DIS at high Q^2)
  - increased sensitivity to new physics

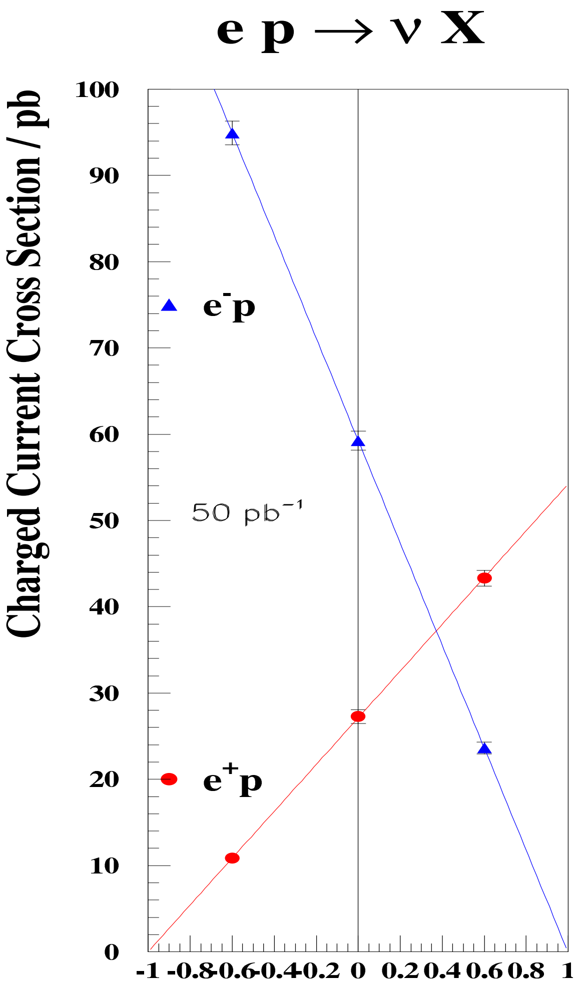

Example Measurement

CC cross section as a function of e polarization P:

$$\sigma^{\text{CC}}(e^{\pm}p) \propto (1 \pm P)$$

- deviations would indicate right-handed charged currents
- sensitivity e.g. to heavy gauge boson W_R
- W_R mass limits of $\mathcal{O}(400\,\text{GeV})$ achievable

The Post-HERA Future

History shows that improvements in spatial resolution obtained in scattering experiments are crucial for the progress of particle physics:

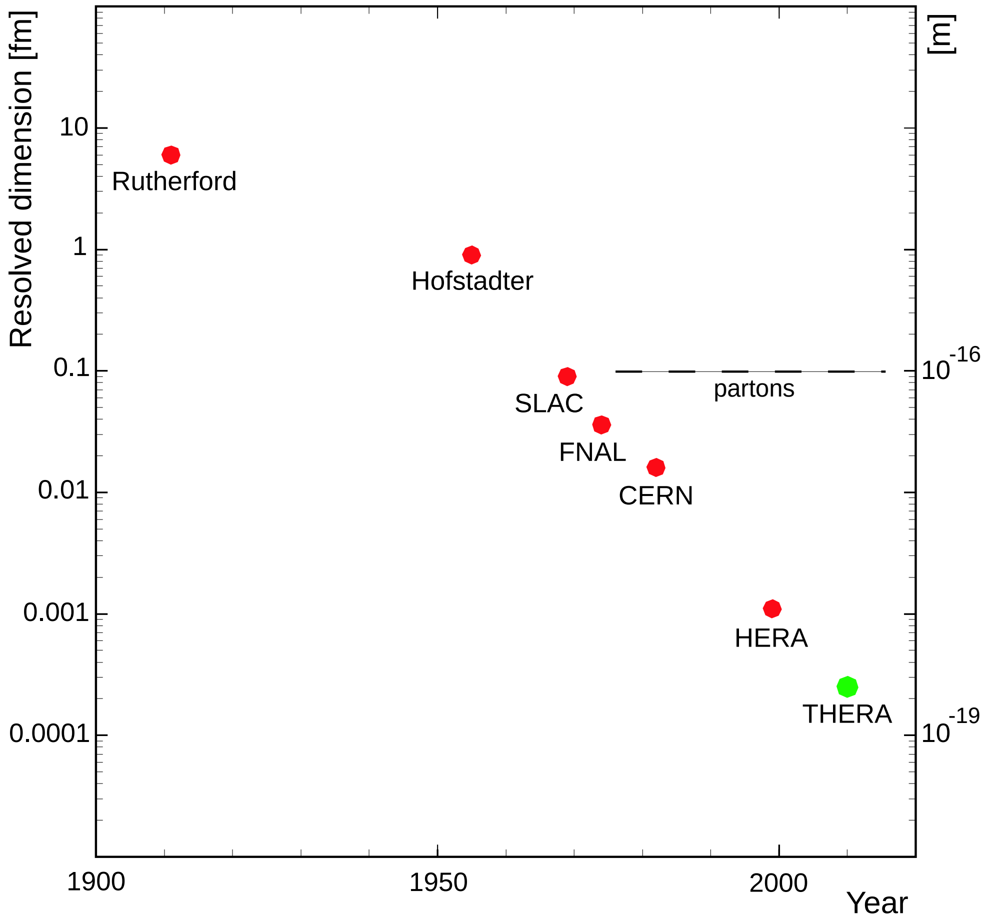

Future ep colliders are under discussion, e.g. a TESLA×HERA option (THERA)

~ 1 TeV center-of-mass-energy,
up to $\mathcal{O}(100\,\mathrm{pb}^{-1})$ luminosity per year ...